Cosmic birefringence

CMB polarisation as a probe for ultra-light axions

Patricia Diego-Palazuelos

COSMIC WISPers kick-off meeting
Laboratori Nazionali di Frascati, Italy
February 23-24 2023

Searching for ULA through their gravitational imprint

CMB Rogers+[arXiv:2301.08361]
kSZ Farren+[arXiv:2109.13268]
Galaxy clustering Laguë+[arXiv:2104.07802]
Galaxy weak lensing Dentler+[arXiv:2111.01199]
Lyman-alpha forest Rogers&Peiris[arXiv:2007.12705]
Dwarf galaxies Dalal&Kravtsov[arXiv:2203.05750]
21cm observations Flitter&Kovetz[arXiv:2207.05083]

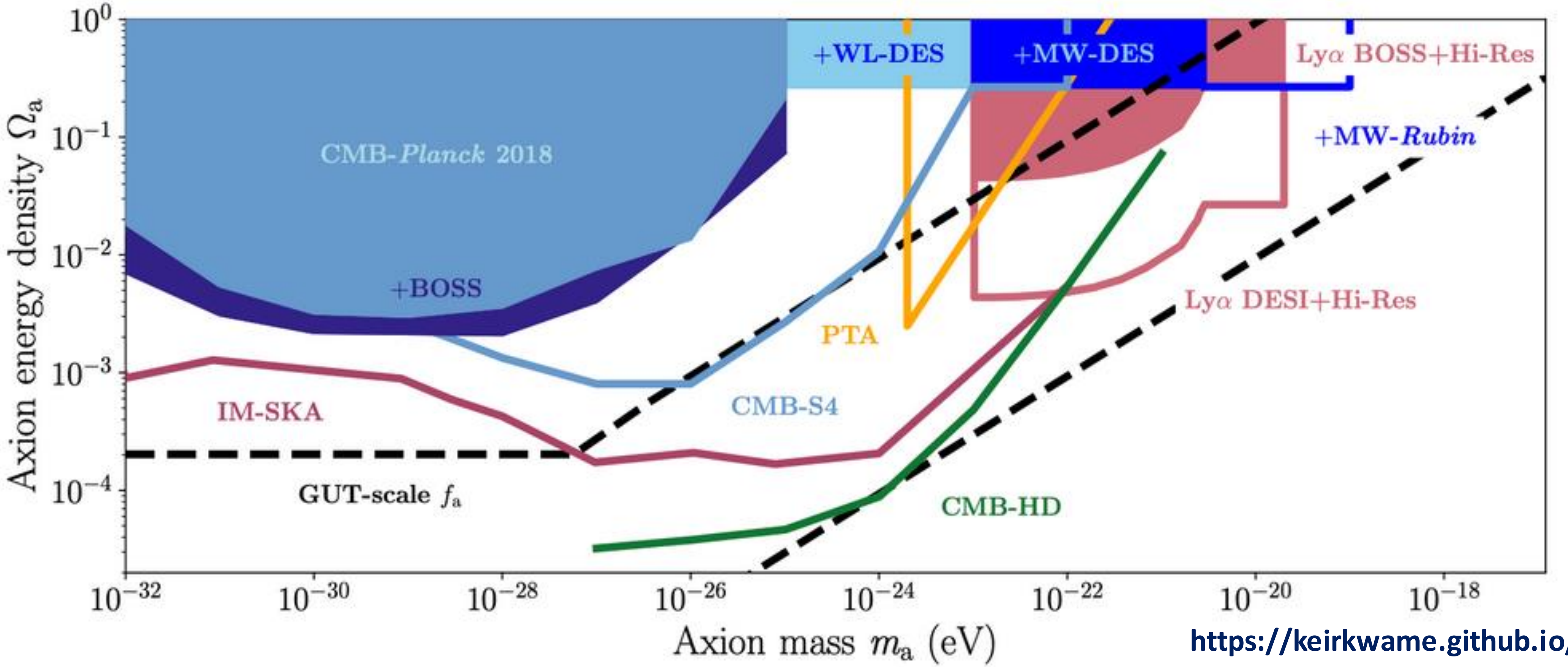

https://keirkwame.github.io/DM_limits

Searching for ULA through their (potential) coupling to EM

ALP can couple to EM through a Chern-Simons interaction

$$\frac{1}{4} g_{\phi\gamma} \phi F_{\mu\nu} \tilde{F}_{\mu\nu}$$

Searching for ULA through their (potential) coupling to EM

ALP can couple to EM through a Chern-Simons interaction

$$\frac{1}{4} g_{\phi\gamma} \phi F_{\mu\nu} \tilde{F}_{\mu\nu}$$

rotation of the plane of linear polarization clockwise on the sky

$$\beta = -\frac{1}{2} g_{\phi\gamma} \int \frac{\partial \phi}{\partial t} dt$$

Cosmic birefringence

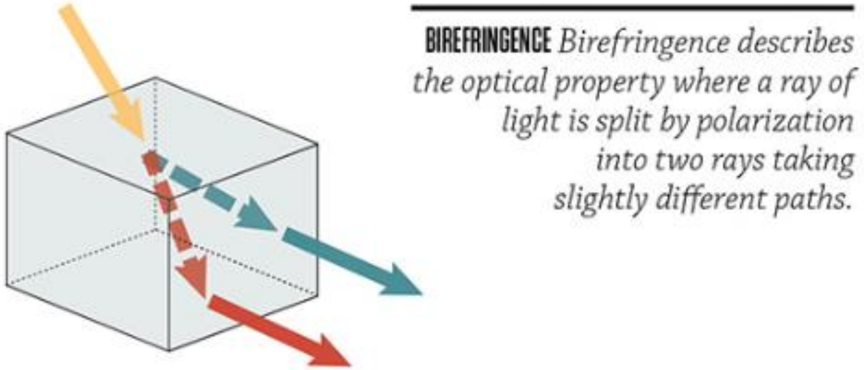

Searching for ULA through their (potential) coupling to EM

ALP can couple to EM through a Chern-Simons interaction

$$\frac{1}{4} g_{\phi\gamma} \phi F_{\mu\nu} \tilde{F}_{\mu\nu}$$

rotation of the plane of linear polarization clockwise on the sky

$$\beta = -\frac{1}{2} g_{\phi\gamma} \int \frac{\partial \phi}{\partial t} dt$$

Applicable to any source of linearly polarised light that is...

... very well-known ← measure a small angle

... situated very far away ← depends on m_φ but, in general, $g_{\varphi\gamma}\partial\varphi/\partial t$ expected to be small

Cosmic birefringence

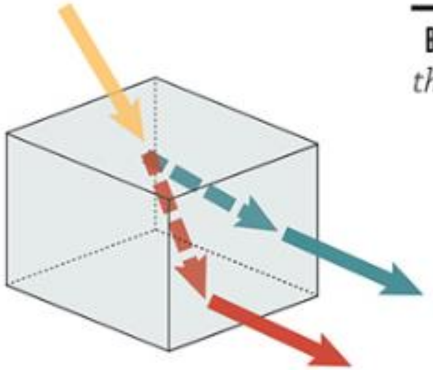

BIREFRINGENCE *Birefringence describes the optical property where a ray of light is split by polarization into two rays taking slightly different paths.*

Searching for ULA through their (potential) coupling to EM

ALP can couple to EM through a Chern-Simons interaction

$$\frac{1}{4} g_{\phi\gamma} \phi F_{\mu\nu} \tilde{F}_{\mu\nu}$$

rotation of the plane of linear polarization clockwise on the sky

$$\beta = -\frac{1}{2} g_{\phi\gamma} \int \frac{\partial \phi}{\partial t} dt$$

Cosmic birefringence

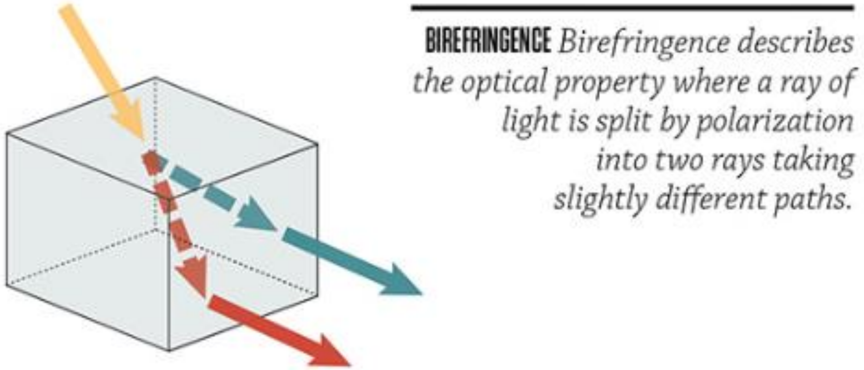

Applicable to any source of linearly polarised light that is...

... very well-known ← measure a small angle

accurately predicted by ΛCDM

... situated very far away ← depends on m_φ but, in general, $g_{\varphi\gamma}\partial\varphi/\partial t$ expected to be small

z≈1100

CMB!

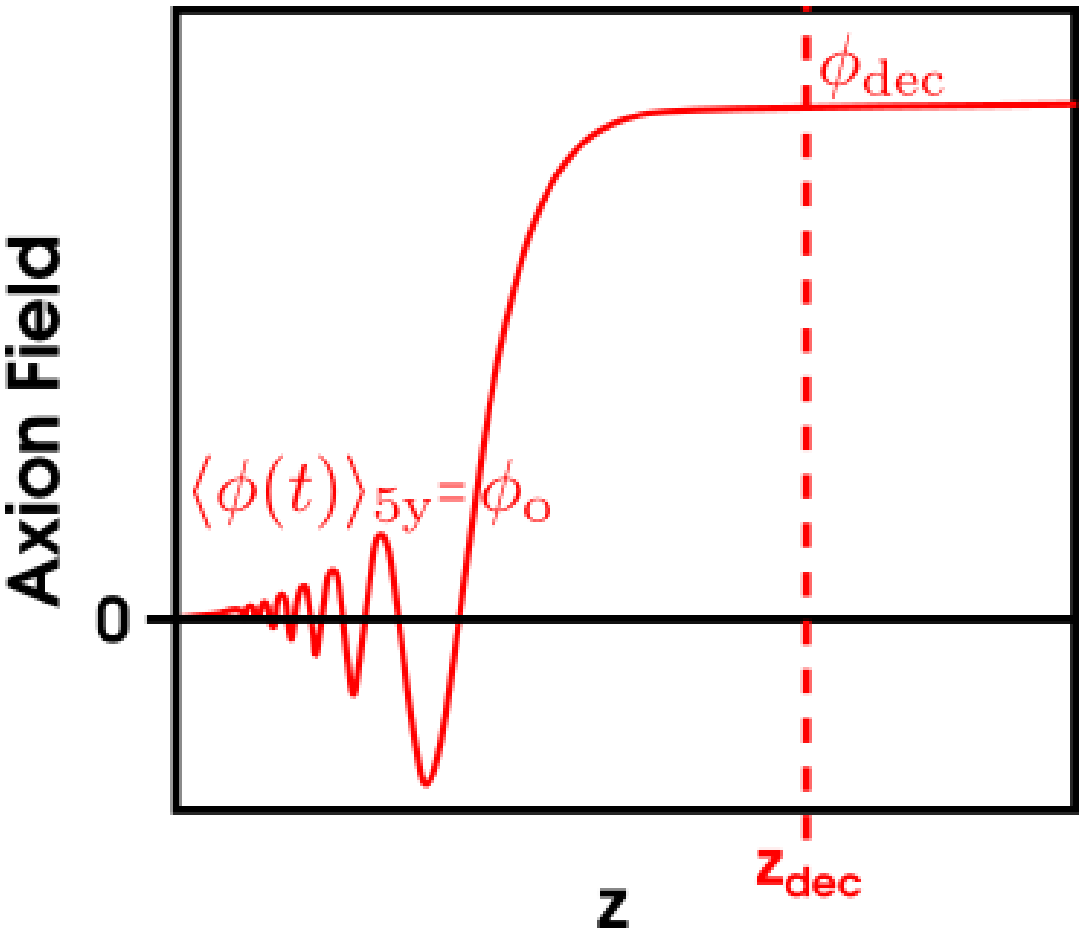

Suppose that ALP field is homogeneous and varies with time

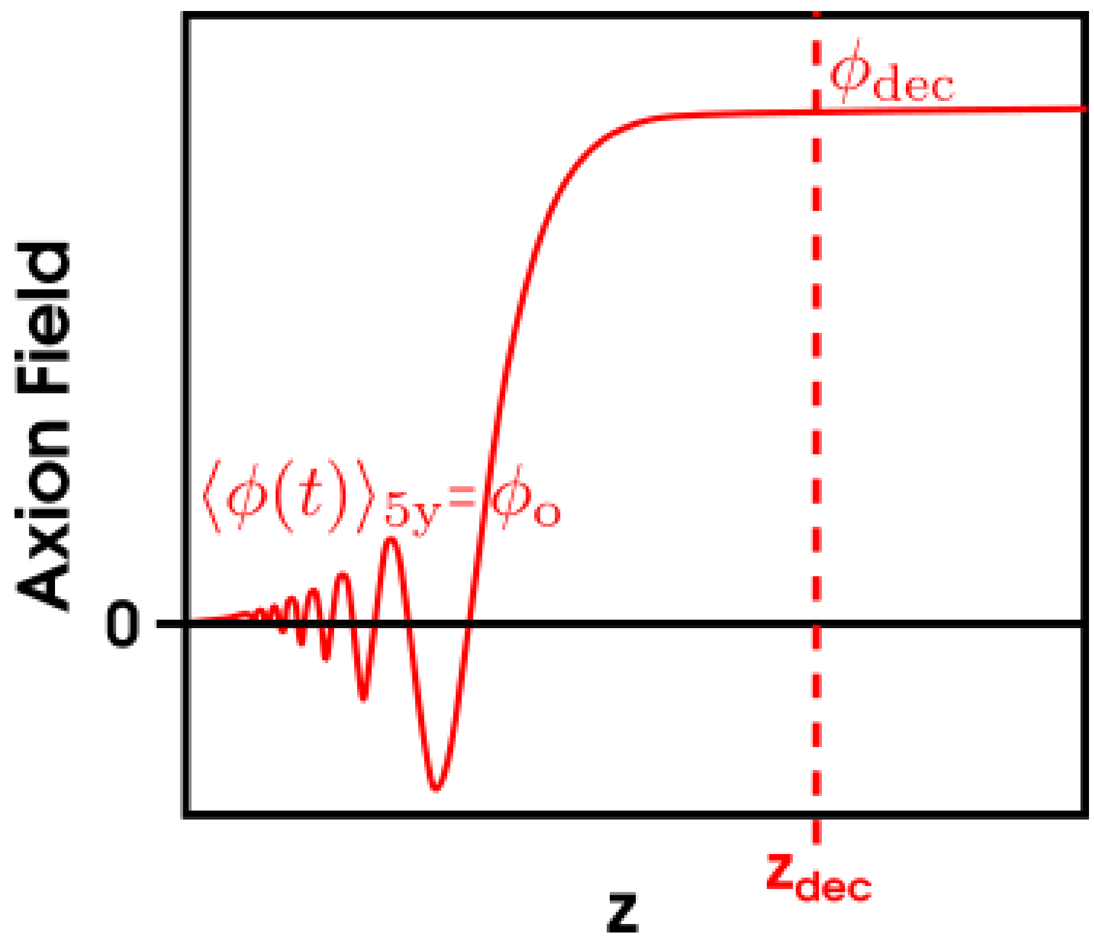

Suppose that ALP field is homogeneous and varies with time

$m_\phi \leq H_{dec}$ For ALP to start oscillating after decoupling

$m_\phi \geq H_o$ For ALP to start oscillating before today

$$10^{-33}\text{eV} \leq m_\phi \leq 10^{-28}\text{eV}$$

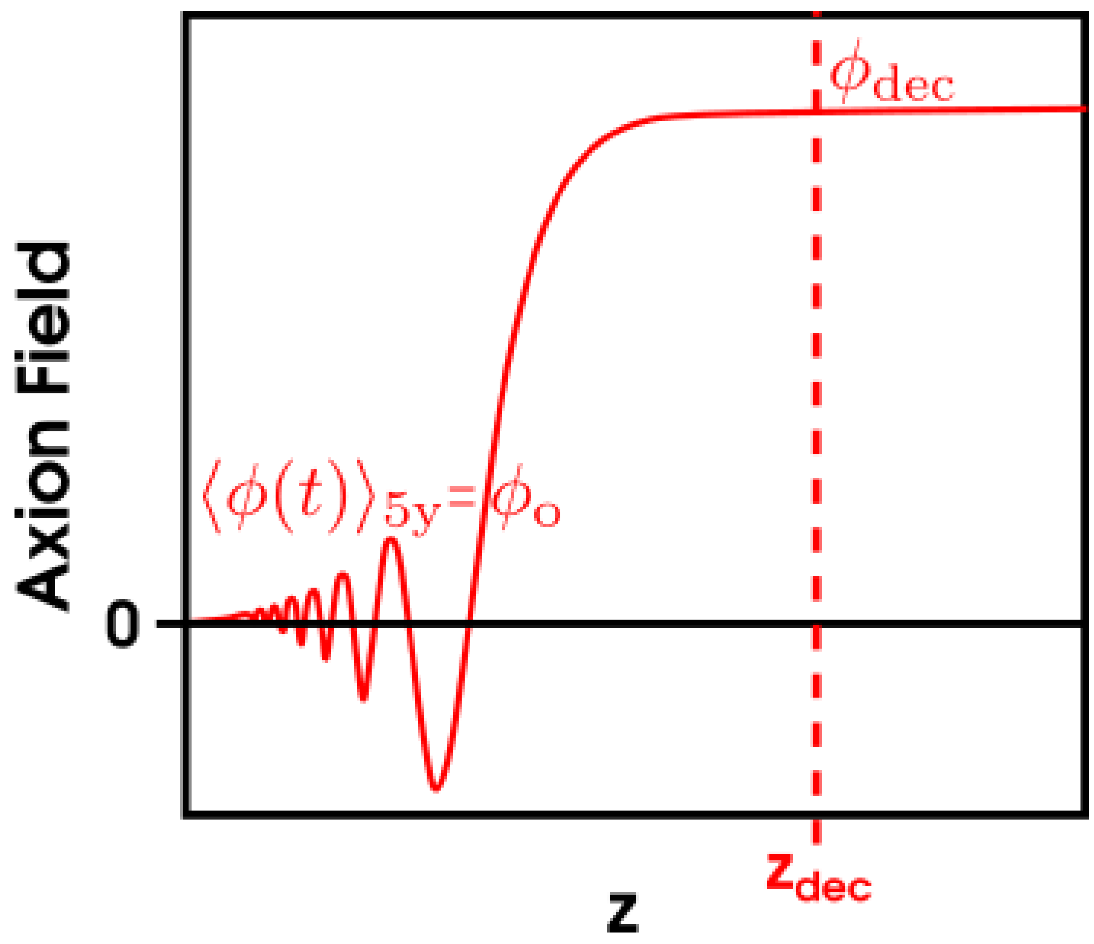

Suppose that ALP field is homogeneous and varies with time

$m_\phi \leq H_{\rm dec}$ For ALP to start oscillating after decoupling

$m_\phi \geq H_{\rm o}$ For ALP to start oscillating before today

$$10^{-33}{\rm eV} \leq m_\phi \leq 10^{-28}{\rm eV}$$

Constant birefringence angle, mainly sensitive to the ALP field value during decoupling

$$\beta = -\frac{1}{2}g_{\phi\gamma}\int\frac{\partial\phi}{\partial t}dt = -\frac{1}{2}g_{\phi\gamma}(\phi_{\rm o} - \phi_{\rm dec}) \approx \frac{1}{2}g_{\phi\gamma}\phi_{\rm dec}$$

Cosmic birefringence rotates the observed CMB

$$\begin{pmatrix} E^{\rm o}_{\ell m} \\ B^{\rm o}_{\ell m} \end{pmatrix} = \begin{pmatrix} \cos(2\beta) & -\sin(2\beta) \\ \sin(2\beta) & \cos(2\beta) \end{pmatrix} \begin{pmatrix} E^{\rm cmb}_{\ell m} \\ B^{\rm cmb}_{\ell m} \end{pmatrix}$$

so the observed angular power spectrum becomes

$$C_\ell^{EB,{\rm o}} = \frac{1}{2}\sin(4\beta)\left(C_\ell^{EE,{\rm cmb}} - C_\ell^{BB,{\rm cmb}}\right) + \cos(4\beta)C_\ell^{EB,{\rm cmb}}$$

ΛCDM

Cosmic birefringence

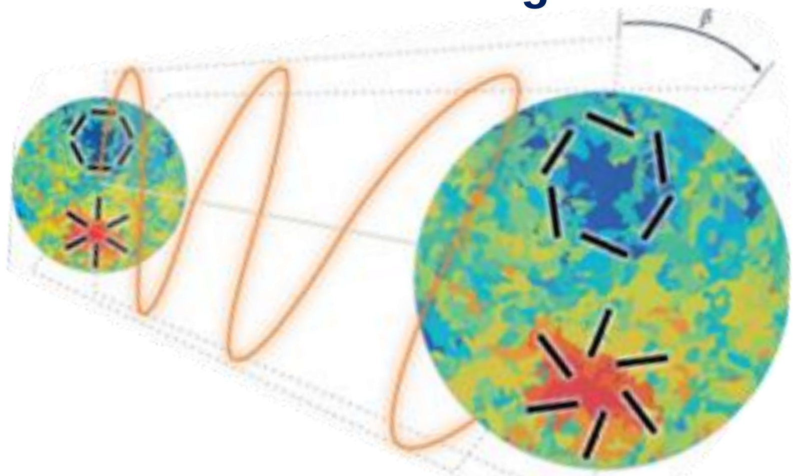

©Y. Minami

Cosmic birefringence rotates the observed CMB

$$\begin{pmatrix} E^{\rm o}_{\ell m} \\ B^{\rm o}_{\ell m} \end{pmatrix} = \begin{pmatrix} \cos(2\beta) & -\sin(2\beta) \\ \sin(2\beta) & \cos(2\beta) \end{pmatrix} \begin{pmatrix} E^{\rm cmb}_{\ell m} \\ B^{\rm cmb}_{\ell m} \end{pmatrix}$$

so the observed angular power spectrum becomes

$$C_\ell^{EB,{\rm o}} = \frac{1}{2}\sin(4\beta)\left(C_\ell^{EE,{\rm cmb}} - C_\ell^{BB,{\rm cmb}}\right) + \cos(4\beta)\,C_\ell^{EB,{\rm cmb}}$$

ΛCDM

$$C_\ell^{EB,{\rm o}} = \frac{1}{2}\tan(4\beta)\left(C_\ell^{EE,{\rm o}} - C_\ell^{BB,{\rm o}}\right)$$

Base of most methodologies applied in the past

Cosmic birefringence

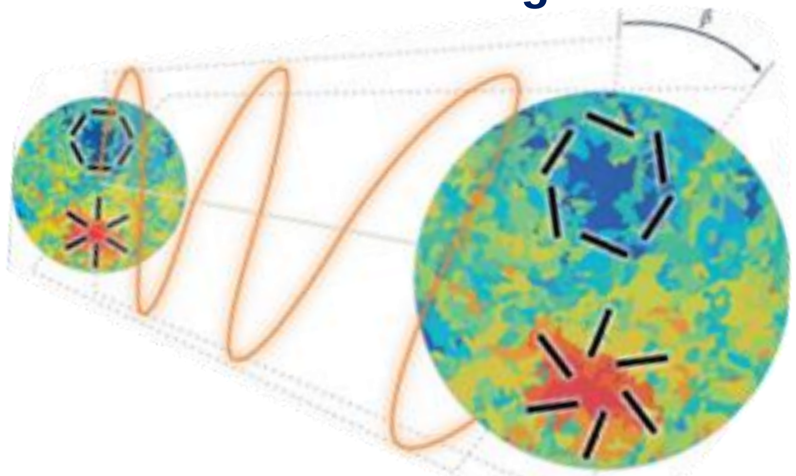

©Y. Minami

Cosmic birefringence rotates the observed CMB

$$\begin{pmatrix} E^{\rm o}_{\ell m} \\ B^{\rm o}_{\ell m} \end{pmatrix} = \begin{pmatrix} \cos(2\beta) & -\sin(2\beta) \\ \sin(2\beta) & \cos(2\beta) \end{pmatrix} \begin{pmatrix} E^{\rm cmb}_{\ell m} \\ B^{\rm cmb}_{\ell m} \end{pmatrix}$$

so the observed angular power spectrum becomes

$$C_\ell^{EB,{\rm o}} = \frac{1}{2}\sin(4\beta)\left(C_\ell^{EE,{\rm cmb}} - C_\ell^{BB,{\rm cmb}}\right) + \cos(4\beta)C_\ell^{EB,{\rm cmb}}$$

ΛCDM

$$C_\ell^{EB,{\rm o}} = \frac{1}{2}\tan(4\beta)\left(C_\ell^{EE,{\rm o}} - C_\ell^{BB,{\rm o}}\right)$$

Base of most methodologies applied in the past

Cosmic birefringence

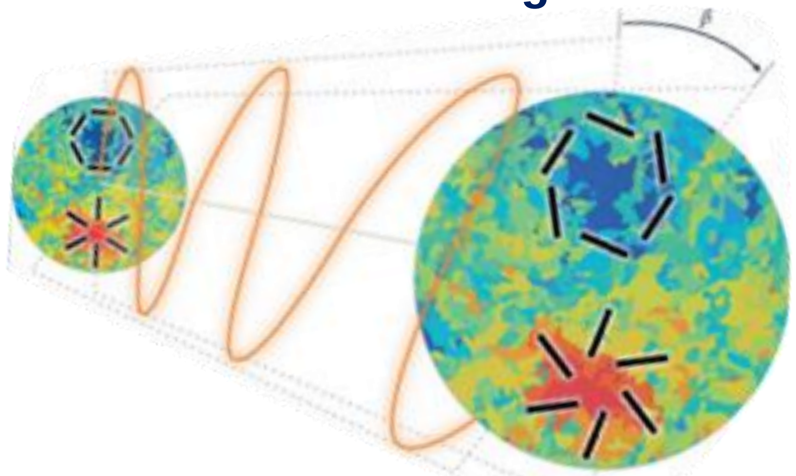

©Y. Minami

OR

Miscalibration of the detector's polarisation angle

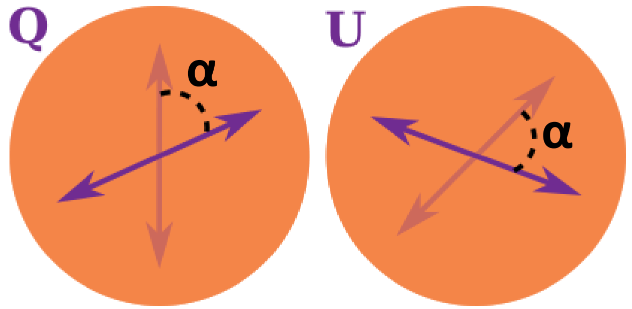

Unknown α miscalibration
Completely degenerate with birefringence

Krachmalnicoff+[arXiv:2111.09140]

The observed signal is actually

$$\begin{pmatrix} E^{\rm o}_{\ell m} \\ B^{\rm o}_{\ell m} \end{pmatrix} = \begin{pmatrix} \cos(2\alpha+2\beta) & -\sin(2\alpha+2\beta) \\ \sin(2\alpha+2\beta) & \cos(2\alpha+2\beta) \end{pmatrix} \begin{pmatrix} E^{\rm cmb}_{\ell m} \\ B^{\rm cmb}_{\ell m} \end{pmatrix}$$

so that EB yields α+β

$$C_\ell^{EB,{\rm o}} = \frac{1}{2}\tan(4\alpha+4\beta)\left(C_\ell^{EE,{\rm o}} - C_\ell^{BB,{\rm o}}\right)$$

Cosmic birefringence

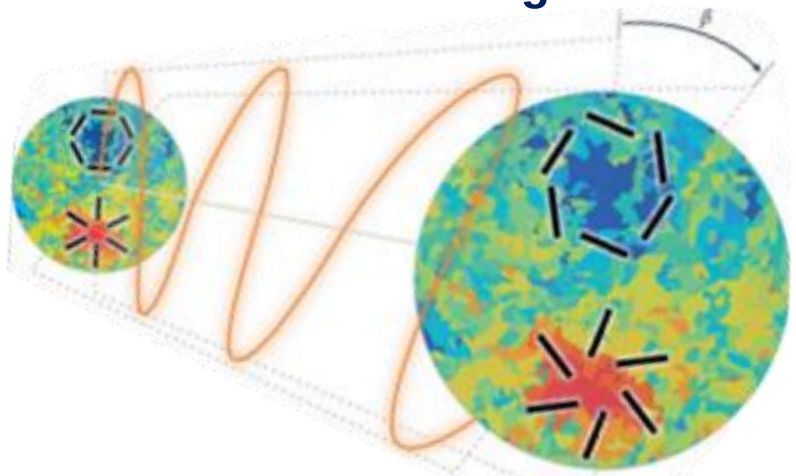

©Y. Minami

OR

Miscalibration of the detector's polarisation angle

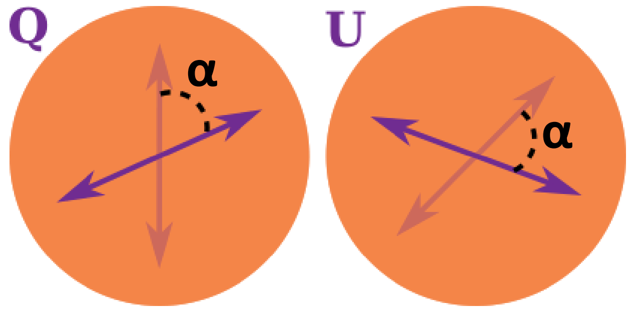

Unknown α miscalibration
Completely degenerate with birefringence

Krachmalnicoff+[arXiv:2111.09140]

The observed signal is actually

$$\begin{pmatrix} E^{\rm o}_{\ell m} \\ B^{\rm o}_{\ell m} \end{pmatrix} = \begin{pmatrix} \cos(2\alpha+2\beta) & -\sin(2\alpha+2\beta) \\ \sin(2\alpha+2\beta) & \cos(2\alpha+2\beta) \end{pmatrix} \begin{pmatrix} E^{\rm cmb}_{\ell m} \\ B^{\rm cmb}_{\ell m} \end{pmatrix}$$

so that EB yields α+β

$$C_\ell^{EB,{\rm o}} = \frac{1}{2}\tan(4\alpha+4\beta)\left(C_\ell^{EE,{\rm o}} - C_\ell^{BB,{\rm o}}\right)$$

Requires absolute calibration of instrumental polarisation angles

Previous measurements limited to ≈ 0.5°- 1°

QUaD Wu+[arXiv:0811.0618]	β = 0.55° ± 0.82° (stat) ± 0.5° (sys)
WMAP 9-year Hinshaw+[arXiv:1212.5226]	β = - 0.36° ± 1.24° (stat) ± 1.5° (sys)
Planck 2016 *Planck* Collab [arXiv:1605.08633]	β = 0.31° ± 0.05° (stat) ± 0.28° (sys)

⋮

Cosmic birefringence

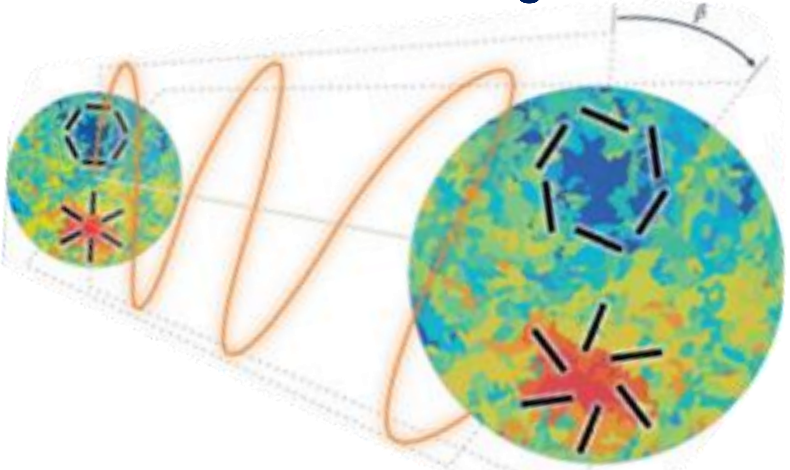

©Y. Minami

OR

Miscalibration of the detector's polarisation angle

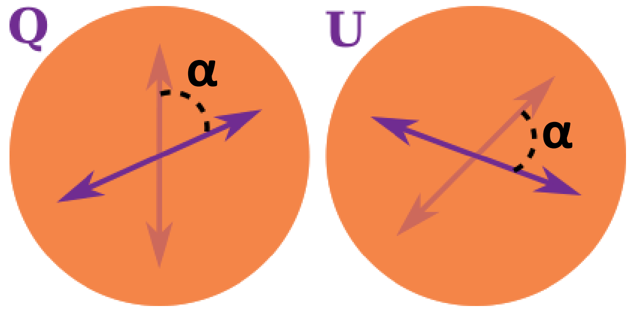

Unknown α miscalibration

Completely degenerate with birefringence

Krachmalnicoff+[arXiv:2111.09140]

Improved calibration strategies for upcoming data

Artificial calibrators:

- **Rotating polarised source**

  BICEP3 recently achieved ≈ 0.03° precision Cornelison+[arXiv:2207.14796]

  Exciting results coming soon!

Improved calibration strategies for upcoming data

Artificial calibrators:

- Rotating polarised source
  BICEP3 recently achieved ≈ 0.03° precision Cornelison+[arXiv:2207.14796]
  Exciting results coming soon!

- Drone/satellite carrying a polarised source
  Expected to reach ≈ 0.01° Nati+[arXiv:1704.02704], Casas-Reinares+[DOI:10.3390/s21103361]

Improved calibration strategies for upcoming data

Artificial calibrators:

- Rotating polarised source
  BICEP3 recently achieved ≈ 0.03° precision Cornelison+[arXiv:2207.14796]
  Exciting results coming soon!

- Drone/satellite carrying a polarised source
  Expected to reach ≈ 0.01° Nati+[arXiv:1704.02704], Casas-Reinares+[DOI:10.3390/s21103361]

Astrophysical calibrators:

- Crab Nebula
  Measured to 0.33° precision Ritacco+[arXiv:1804.09581], Aumont+[arXiv:1805.10475]

Improved calibration strategies for upcoming data

Artificial calibrators:

- Rotating polarised source
  BICEP3 recently achieved ≈ 0.03° precision Cornelison+[arXiv:2207.14796]
  Exciting results coming soon!

- Drone/satellite carrying a polarised source
  Expected to reach ≈ 0.01° Nati+[arXiv:1704.02704], Casas-Reinares+[DOI:10.3390/s21103361]

Astrophysical calibrators:

- Crab Nebula
  Measured to 0.33° precision Ritacco+[arXiv:1804.09581], Aumont+[arXiv:1805.10475]

- Galactic thermal dust emission Minami+[arXiv:1904.12440], Minami&Komatsu[arXiv:2011.11254]

$$\beta = -\frac{1}{2} g_{\phi\gamma} \int \frac{\partial \phi}{\partial t} dt$$

Galactic foreground emission should not be significantly affected by birefringence

Use foregrounds as our calibrator

Minami+[arXiv:1904.12440]
Minami&Komatsu[arXiv:2006.15982]

$$\beta = -\frac{1}{2} g_{\phi\gamma} \int \frac{\partial \phi}{\partial t} dt$$

Galactic foreground emission should not be significantly affected by birefringence

Use foregrounds as our calibrator

Minami+[arXiv:1904.12440]
Minami&Komatsu[arXiv:2006.15982]

Observed signal is a rotation of the CMB and Galactic foreground emissions

$$\begin{pmatrix} E^{\rm o}_{\ell m} \\ B^{\rm o}_{\ell m} \end{pmatrix} = \begin{pmatrix} \cos(2\alpha) & -\sin(2\alpha) \\ \sin(2\alpha) & \cos(2\alpha) \end{pmatrix} \begin{pmatrix} E^{\rm fg}_{\ell m} \\ B^{\rm fg}_{\ell m} \end{pmatrix} + \begin{pmatrix} \cos(2\alpha+2\beta) & -\sin(2\alpha+2\beta) \\ \sin(2\alpha+2\beta) & \cos(2\alpha+2\beta) \end{pmatrix} \begin{pmatrix} E^{\rm cmb}_{\ell m} \\ B^{\rm cmb}_{\ell m} \end{pmatrix}$$

so the observed EB angular power spectrum is

$$C_\ell^{EB,{\rm o}} = \frac{\tan(4\alpha)}{2}\left(C_\ell^{EE,{\rm o}} - C_\ell^{BB,{\rm o}}\right) + \frac{1}{\cos(4\alpha)} C_\ell^{EB,{\rm fg}} + \frac{\sin(4\beta)}{2\cos(4\alpha)}\left(C_\ell^{EE,{\rm cmb}} - C_\ell^{BB,{\rm cmb}}\right)$$

$$\beta = -\frac{1}{2} g_{\phi\gamma} \int \frac{\partial \phi}{\partial t} dt$$

Galactic foreground emission should not be significantly affected by birefringence

Use foregrounds as our calibrator

Minami+[arXiv:1904.12440]
Minami&Komatsu[arXiv:2006.15982]

Observed signal is a rotation of the CMB and Galactic foreground emissions

$$\begin{pmatrix} E^{\mathrm{o}}_{\ell m} \\ B^{\mathrm{o}}_{\ell m} \end{pmatrix} = \begin{pmatrix} \cos(2\alpha) & -\sin(2\alpha) \\ \sin(2\alpha) & \cos(2\alpha) \end{pmatrix} \begin{pmatrix} E^{\mathrm{fg}}_{\ell m} \\ B^{\mathrm{fg}}_{\ell m} \end{pmatrix} + \begin{pmatrix} \cos(2\alpha+2\beta) & -\sin(2\alpha+2\beta) \\ \sin(2\alpha+2\beta) & \cos(2\alpha+2\beta) \end{pmatrix} \begin{pmatrix} E^{\mathrm{cmb}}_{\ell m} \\ B^{\mathrm{cmb}}_{\ell m} \end{pmatrix}$$

so the observed EB angular power spectrum is

$$C_\ell^{EB,\mathrm{o}} = \frac{\tan(4\alpha)}{2}\left(C_\ell^{EE,\mathrm{o}} - C_\ell^{BB,\mathrm{o}}\right) + \frac{1}{\cos(4\alpha)} \boxed{C_\ell^{EB,\mathrm{fg}}} + \frac{\sin(4\beta)}{2\cos(4\alpha)}\left(C_\ell^{EE,\mathrm{cmb}} - C_\ell^{BB,\mathrm{cmb}}\right)$$

$$\beta = -\frac{1}{2} g_{\phi\gamma} \int \frac{\partial \phi}{\partial t} dt$$

Galactic foreground emission should not be significantly affected by birefringence

Use foregrounds as our calibrator

Minami+[arXiv:1904.12440]
Minami&Komatsu[arXiv:2006.15982]

Observed signal is a rotation of the CMB and Galactic foreground emissions

$$\begin{pmatrix} E^{\rm o}_{\ell m} \\ B^{\rm o}_{\ell m} \end{pmatrix} = \begin{pmatrix} \cos(2\alpha) & -\sin(2\alpha) \\ \sin(2\alpha) & \cos(2\alpha) \end{pmatrix} \begin{pmatrix} E^{\rm fg}_{\ell m} \\ B^{\rm fg}_{\ell m} \end{pmatrix} + \begin{pmatrix} \cos(2\alpha+2\beta) & -\sin(2\alpha+2\beta) \\ \sin(2\alpha+2\beta) & \cos(2\alpha+2\beta) \end{pmatrix} \begin{pmatrix} E^{\rm cmb}_{\ell m} \\ B^{\rm cmb}_{\ell m} \end{pmatrix}$$

so the observed EB angular power spectrum is

$$C_\ell^{EB,{\rm o}} = \frac{\tan(4\alpha)}{2}\left(C_\ell^{EE,{\rm o}} - C_\ell^{BB,{\rm o}}\right) + \frac{1}{\cos(4\alpha)} C_\ell^{EB,{\rm fg}} + \frac{\sin(4\beta)}{2\cos(4\alpha)}\left(C_\ell^{EE,{\rm cmb}} - C_\ell^{BB,{\rm cmb}}\right)$$

Synch EB statistically compatible with null

Martire+[arXiv:2110.12803]
QUIJOTE [arXiv:2301.05113]

$$\beta = -\frac{1}{2} g_{\phi\gamma} \int \frac{\partial \phi}{\partial t} dt$$

Galactic foreground emission should not be significantly affected by birefringence

Use foregrounds as our calibrator

Minami+[arXiv:1904.12440]
Minami&Komatsu[arXiv:2006.15982]

Observed signal is a rotation of the CMB and Galactic foreground emissions

$$\begin{pmatrix} E^{\mathrm{o}}_{\ell m} \\ B^{\mathrm{o}}_{\ell m} \end{pmatrix} = \begin{pmatrix} \cos(2\alpha) & -\sin(2\alpha) \\ \sin(2\alpha) & \cos(2\alpha) \end{pmatrix} \begin{pmatrix} E^{\mathrm{fg}}_{\ell m} \\ B^{\mathrm{fg}}_{\ell m} \end{pmatrix} + \begin{pmatrix} \cos(2\alpha+2\beta) & -\sin(2\alpha+2\beta) \\ \sin(2\alpha+2\beta) & \cos(2\alpha+2\beta) \end{pmatrix} \begin{pmatrix} E^{\mathrm{cmb}}_{\ell m} \\ B^{\mathrm{cmb}}_{\ell m} \end{pmatrix}$$

so the observed EB angular power spectrum is

$$C_\ell^{EB,\mathrm{o}} = \frac{\tan(4\alpha)}{2}\left(C_\ell^{EE,\mathrm{o}} - C_\ell^{BB,\mathrm{o}}\right) + \frac{1}{\cos(4\alpha)} C_\ell^{EB,\mathrm{fg}} + \frac{\sin(4\beta)}{2\cos(4\alpha)}\left(C_\ell^{EE,\mathrm{cmb}} - C_\ell^{BB,\mathrm{cmb}}\right)$$

Synch EB statistically compatible with null

Martire+[arXiv:2110.12803]
QUIJOTE [arXiv:2301.05113]

Misalignment between dust filaments and Galactic magnetic fields creates TB and EB correlations

Clark+[arXiv:2105.00120]
Cukierman+[arXiv:2208.07382]

***Planck* reported :**

- **Dust TB > 0**
- **A hint of dust EB > 0**

Planck Collab [arXiv:1801.04945]

Using dust as a calibrator, birefringence measurements are…

… robust against the miscalibration of polarisation angles and other systematics

… sensitive to dust EB

PDP+[arXiv:2201.07682]
PDP+[arXiv:2210.07655]

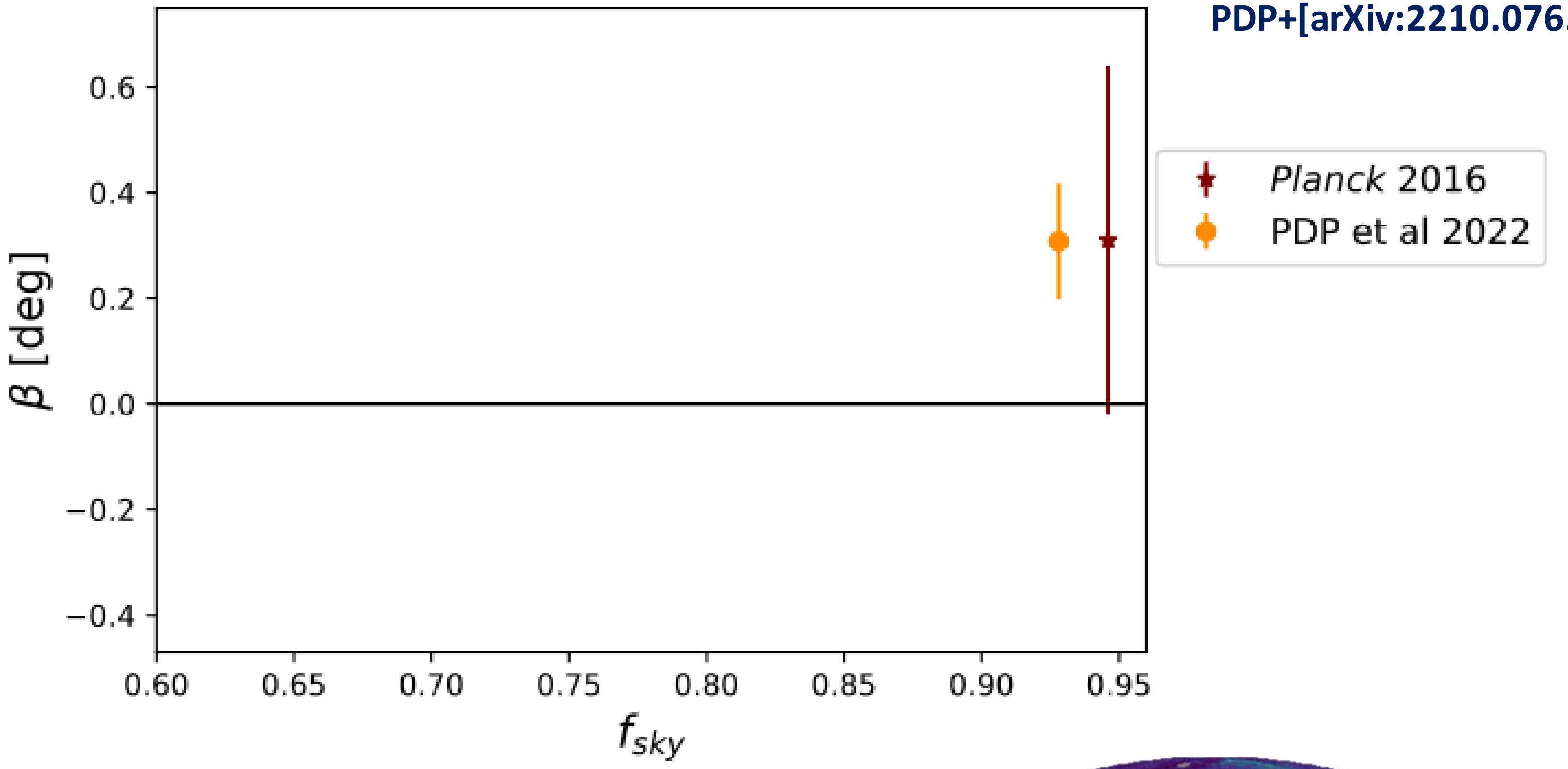

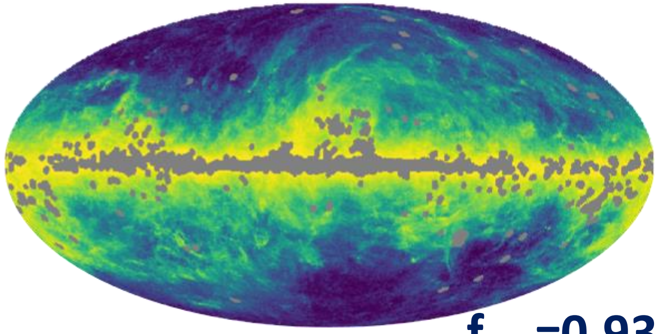

f_{sky}=0.93

Using dust as a calibrator, birefringence measurements are...

... robust against the miscalibration of polarisation angles and other systematics

... sensitive to dust EB

PDP+[arXiv:2201.07682]
PDP+[arXiv:2210.07655]

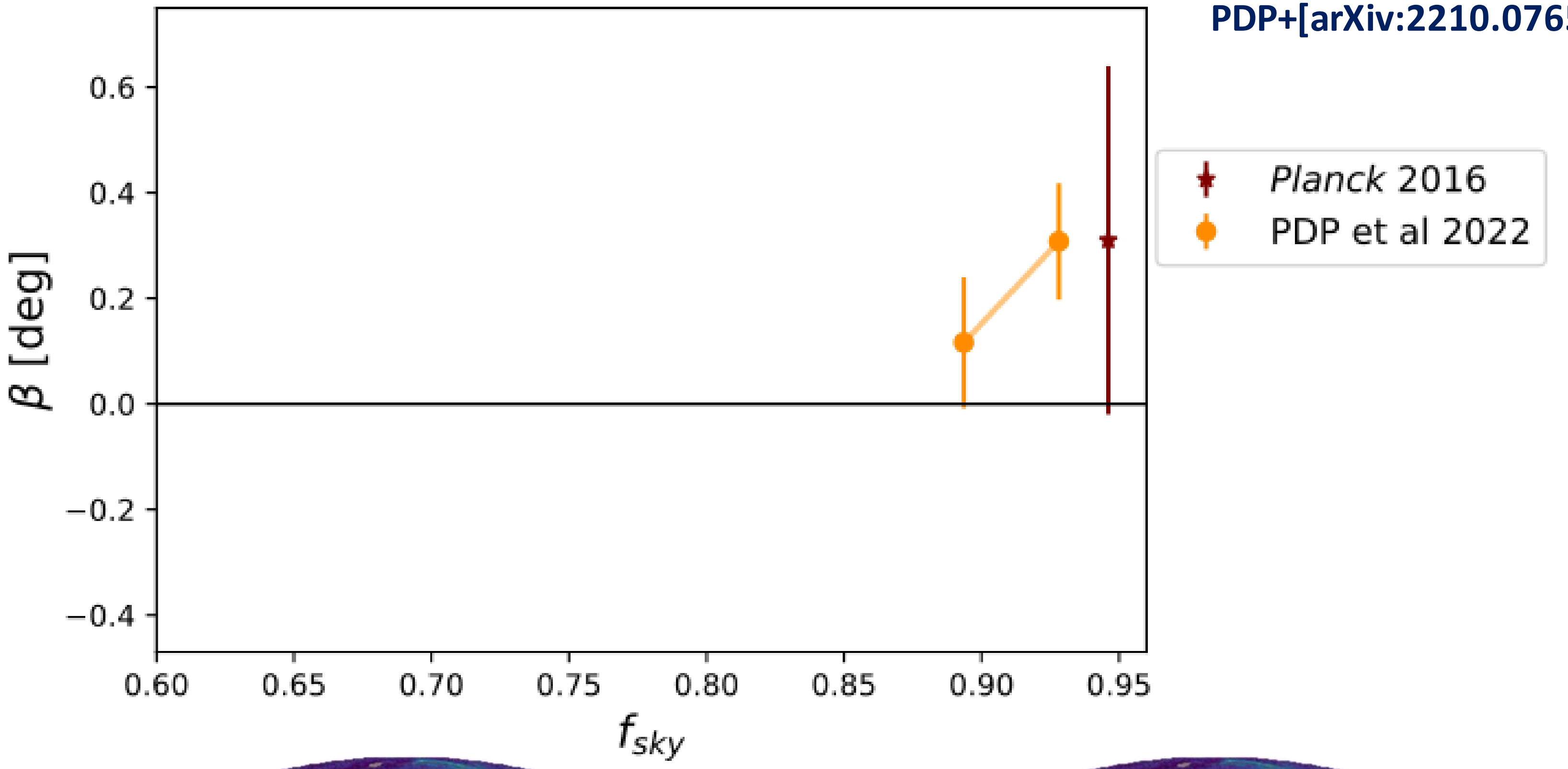

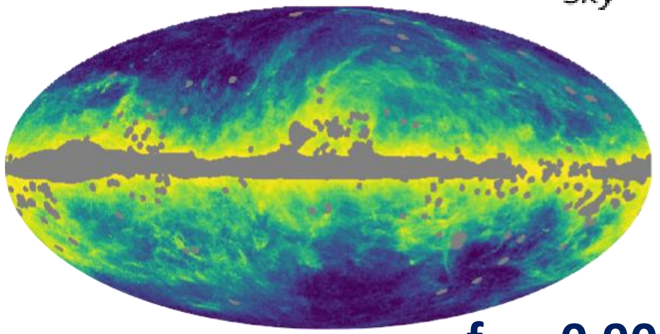

f_{sky}=0.90

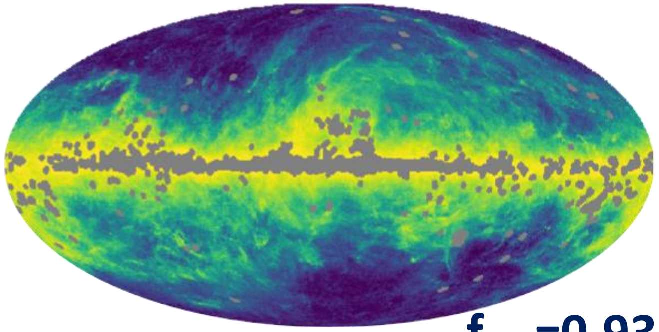

f_{sky}=0.93

Using dust as a calibrator, birefringence measurements are…

… robust against the miscalibration of polarisation angles and other systematics

… sensitive to dust EB

PDP+[arXiv:2201.07682]
PDP+[arXiv:2210.07655]

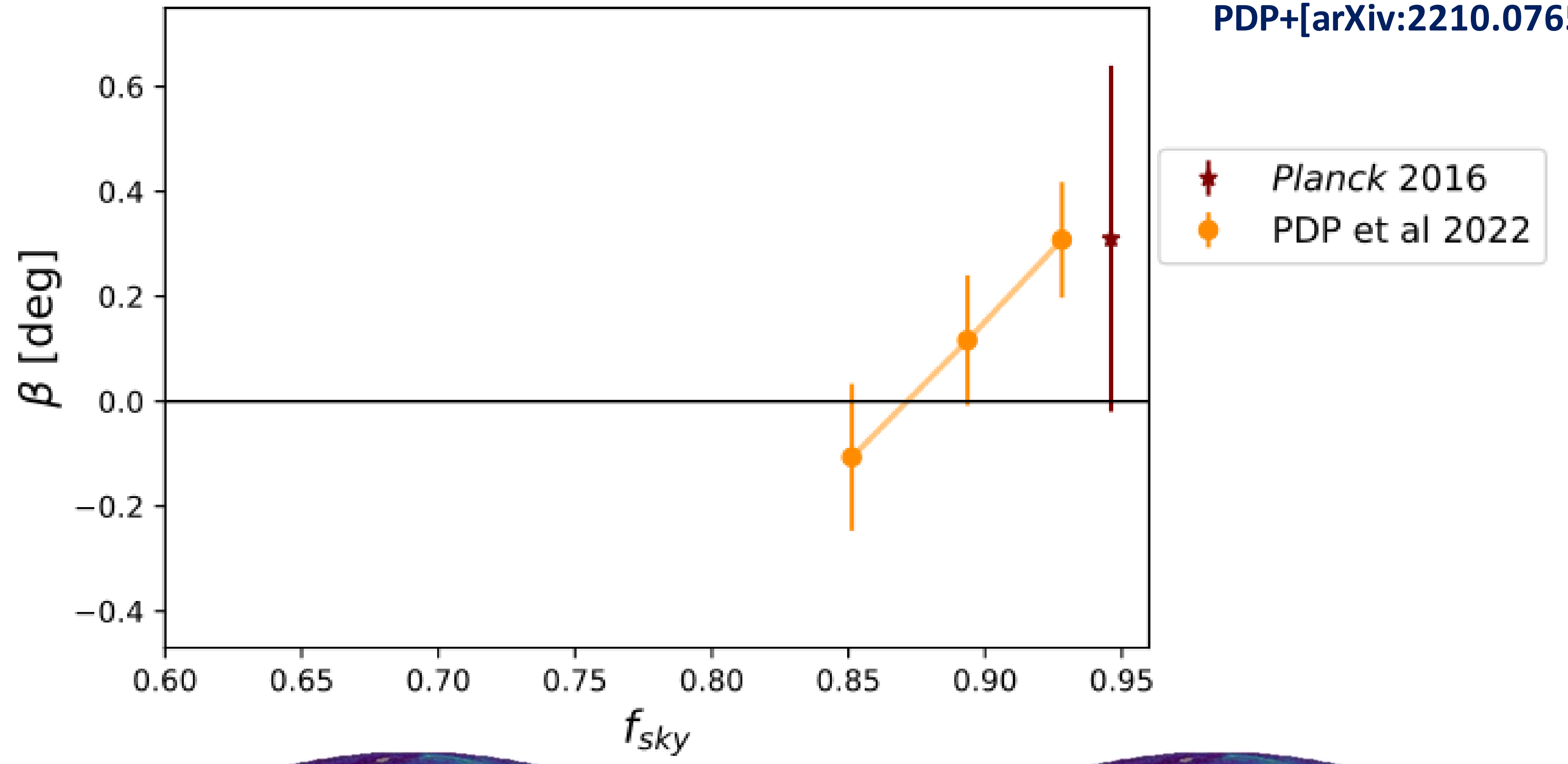

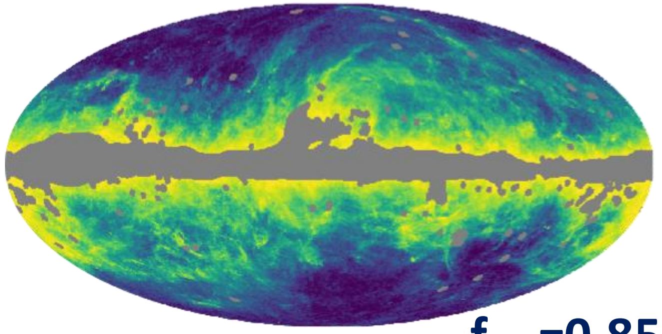

f_{sky}=0.85

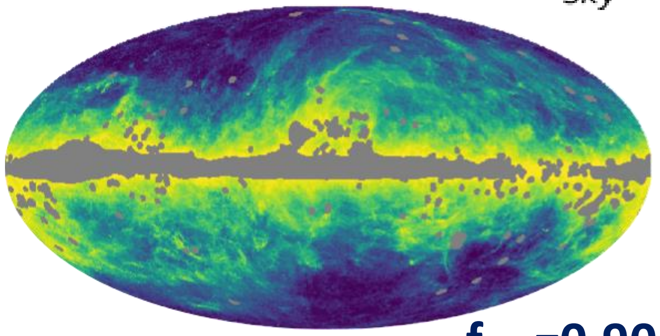

f_{sky}=0.90

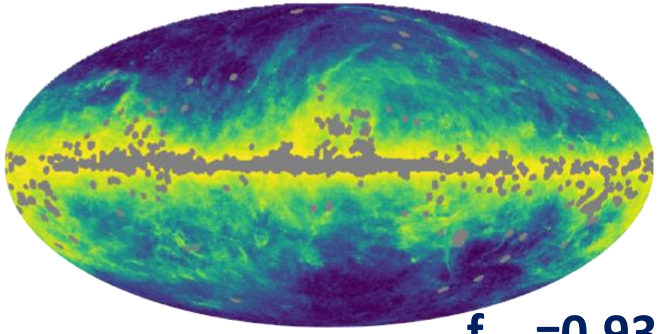

f_{sky}=0.93

Using dust as a calibrator, birefringence measurements are…

… robust against the miscalibration of polarisation angles and other systematics

… sensitive to dust EB

PDP+[arXiv:2201.07682]
PDP+[arXiv:2210.07655]

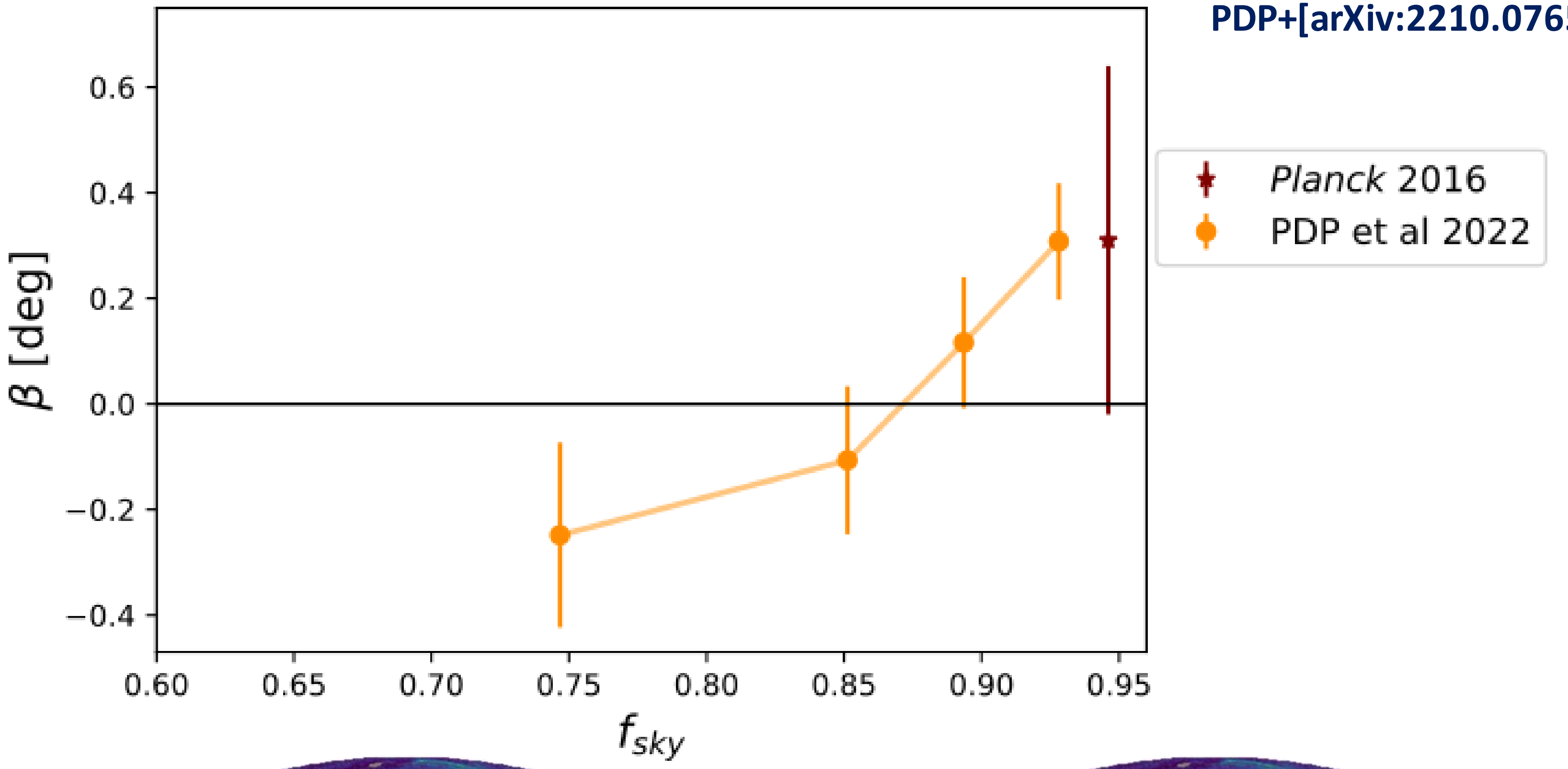

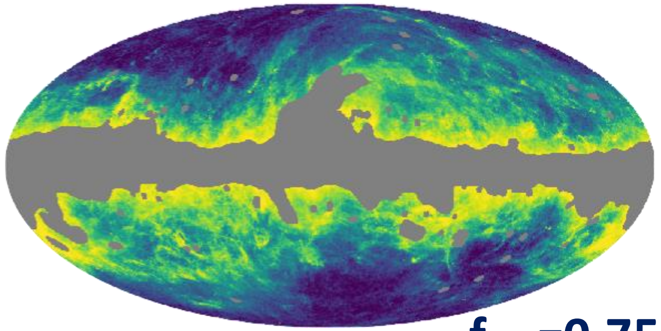

f_{sky}=0.75

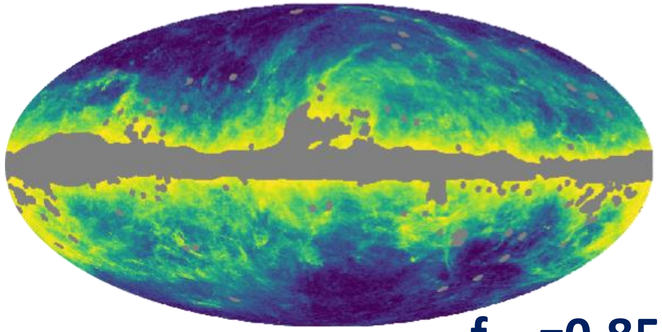

f_{sky}=0.85

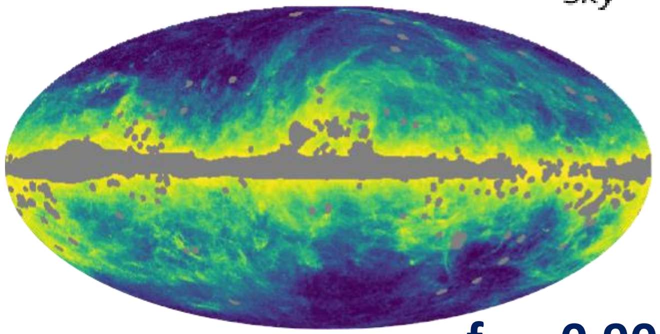

f_{sky}=0.90

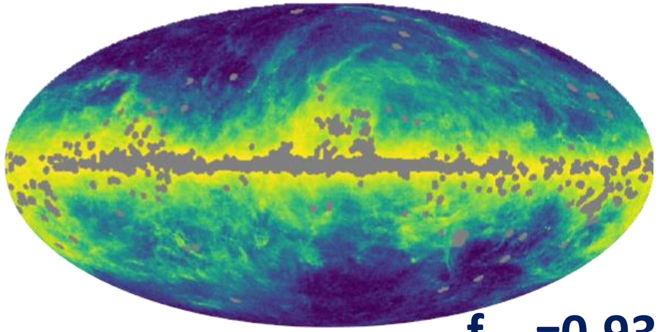

f_{sky}=0.93

Using dust as a calibrator, birefringence measurements are…

… robust against the miscalibration of polarisation angles and other systematics

… sensitive to dust EB

PDP+[arXiv:2201.07682]
PDP+[arXiv:2210.07655]

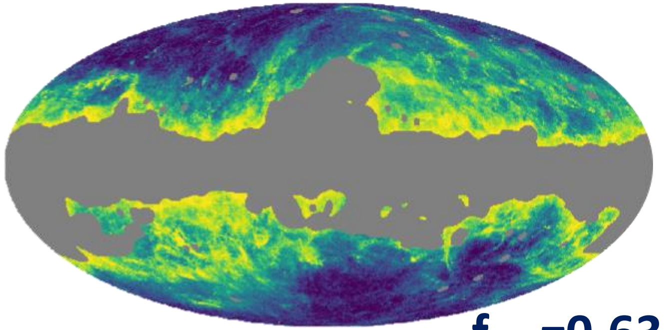

f_{sky}=0.63

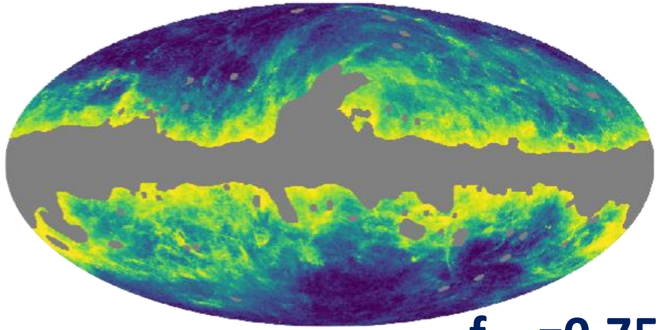

f_{sky}=0.75

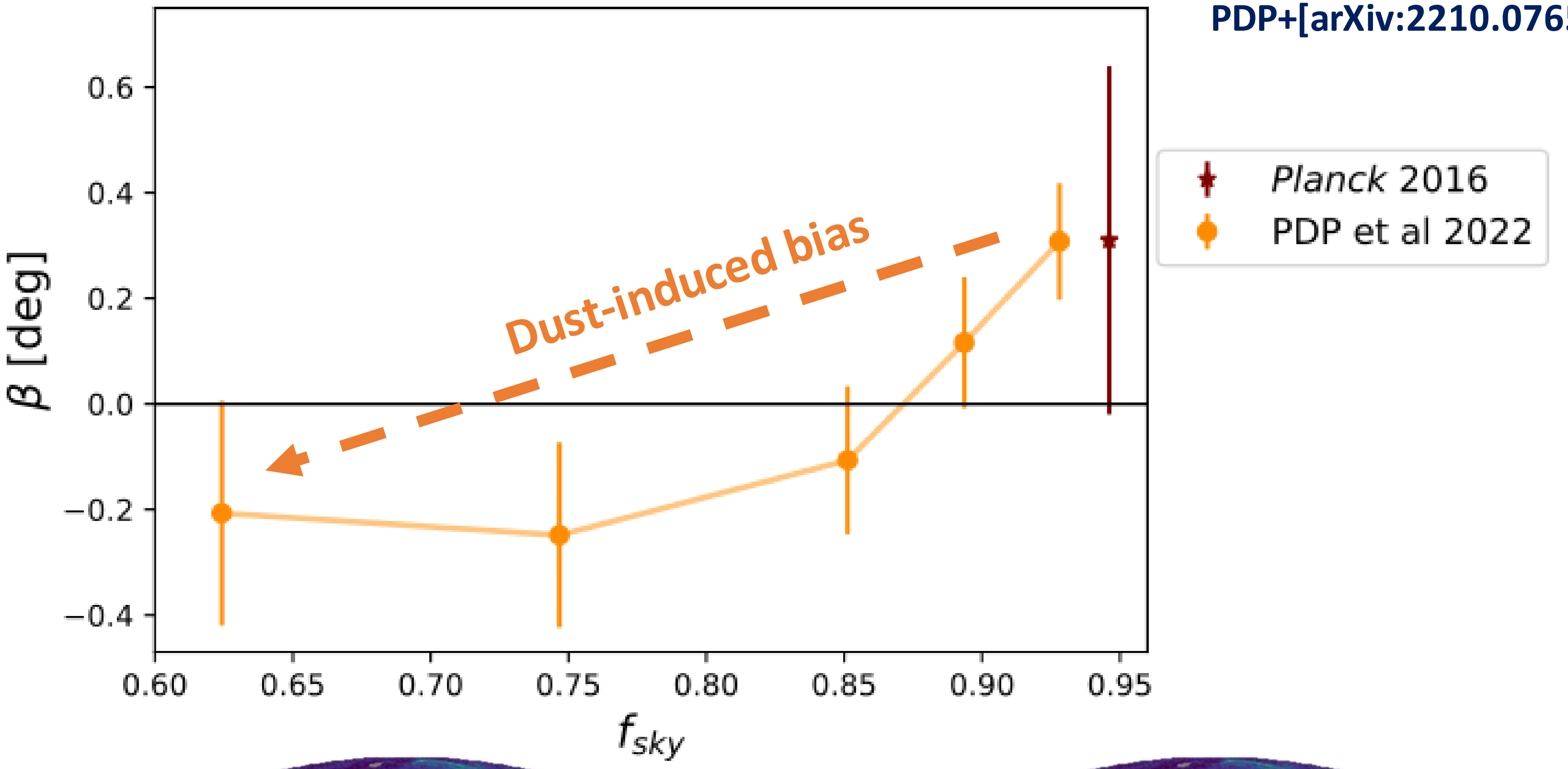

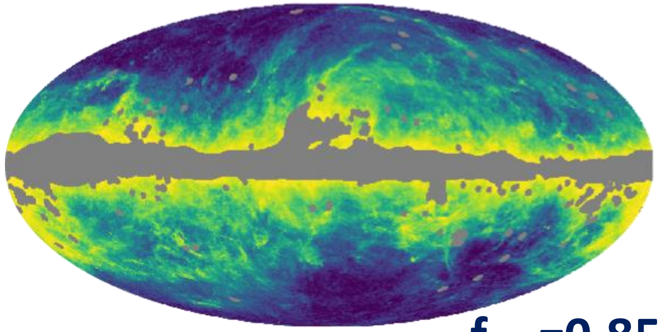

f_{sky}=0.85

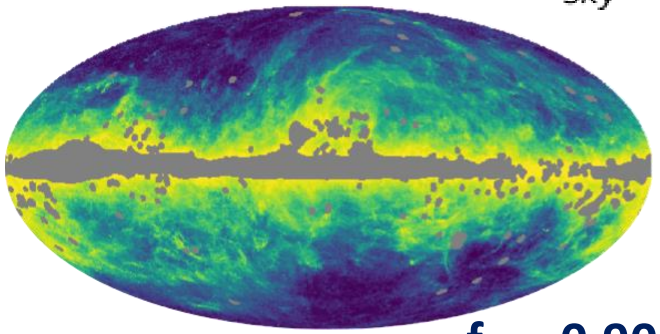

f_{sky}=0.90

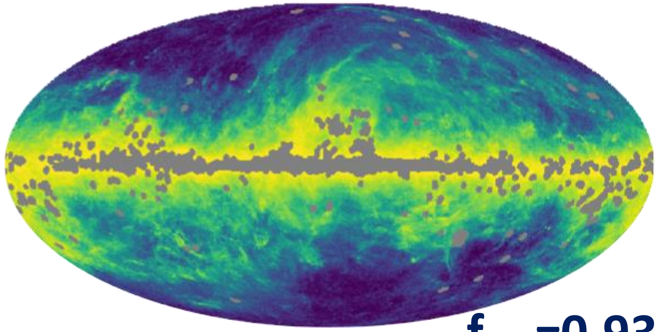

f_{sky}=0.93

Modeling dust EB

Misalignment ansatz to predict sign and amplitude of dust EB

$$C_\ell^{EB,\mathrm{dust}} \approx A_\ell C_\ell^{EE,\mathrm{dust}} \frac{C_\ell^{TB,\mathrm{dust}}}{C_\ell^{TE,\mathrm{dust}}}$$

Clark+[arXiv:2105.00120]
Cukierman+[arXiv:2208.07382]

Modeling dust EB

Misalignment ansatz to predict sign and amplitude of dust EB

$$C_\ell^{EB,\mathrm{dust}} \approx A_\ell C_\ell^{EE,\mathrm{dust}} \frac{C_\ell^{TB,\mathrm{dust}}}{C_\ell^{TE,\mathrm{dust}}}$$

Clark+[arXiv:2105.00120]
Cukierman+[arXiv:2208.07382]

Planck Collab [arXiv:1807.06208]

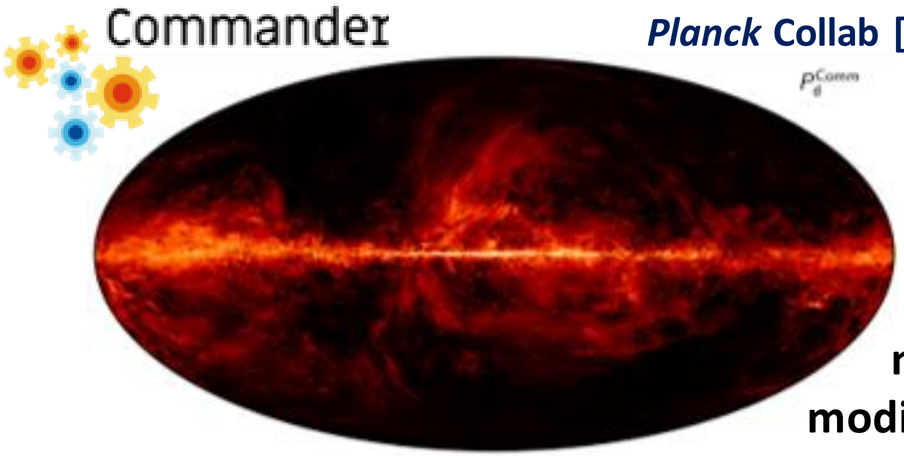

Parametric templates that model dust as a modified blackbody

Modeling dust EB

Misalignment ansatz to predict sign and amplitude of dust EB

$$C_\ell^{EB,\mathrm{dust}} \approx A_\ell C_\ell^{EE,\mathrm{dust}} \frac{C_\ell^{TB,\mathrm{dust}}}{C_\ell^{TE,\mathrm{dust}}}$$

Clark+[arXiv:2105.00120]
Cukierman+[arXiv:2208.07382]

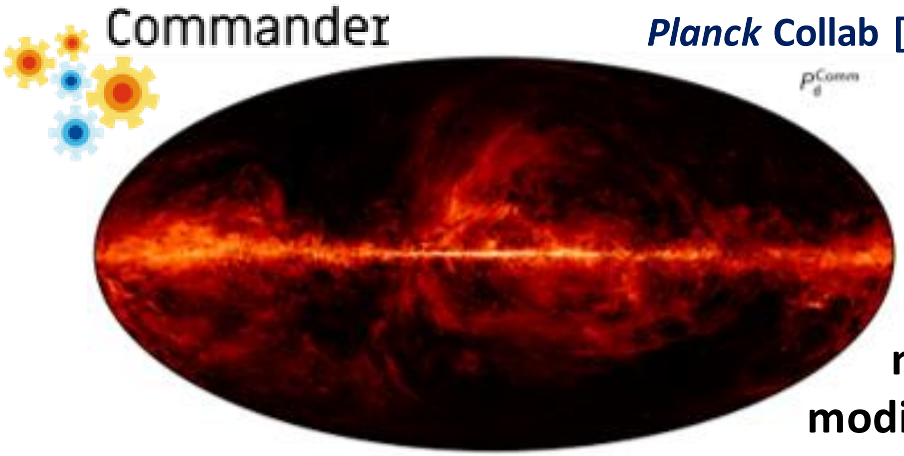

Planck Collab [arXiv:1807.06208]

Parametric templates that model dust as a modified blackbody

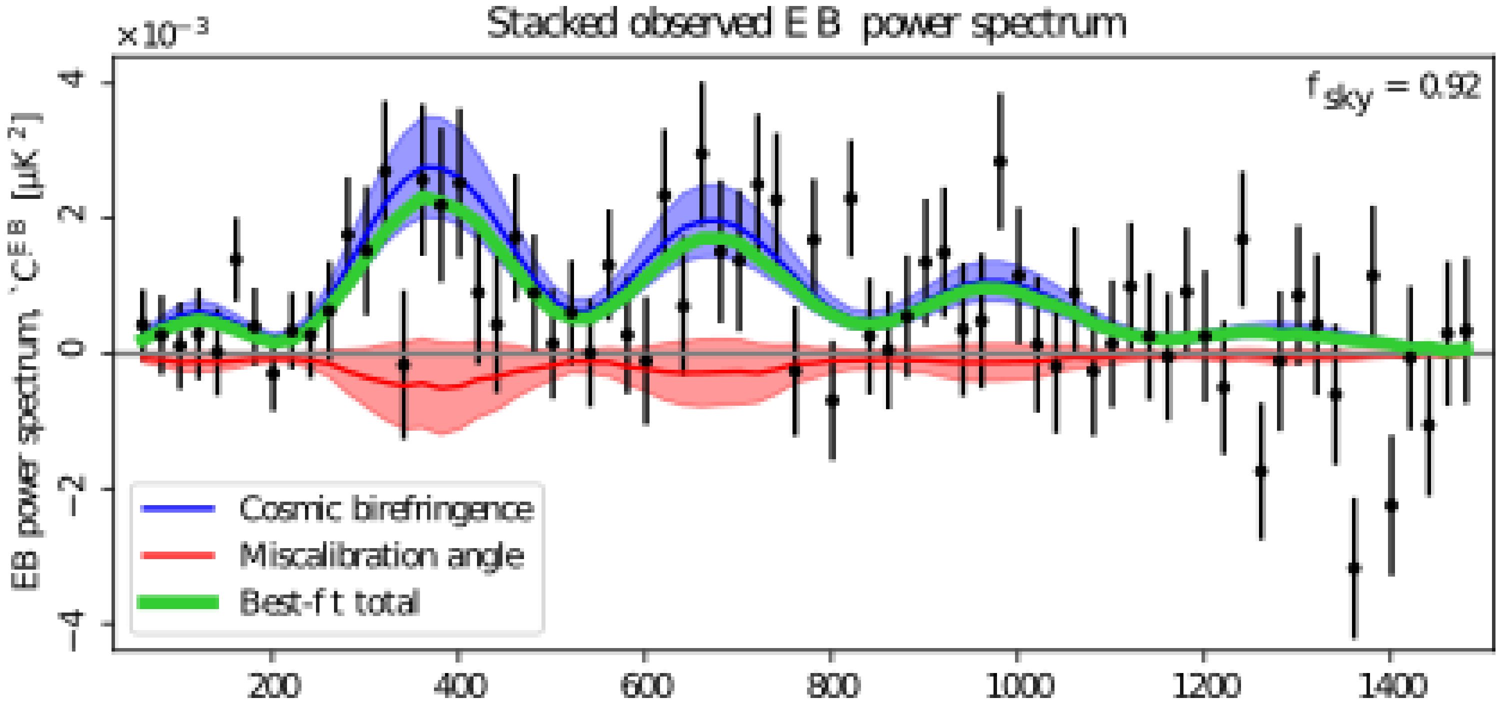

Eskilt&Komatsu [arXiv:2205.13962]

Joint analysis of *Planck* and WMAP data

Tightest constraint to date (3.6σ)

$$\beta = 0.342^\circ {}^{+0.094^\circ}_{-0.091^\circ}$$

favouring a **frequency-independent** rotation

Eskilt [arXiv:2201.13347]

Constraining power of CMB observations alone was the β ≈ 0.3° measurement confirmed

Fujita+[arXiv:2008.02473]

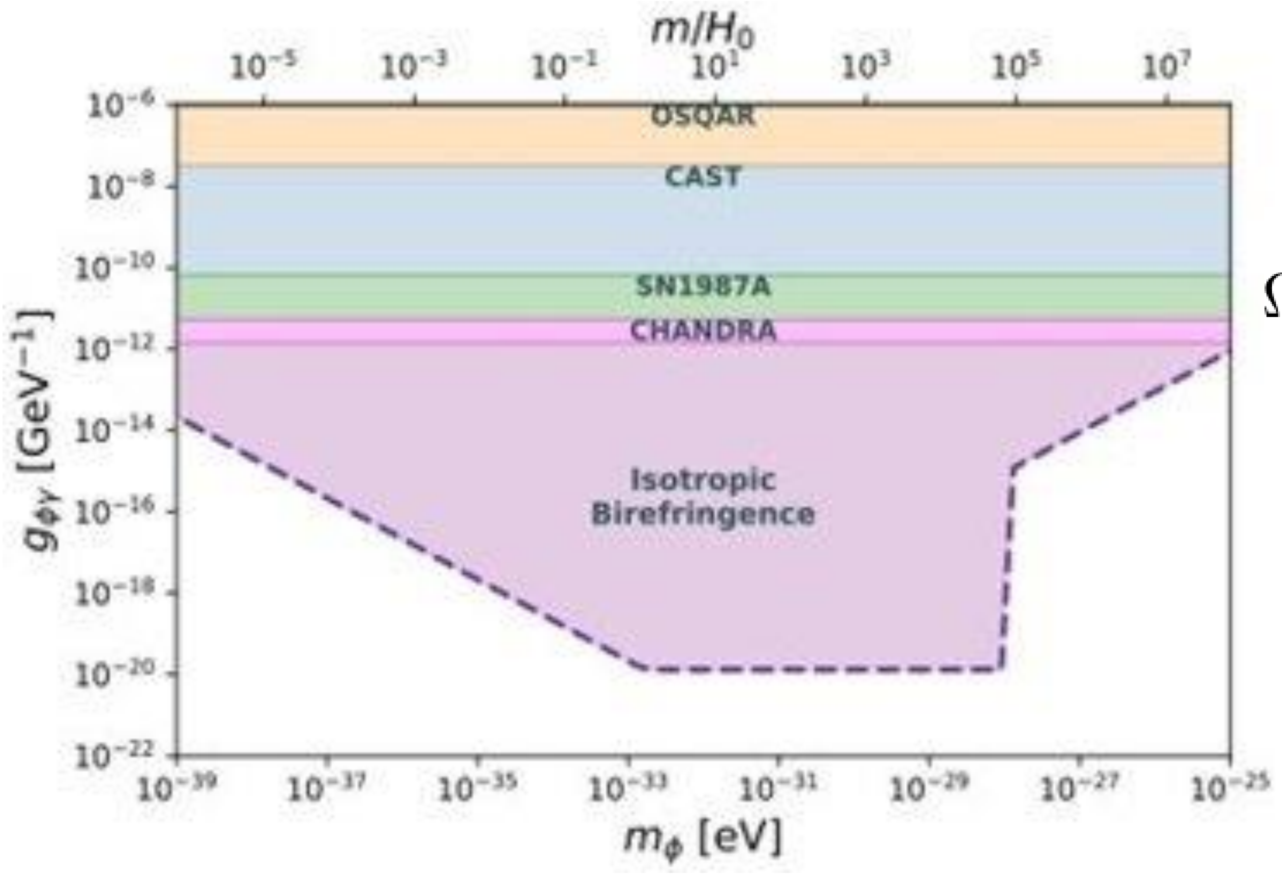

Assuming the largest ALP abundance allowed

$$\Omega_\phi \begin{cases} \Omega_\Lambda = 0.69 & m_\phi \le 9.26 \times 10^{-34}\mathrm{eV} \\ 0.006h^{-2} & 10^{-32}\mathrm{eV} \le m_\phi \le 10^{-25.5}\mathrm{eV} \end{cases}$$

Planck Collab [arXiv:1807.06209]

with ALP density only bounded from above, putting an upper constraint on the ALP-photon coupling is not possible

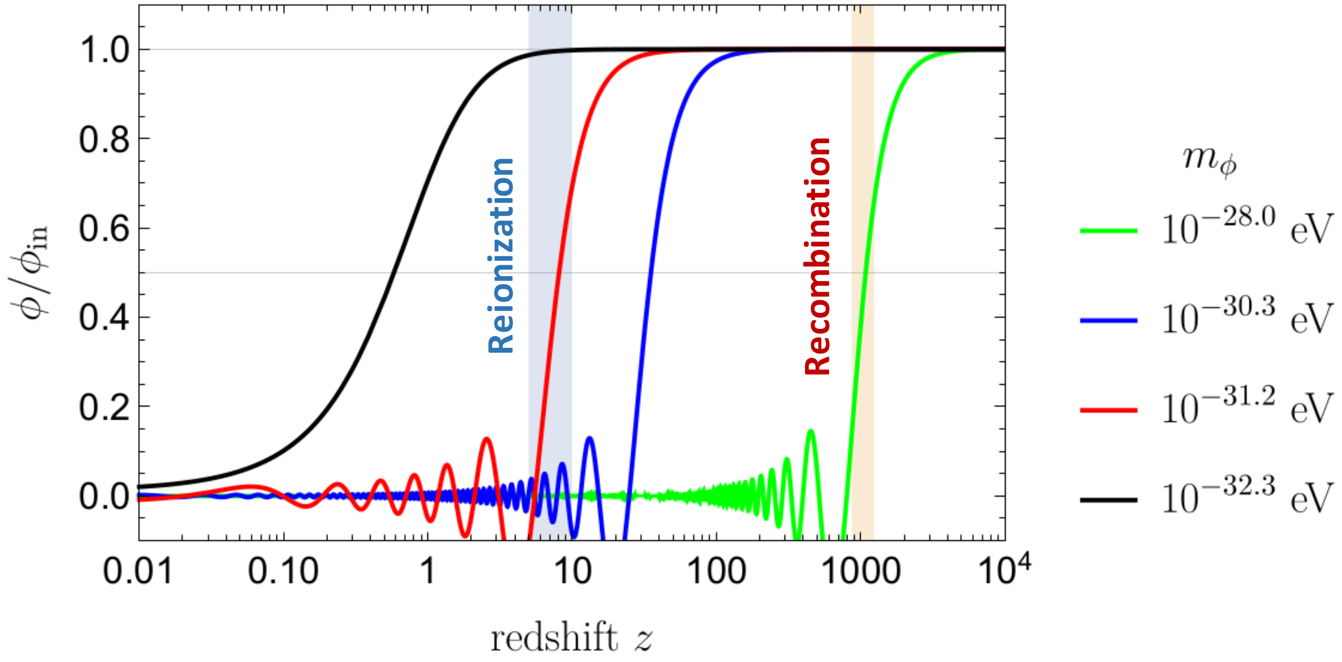

Nakatsuka+[arXiv:2203.08560]

$$\beta(z) = \begin{cases} 0 & \text{for} \quad z = 0 \\ \beta_{\rm rei} & \text{for} \quad 0 < z \leq 10 \\ \beta_{\rm rec} & \text{for} \quad 10 < z \end{cases} ,$$

Nakatsuka+[arXiv:2203.08560]

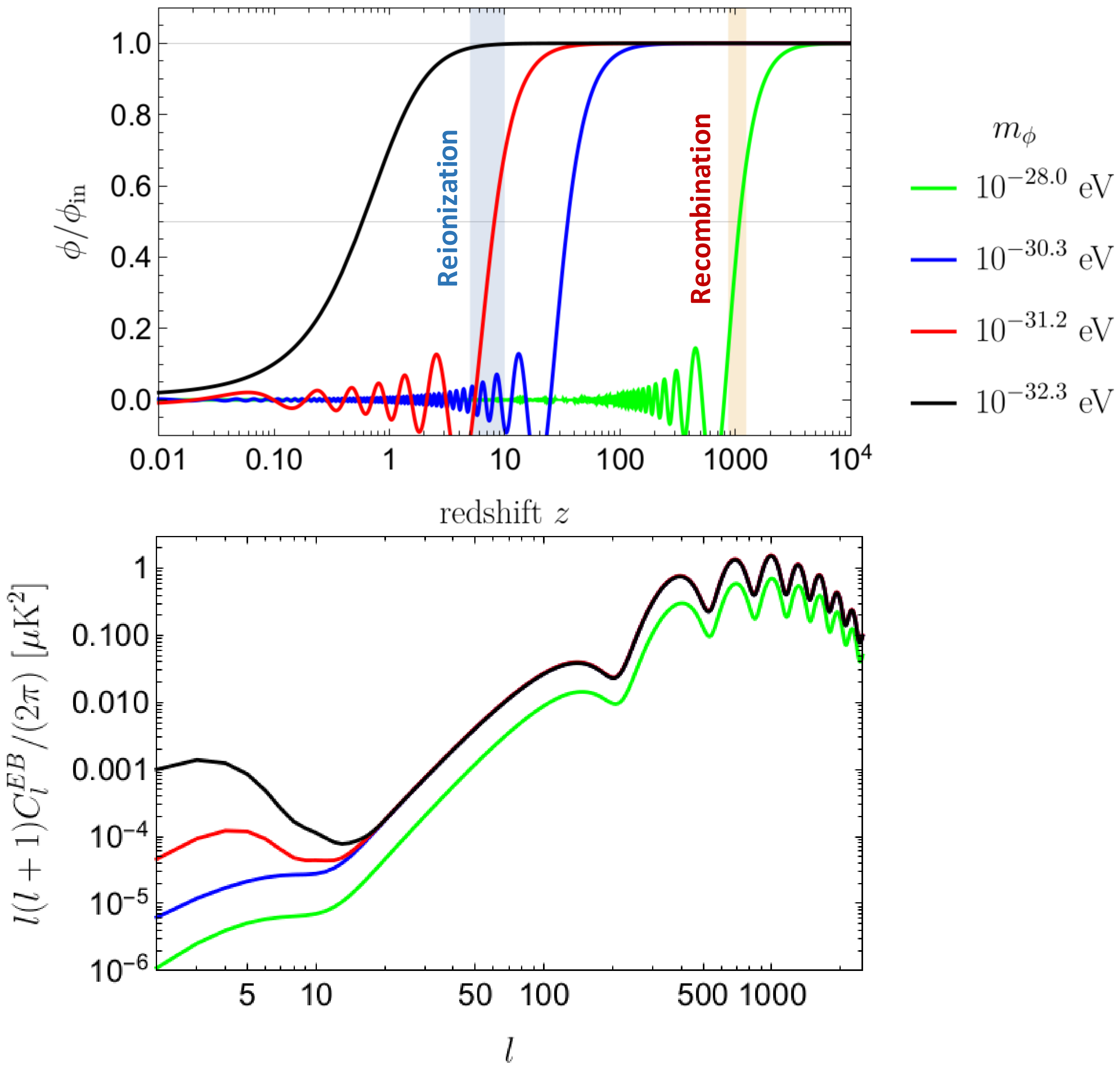

$$\beta(z) = \begin{cases} 0 & \text{for} \quad z = 0 \\ \beta_{\rm rei} & \text{for} \quad 0 < z \leq 10 \\ \beta_{\rm rec} & \text{for} \quad 10 < z \end{cases} ,$$

CMB photons emitted at recombination and reionization will suffer different rotations

$$C_\ell^{EB,\rm o} \approx \frac{1}{2}\sin(4\beta_{\rm rec})C_\ell^{E_{\rm rec}E_{\rm rec}} + \frac{1}{2}\sin(4\beta_{\rm rei})C_\ell^{E_{\rm rei}E_{\rm rei}} + \sin(2\beta_{\rm rec}+2\beta_{\rm rei})C_\ell^{E_{\rm rec}E_{\rm rei}}$$

The study of low-multipoles gives a tomographic view of the ALP field

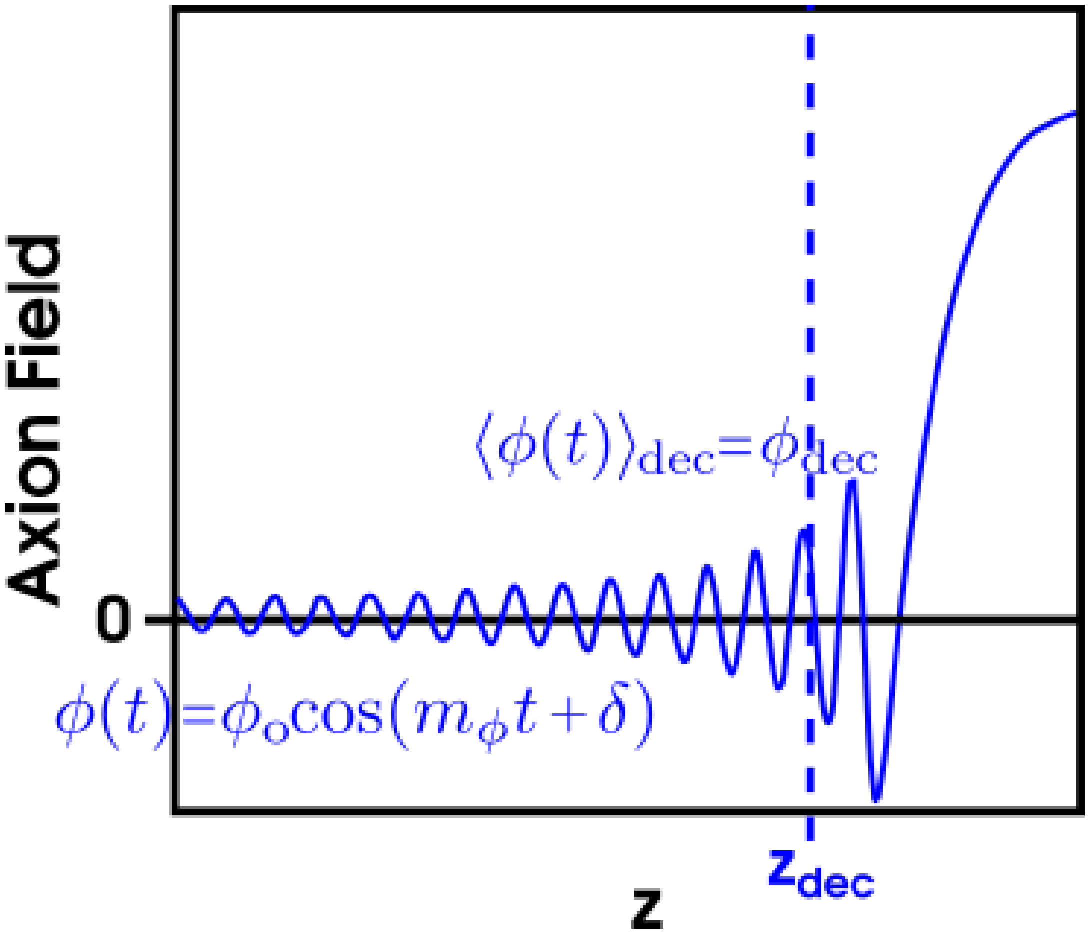

Suppose that ALP field is homogeneous and varies with time

$$m_\phi \geq H_{\rm dec}$$

For ALP to start oscillating before decoupling

$$\Rightarrow \quad 10^{-28}{\rm eV} \leq m_\phi$$

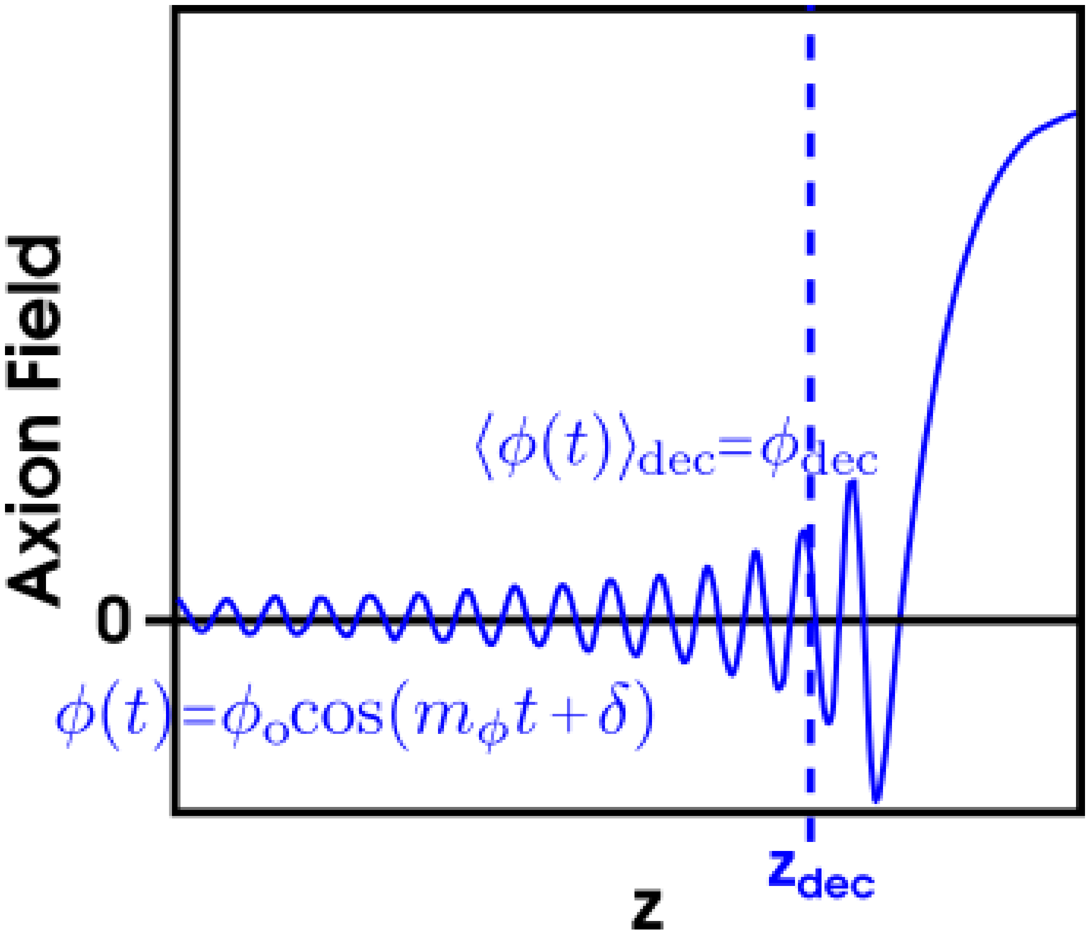

Suppose that ALP field is homogeneous and varies with time

$$m_\phi \geq H_{\rm dec}$$

For ALP to start oscillating before decoupling

$$10^{-28}{\rm eV} \leq m_\phi$$

$$(Q \pm iU)(t,\vec{n}) = J_0[g_{\phi\gamma}\phi_{\rm dec}]\exp[\mp 2i(\tfrac{g_{\phi\gamma}}{2}\phi_{\rm o}\cos(m_\phi t+\delta))](Q \pm iU)_0(\vec{n})$$

Fedderke+[arXiv:1903.02666]

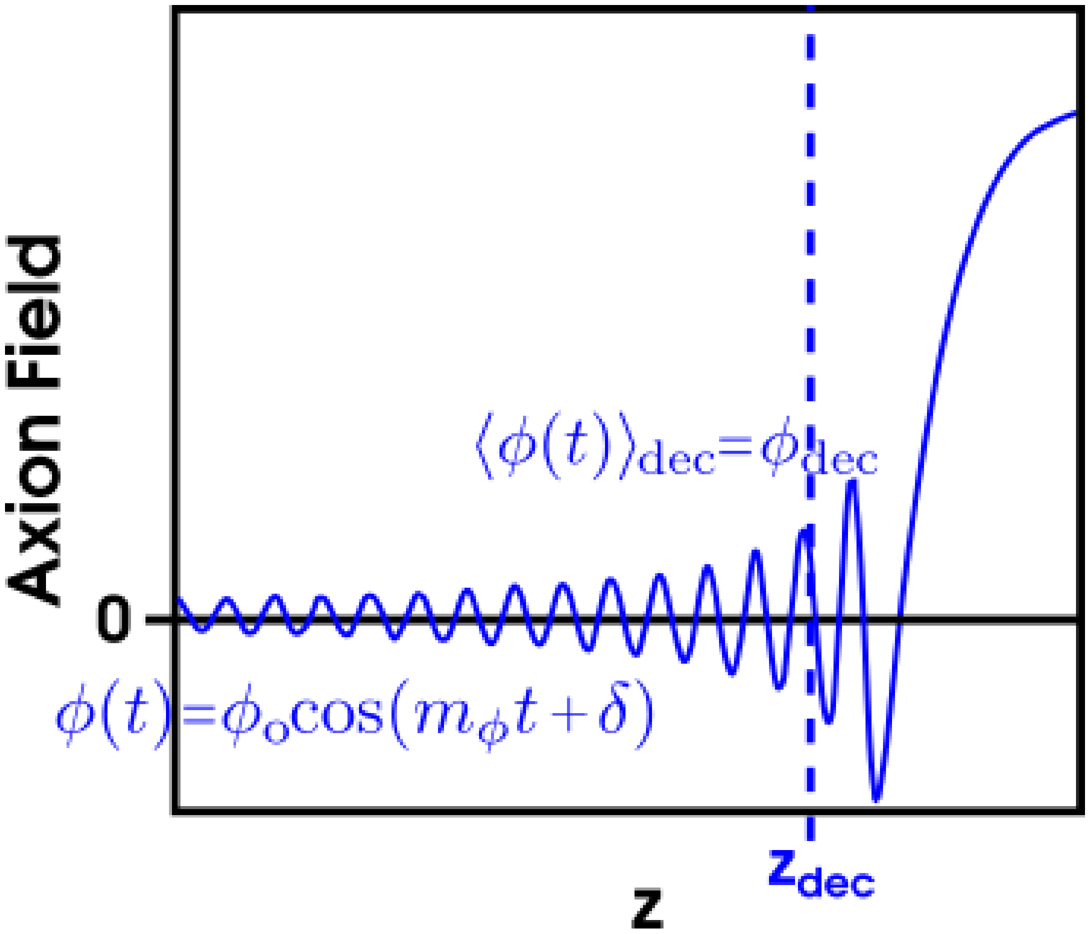

Suppose that ALP field is homogeneous and varies with time

$$m_\phi \geq H_{dec}$$

For ALP to start oscillating before decoupling

$$\Rightarrow \quad 10^{-28}\text{eV} \leq m_\phi$$

(Q,U) rotating as if the polarisation angle oscillated with a period

$$T_\phi \sim 1\text{y}\left(\frac{10^{-22}\text{eV}}{m_\phi}\right)$$

***Planck*, LiteBIRD** $\sim 1\text{y}$

BICEP/Keck, SPT $\sim 1\text{h}$

$$10^{-24}\text{eV} \leq m_\phi \leq 10^{-19}\text{eV}$$

Oscillation depending on ALP field at absorption

$$(Q \pm iU)(t,\vec{n}) = J_0[g_{\phi\gamma}\phi_{dec}]\exp[\mp 2i(\underbrace{\tfrac{g_{\phi\gamma}}{2}\phi_o\cos(m_\phi t+\delta)}))](Q \pm iU)_0(\vec{n})$$

Fedderke+[arXiv:1903.02666]

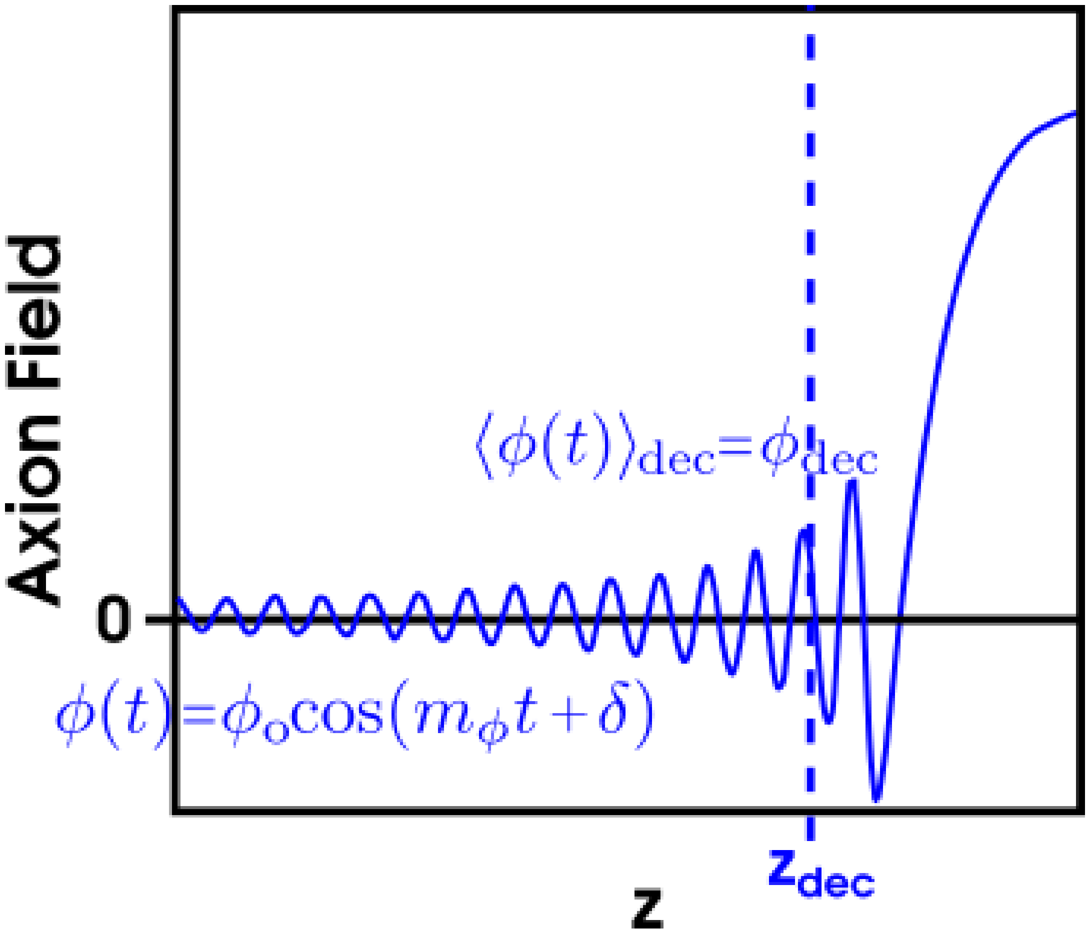

Suppose that ALP field is homogeneous and varies with time

$$m_\phi \geq H_{\rm dec}$$

For ALP to start oscillating before decoupling

$$\Rightarrow \quad 10^{-28}{\rm eV} \leq m_\phi$$

(Q,U) rotating as if the polarisation angle oscillated with a period

$$T_\phi \sim 1{\rm y}\left(\frac{10^{-22}{\rm eV}}{m_\phi}\right)$$

***Planck*, LiteBIRD** $\sim 1{\rm y}$

BICEP/Keck, SPT $\sim 1{\rm h}$

$$10^{-24}{\rm eV} \leq m_\phi \leq 10^{-19}{\rm eV}$$

Oscillation depending on ALP field at absorption

$$(Q \pm iU)(t,\vec{n}) = J_0[g_{\phi\gamma}\phi_{\rm dec}]\exp[\mp 2i(\tfrac{g_{\phi\gamma}}{2}\phi_o\cos(m_\phi t+\delta))](Q \pm iU)_0(\vec{n})$$

Washout depending on ALP field at emission

Fedderke+[arXiv:1903.02666]

Fedderke+[arXiv:1903.02666]

Washout is a consequence of decoupling not being an instantaneous process

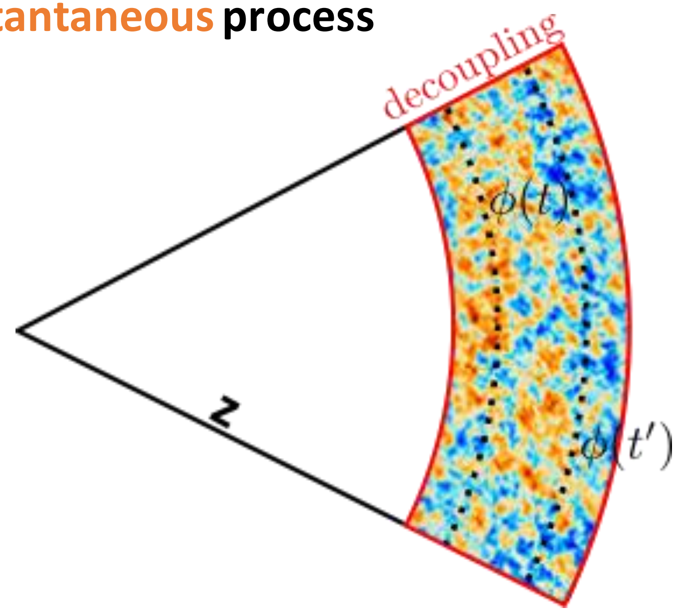

Fedderke+[arXiv:1903.02666]

Washout is a consequence of **decoupling not being an instantaneous** process

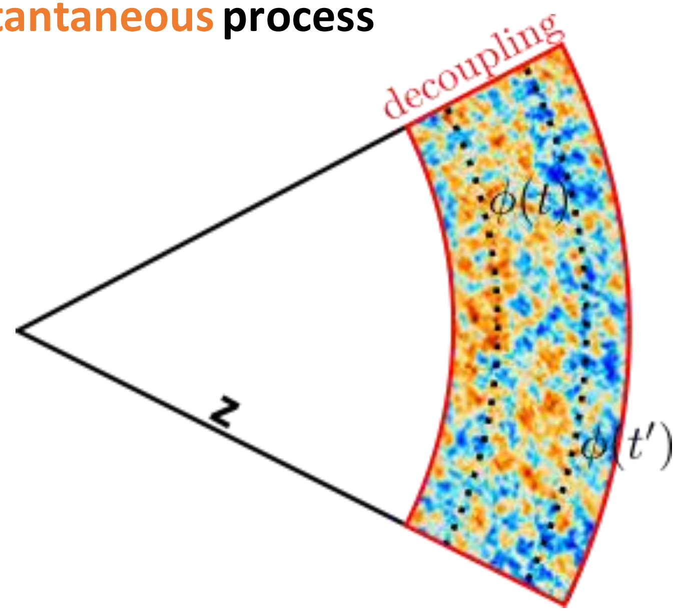

Photons emitted at different times…

… see a slightly different ALP field

… are rotated by a slightly different angle

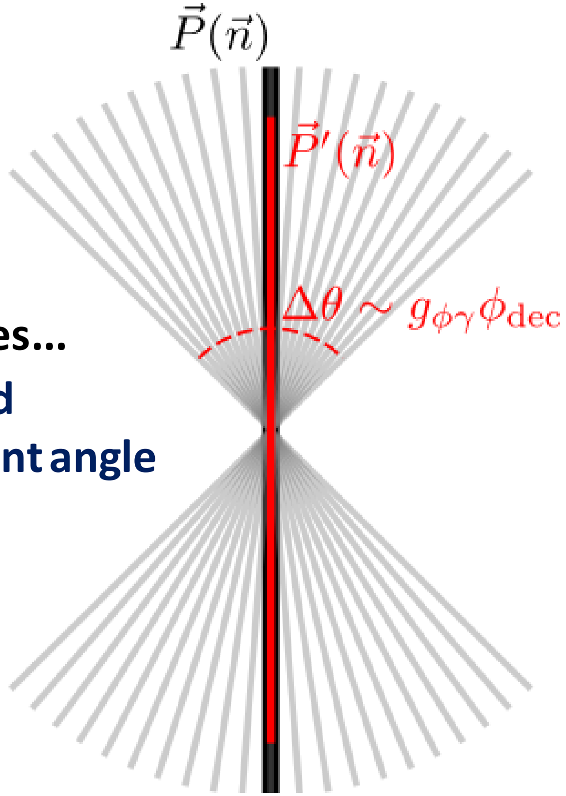

Fedderke+[arXiv:1903.02666]

Washout is a consequence of decoupling not being an instantaneous process

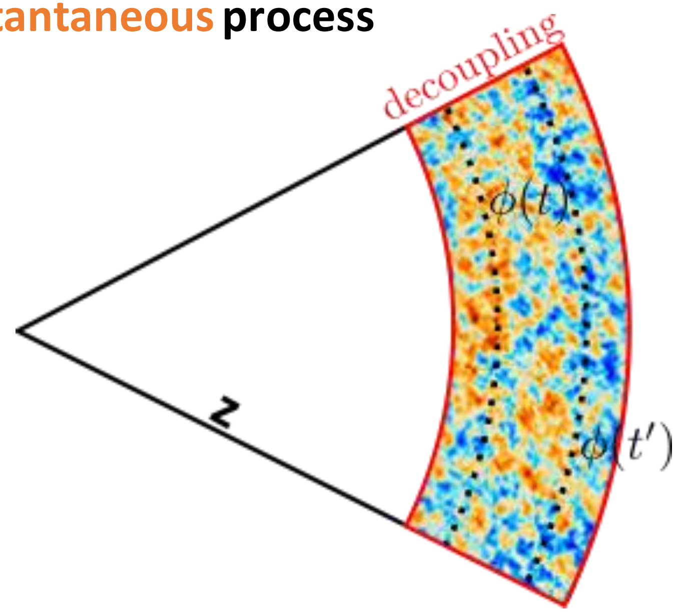

Photons emitted at different times…

… see a slightly different ALP field

… are rotated by a slightly different angle

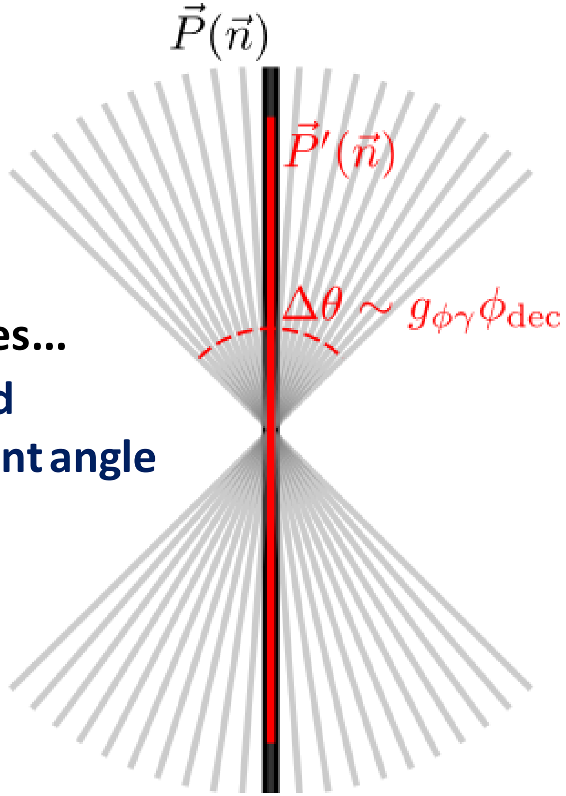

CMB detectors do an incoherent sum over the fanned-out states

Reduction of polarization intensity

$$J_0[g_{\phi\gamma}\phi_{\rm dec}] \approx 1 - \frac{1}{4}(g_{\phi\gamma}\phi_{\rm dec})^2$$

Constraints from time-dependent birefringence

Planck washout

Fedderke+[arXiv:1903.02666]

$$g_{\phi\gamma} \lesssim 9.6 \times 10^{-13}\,\mathrm{GeV}^{-1} \times \left(\frac{m_\phi}{10^{-21}\,\mathrm{eV}}\right) \times \left(\kappa \times \frac{\Omega_c^0 h^2}{0.11933}\right)^{-1/2}$$

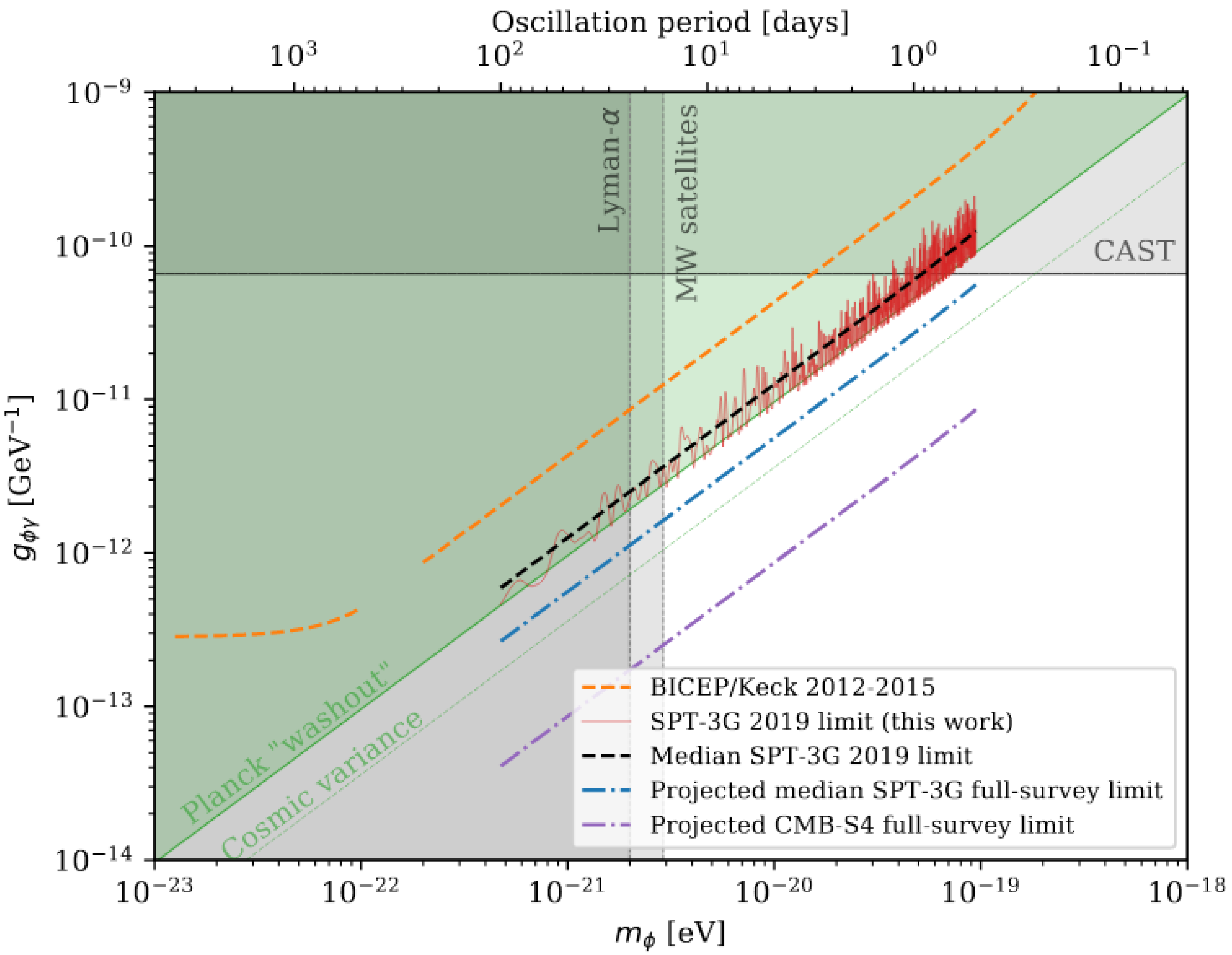

Constraints from time-dependent birefringence

Planck washout

Fedderke+[arXiv:1903.02666]

$$g_{\phi\gamma} \lesssim 9.6 \times 10^{-13}\,\mathrm{GeV}^{-1} \times \left(\frac{m_\phi}{10^{-21}\,\mathrm{eV}}\right) \times \left(\kappa \times \frac{\Omega_c^0 h^2}{0.11933}\right)^{-1/2}$$

SPT-3G data

Ferguson+[arXiv:2203.16567]

For periods 1 day ≤ T_φ ≤ 100 days …

… probing 10^{-22}eV ≤ m_φ ≤ 10^{-19}eV

… upper limit (β+α)(t) ≤ 0.071°

Assuming DM made of one ALP species with local density of 0.3 GeV/cm³

$$g_{\phi\gamma} < 1.18 \times 10^{-12}\ \mathrm{GeV}^{-1} \times \left(\frac{m_\phi}{1.0 \times 10^{-21}\ \mathrm{eV}}\right)$$

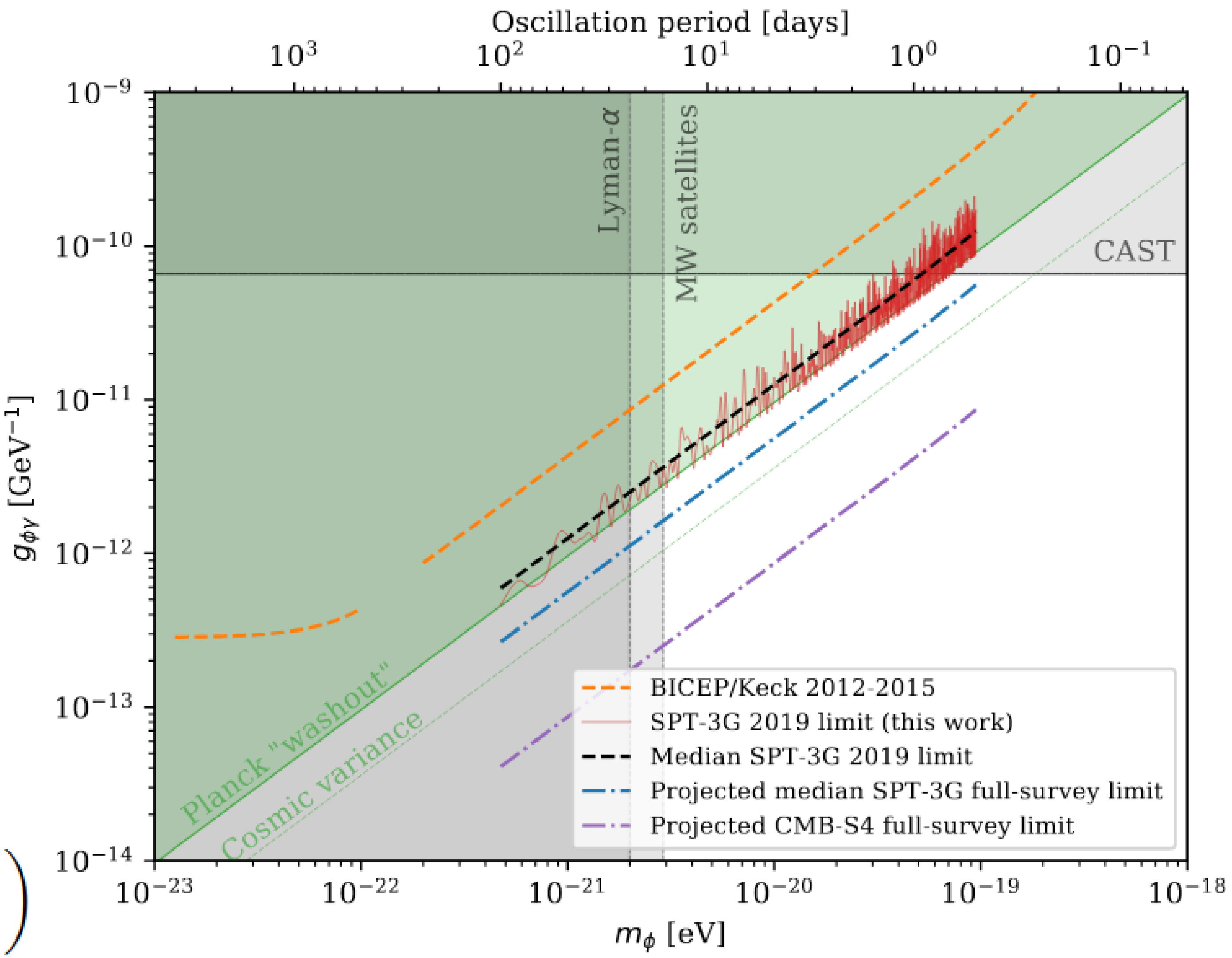

Outlook

From the CMB community side:

- High-precision CMB polarisation data is on the way

  SPT-3G, BICEP3, Simons Observatory, LiteBIRD...

- Improved artificial calibrators are being deployed

  Watch out for BICEP3 results!

- Working towards a better understanding and modeling of Galactic dust EB

Outlook

From the CMB community side:

- High-precision CMB polarisation data is on the way
  SPT-3G, BICEP3, Simons Observatory, LiteBIRD...
- Improved artificial calibrators are being deployed
  Watch out for BICEP3 results!
- Working towards a better understanding and modeling of Galactic dust EB

From you, COSMIC WISPers experts:

- How to get the most out of this data?
  Well-motivated models to test? Combination with other probes/observables?
- Coherent search combining birefringence with the gravitational effect of ULA

⋮

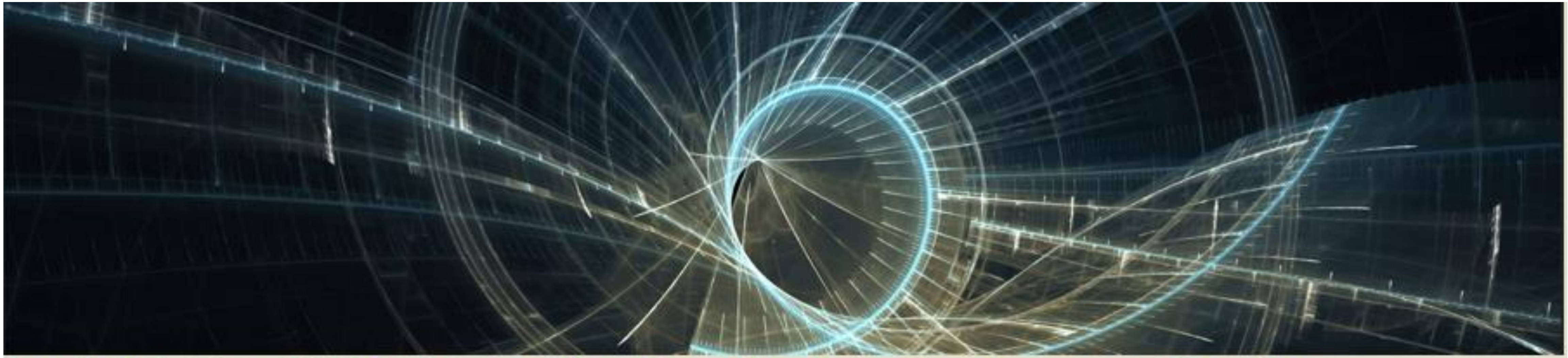

Dark Matter 2023: From the Smallest to the Largest Scales

May 29 – Jun 2, 2023

Discussing the latest developments in the field of dark matter, from experiments to theory and phenomenology

Registration is now open **until 18th May 2023**
Abstract submission is open **until 10th March 2023**

https://indico.ifca.es/event/2675/

Confirmed speakers include:

- Susmita Adhikari
- Kim Boddy
- Pierluca Carenza
- Katy Clough
- Pippa Cole
- Chris Conselice
- Graciela Gelmini
- Suchita Kulkarni
- Gaia Lanfranchi
- María Martínez

Backup slides

Based on...

- Minami et al 2019, PTEP, 083E02 — The original presentation of the methodology
- Minami 2020, PTEP, 063E01 — Extension to partial-sky observations
- Minami & Komatsu 2020, PTEP, 103E02 — Extension to frequency cross-spectra
- Minami & Komatsu 2020, PRL, 125, 221301 — Application to *Planck* HFI PR3
  - Without foreground modeling
- PDP et al 2022, PRL, 128, 091302 — Application to *Planck* HFI PR4
  - With foreground modeling
- Eskilt 2022, A&A, 662, A10 — Application to *Planck* LFI & HFI PR4
  - Study of the frequency dependence of birefringence
- Eskilt & Komatsu 2022, PRD, 106, 063503 — Joint analysis of *Planck* LFI & HFI PR4 and WMAP 9-year
- PDP et al 2022 [arXiv:2210.07655] Accepted at JCAP — Alternative semi-analytical implementation
  - Simulation study and assessment of the impact of systematics

Polarization primer

Cabella & Kamionkowski 2003 [arXiv:astro-ph/0403392]

Linearly polarized light propagating along the z direction

$$E_x = a_x \cos(\omega t - \delta_x) \quad E_y = a_y \cos(\omega t - \delta_y)$$

can be described through the Stoke's parameters

$$I = a_x^2 + a_y^2$$

$$Q = a_x^2 - a_y^2$$

$$U = 2 a_x a_y \cos(\delta_x - \delta_y)$$

Helmholtz's theorem

Express vector fields as the sum of curl-free and divergence-free fields

Q and U define a spin-2 field

$$P_{ab} = \frac{1}{2}\begin{pmatrix} Q(\vec{r}) & U(\vec{r}) \\ U(\vec{r}) & -Q(\vec{r}) \end{pmatrix}$$

Express the polarization field in terms of its gradient and curl components

$$\nabla^2 E = \partial_a \partial_b P_{ab} \quad \nabla^2 B = \epsilon_{ac} \partial_b \partial_c P_{ab}$$

Relative to the chosen coordinate system

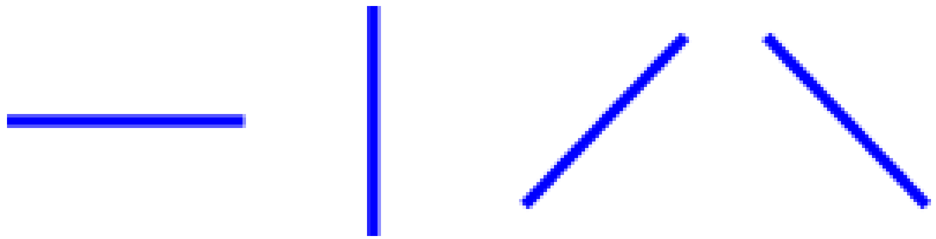

Q > 0	Q < 0	Q = 0	Q = 0
U = 0	U = 0	U > 0	U < 0

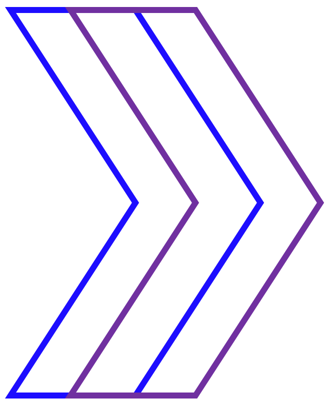

Locally independent

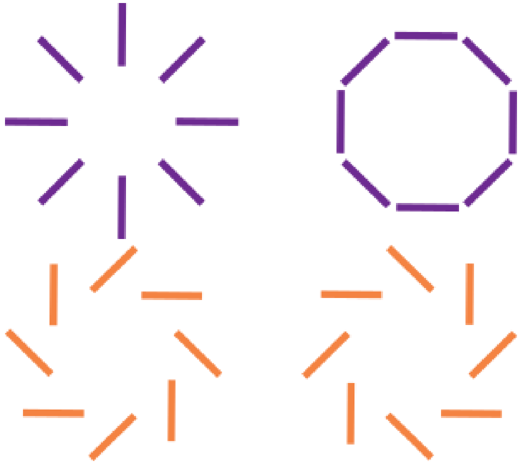

E-modes

B-modes

Decompose CMB maps into spherical harmonics

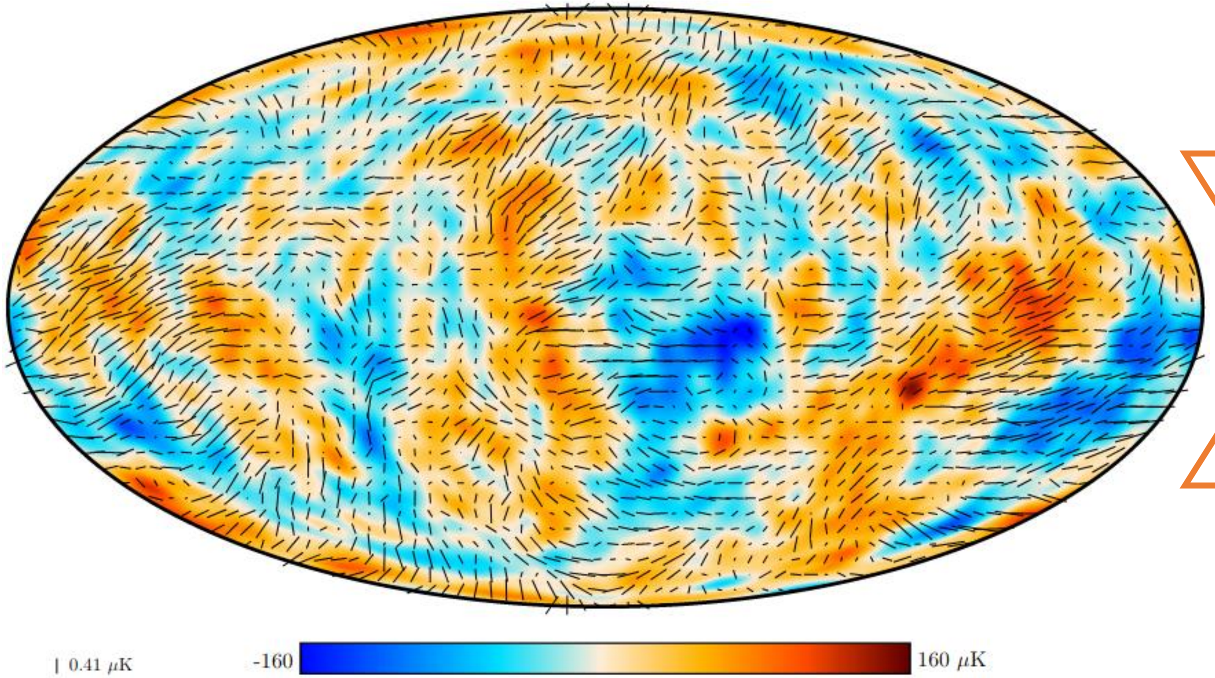

Planck Collaboration I. 2020, A&A, 641, A1

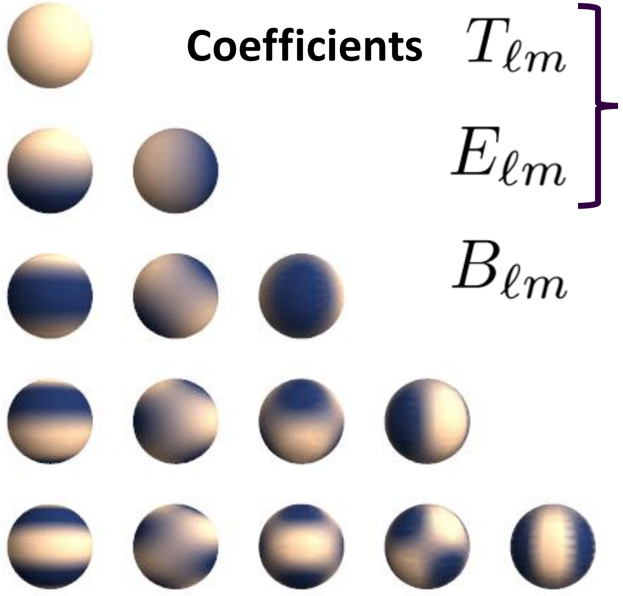

Coefficients $T_{\ell m}$, $E_{\ell m}$ — **Parity-even**

$B_{\ell m}$ — **Parity-odd**

Zaldarriaga & Seljak 1997, PRD, 55, 1830
Kamionkowski et al 1997, PRD, 55, 7368

Analyzing CMB polarization in terms of spherical harmonics

$$\langle E_{\ell m}E^*_{\ell' m'}\rangle = \delta_{mm'}\delta_{\ell\ell'}C_\ell^{EE}$$
$$\langle B_{\ell m}B^*_{\ell' m'}\rangle = \delta_{mm'}\delta_{\ell\ell'}C_\ell^{BB}$$
Parity-even

$$\langle E_{\ell m}B^*_{\ell' m'}\rangle = \delta_{mm'}\delta_{\ell\ell'}C_\ell^{EB}$$
Parity-odd

ΛCDM

The Universe has no preferred direction so the statistics of CMB anisotropies must be invariant under parity transformation

EB≠0 evidence of parity-violating physics

Lue et al 1999, PRL, 83, 1506

Past measurements

early WMAP & BOOMERANG	$\alpha+\beta$ = - 6.0° ± 4.0° (stat) ± ?? (sys)	Feng et al 2006, PRL, 96, 221302
QUaD	$\alpha+\beta$ = 0.55° ± 0.82° (stat) ± 0.5° (sys)	Wu et al 2009, PRL, 102, 161302
WMAP 9-year	$\alpha+\beta$ = - 0.36° ± 1.24° (stat) ± 1.5° (sys)	Hinshaw et al 2013, ApJS, 208, 19
Planck 2015	$\alpha+\beta$ = 0.31° ± 0.05° (stat) ± 0.28° (sys)	*Planck* Collaboration XLIX. 2016, A&A, 596, A110
POLARBEAR 2020	$\alpha+\beta$ = - 0.61° ± 0.22° (stat) ± ?? (sys)	Polarbear Collaboration 2020, ApJ, 897, 55
ACT 2020	$\alpha+\beta$ = - 0.07° ± 0.09° (stat) ± ?? (sys)	Choi et al 2020, JCAP, 12, 045
SPT 2020	$\alpha+\beta$ = 0.63° ± 0.04° (stat) ± ?? (sys)	Bianchini et al 2020, PRD, 102, 083504

Systematic uncertainties dominate the analysis

Current calibration strategies set a ≈0.5°-1° limit

DM/DE could be a **parity-violating pseudoscalar field** $\phi(-\vec{n}) = -\phi(\vec{n})$

Chern-Simons coupling to EM $\frac{1}{4} g_{\phi\gamma} \phi F_{\mu\nu} \tilde{F}_{\mu\nu}$

Carroll at al 1990, PRD, 41, 1231
Carroll & Field 1991, PRD, 43, 3789
Harari & Sikivie 1992, PLB, 289, 67

Axion-like particles
Marsh 2016, Phys Rep, 643, 1

Early Dark Energy
Murai et al 2022 [arXiv:2209.07804]

rotation of the plane of linear polarization clockwise on the sky

$$\beta = -\frac{1}{2} g_{\phi\gamma} \int \frac{\partial \phi}{\partial t} dt$$

Cosmic birefringence

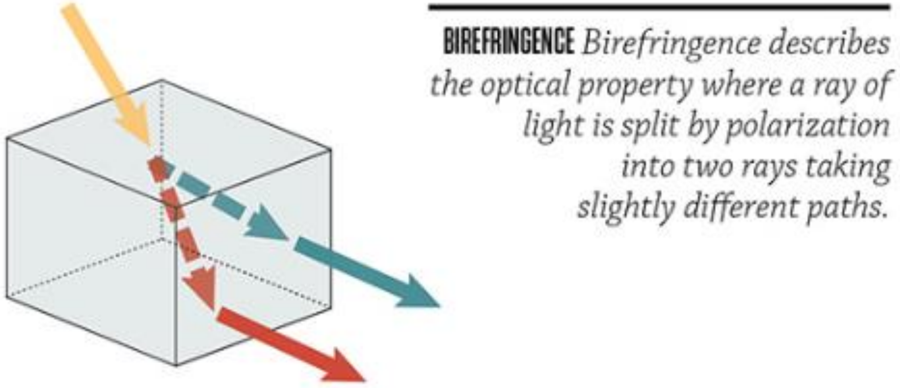

Faraday rotation from primordial magnetic fields
Subramanian 2016, Rep Prog Phys, 79, 076901

Superluminal Lorentz-violating electrodynamics emerging from a non-vanishing Weyl tensor
Shore 2005, Nucl Phys B, 717, 86118

Quantum gravity models that modify the dispersion relation of photons
Gleiser & Kozameh 2001, PRD, 64, 8, 083007

$\beta(\nu)$
disfavored by data
Eskilt 2022, A&A, 662, A10

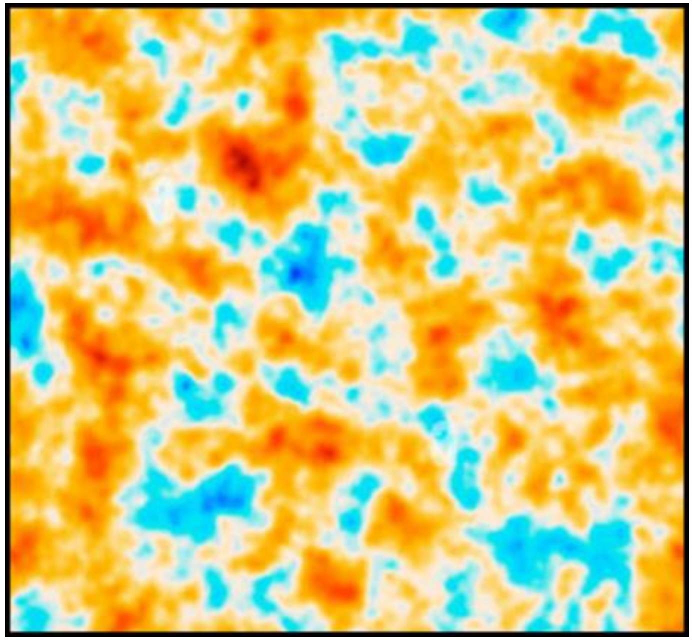

Improve instrument calibration

- Provides tighter constraints and does not directly depend on foregrounds (subject to the foreground residuals)
- Optimal strategy for ground-based experiments as new calibration sources allow a precise measurement of polarization angles

BICEP3: rotating polarized source

systematic error of <0.1° with a ≈0.03° statistical uncertainty on the calibration of polarization angles

Cornelison & Vergès Proc SPIE Int Soc Opt Eng 12190 (2022) 829

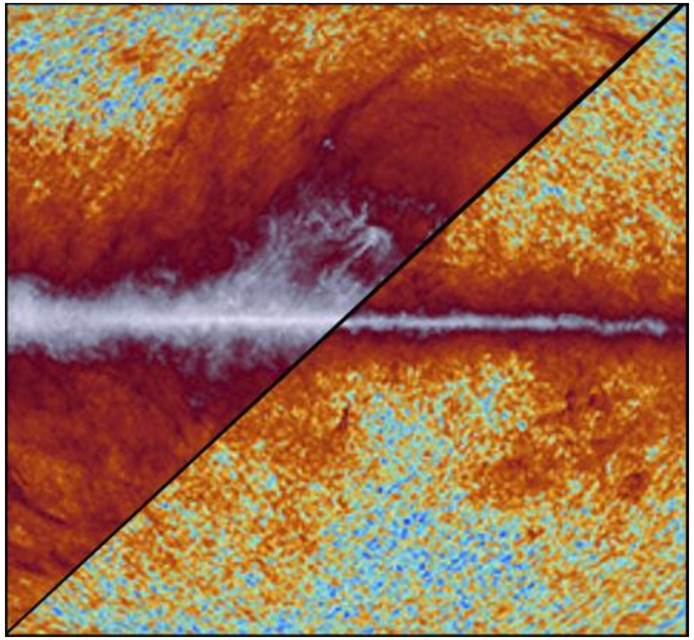

Use Galactic foregrounds as calibrator

- (Currently) optimal strategy for satellite missions where calibration is limited by prior knowledge of astrophysical sources
- Proven to be robust against instrumental systematics but sensitive to dust EB

PDP et al 2022 [arXiv:2210.07655]

PDP et al 2022, PRL, 128, 091302

Tightest constraint to date coming from

Planck PR4 + WMAP-9y $\beta = 0.342° \pm 0.093°$

Eskilt & Komatsu 2022, PRD, 106, 063503

Minami et al 2019, PTEP, 083E02
Minami 2020, PTEP, 063E01
Minami & Komatsu 2020, PTEP, 103E02

Observed signal is a rotation of the CMB and Galactic foreground emissions

$$\begin{pmatrix} E_{\ell m}^{\mathrm{o}} \\ B_{\ell m}^{\mathrm{o}} \end{pmatrix} = \begin{pmatrix} \cos(2\alpha) & -\sin(2\alpha) \\ \sin(2\alpha) & \cos(2\alpha) \end{pmatrix} \begin{pmatrix} E_{\ell m}^{\mathrm{fg}} \\ B_{\ell m}^{\mathrm{fg}} \end{pmatrix} + \begin{pmatrix} \cos(2\alpha+2\beta) & -\sin(2\alpha+2\beta) \\ \sin(2\alpha+2\beta) & \cos(2\alpha+2\beta) \end{pmatrix} \begin{pmatrix} E_{\ell m}^{\mathrm{cmb}} \\ B_{\ell m}^{\mathrm{cmb}} \end{pmatrix}$$

so the observed EB is

$$C_\ell^{EB,\mathrm{o}} = \frac{\tan(4\alpha)}{2}\left(C_\ell^{EE,\mathrm{o}} - C_\ell^{BB,\mathrm{o}}\right) + \frac{1}{\cos(4\alpha)} C_\ell^{EB,\mathrm{fg}} + \frac{\sin(4\beta)}{2\cos(4\alpha)}\left(C_\ell^{EE,\mathrm{cmb}} - C_\ell^{BB,\mathrm{cmb}}\right)$$

Planck Collaboration XI. 2020, A&A, 641, A11
Martire et al 2022, JCAP, 04, 003

Build a Gaussian likelihood to simultaneously determine both angles

$$-2\ln\mathcal{L} = \sum_{b=1}^{N_{\mathrm{bins}}} \left(\mathbf{A}\bar{C}_b^{\mathrm{o}} - \mathbf{B}\bar{C}_b^{\mathrm{cmb}}\right)^T \mathbf{M}_b^{-1} \left(\mathbf{A}\bar{C}_b^{\mathrm{o}} - \mathbf{B}\bar{C}_b^{\mathrm{cmb}}\right) + \sum_{b=1}^{N_{\mathrm{bins}}} \ln|\mathbf{M}_b|$$

Only two ingredients needed:

Cross-correlation of frequency bands of any CMB experiment

$$\bar{C}_b^{\mathrm{o}} = \left(C_b^{E_iE_j,\mathrm{o}}\ C_b^{B_iB_j,\mathrm{o}}\ C_b^{E_iB_j,\mathrm{o}}\right)^T$$

Theoretical prediction for CMB angular power spectra

Planck PR4 (NPIPE reprocessing)

Planck Collaboration 2020, A&A, 643, A42

The NPIPE pipeline processes raw, uncalibrated detector data from both LFI and HFI into polarized frequency and detector-set maps. NPIPE fits and corrects for gain fluctuations, ADCNL, bolometric transfer-function residuals and bandpass mismatch by fitting time-domain templates while solving for the polarized map.

NPIPE achieves a smaller noise by:

(1) including data acquired during repointing maneuvers between scans

(2) better modeling the data via a short baseline offset model for noise, suppressing degree-scale noise residuals

(3) multi-frequency polarization model used in calibration greatly reduces large-scale polarization uncertainty but introduces a pipeline transfer-function that suppresses CMB polarization power at $\ell < 20$

(4) second-order analog-to-digital conversion nonlinearity (ADCNL) model

The net effect on polarization is a scale-dependent reduction in the total uncertainty:

(1) $\sim$ 50 % lower N_ℓ at $\ell \sim 10$

(2) 20–30 % lower N_ℓ at $\ell \sim 100$

(3) 10–20 % lower N_ℓ at $\ell \sim 1000$ (also in temperature)

Planck PR4 (NPIPE reprocessing)

Reprocessing of raw LFI and HFI *Planck* data

Scale-dependent reduction of total uncertainty due to

- Addition of data acquired during repointing maneuvers
- Improved modeling of instrumental noise and systematics

Planck Collaboration 2020, A&A, 643, A42

- NPIPE 100, 143, 217, 353 GHz data
- Focus on small-scale information (ℓ>50) to target the birefringence angle from recombination
- Cross-correlating A/B detector splits → β, α_i (i=1,…,8)
- Start by considering a null foreground EB

PDP et al 2022, PRL, 128, 091302

Consistent results across 4 independent pipelines

Pipeline	Implementation	Pseudo-C_ℓ
JRE	Posterior distribution via MCMC	PolSpice
MT	Posterior distribution via MCMC	Xpol
YM	Posterior distribution via MCMC	NaMaster
PDP	Analytical minimization	NaMaster

PDP et al 2022 [arXiv:2210.07655]

Minami & Komatsu 2020, PRL, 125, 221301

Planck 2018 (PR3)

100, 143, 217, 353 GHz data

Half-mission splits → β, α_i (i=1,…,4)

High-ℓ data → bin C_ℓ/M_ℓ from ℓ_{min}=51 to ℓ_{max}=1490 with $\Delta\ell$ = 20 spacing

Specific mask for each band

Neglecting foreground EB

$\beta = 0.35° \pm 0.14°$ (2.4σ)
for nearly full-sky

PDP et al 2022, PRL, 128, 091302

Planck 2020 (PR4 or NPIPE)

100, 143, 217, 353 GHz data

A/B detector splits → β, α_i (i=1,…,8)

High-ℓ data → bin C_ℓ/M_ℓ from ℓ_{min}=51 to ℓ_{max}=1490 with $\Delta\ell$ = 20 spacing

Common mask for all bands

Correcting for foreground EB

$\beta = 0.30° \pm 0.11°$ (2.7σ)
for nearly full-sky

For nearly full-sky: β = 0.30° ± 0.11° (2.7σ) → Consistent with and more precise than previous measurements!

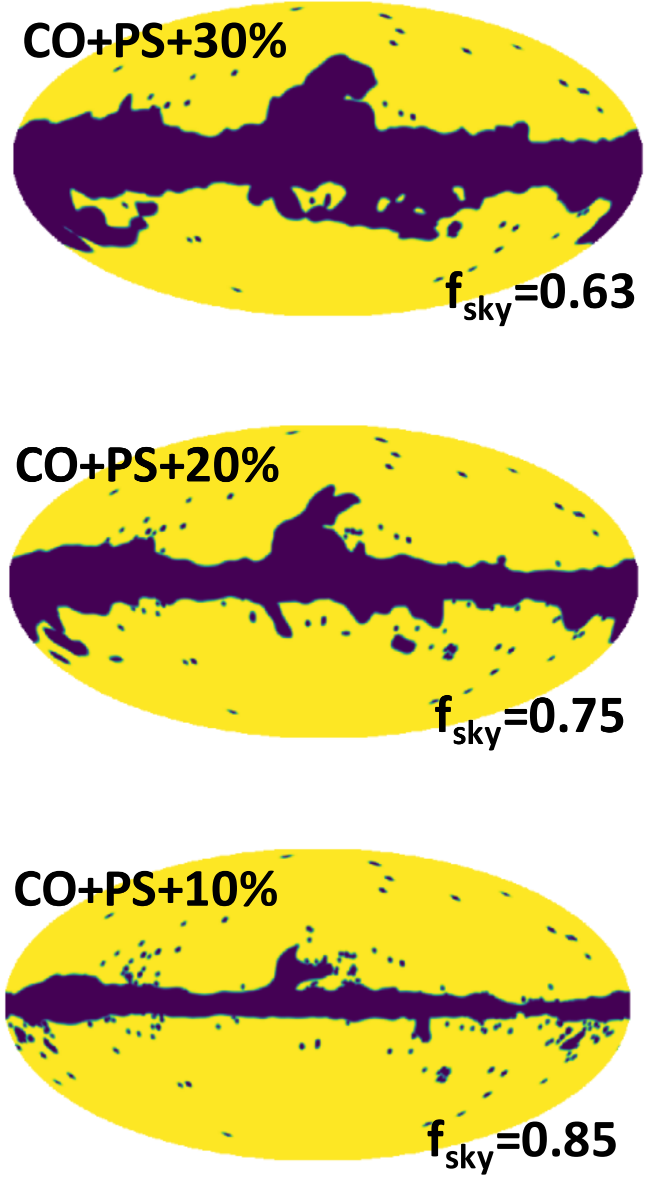

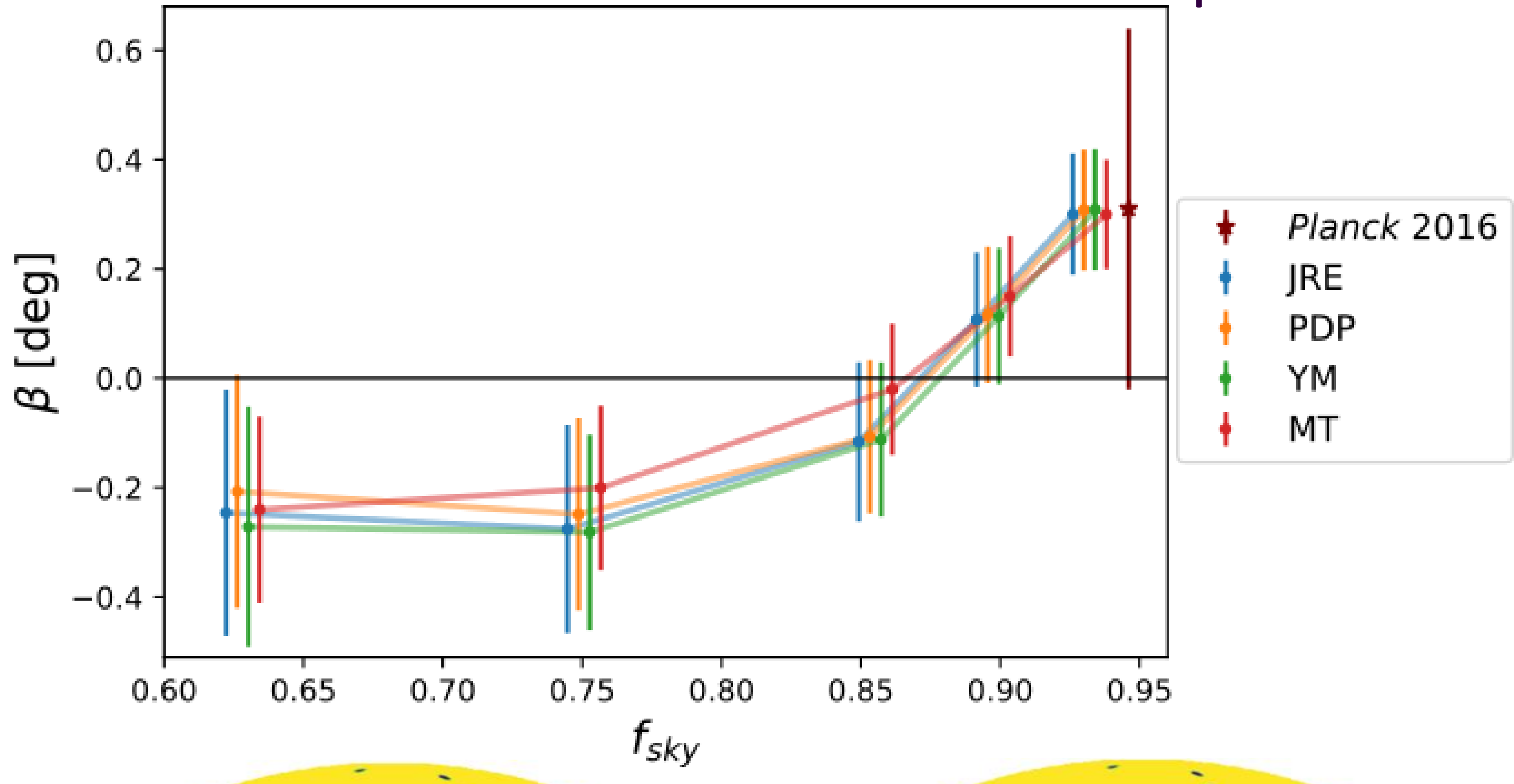

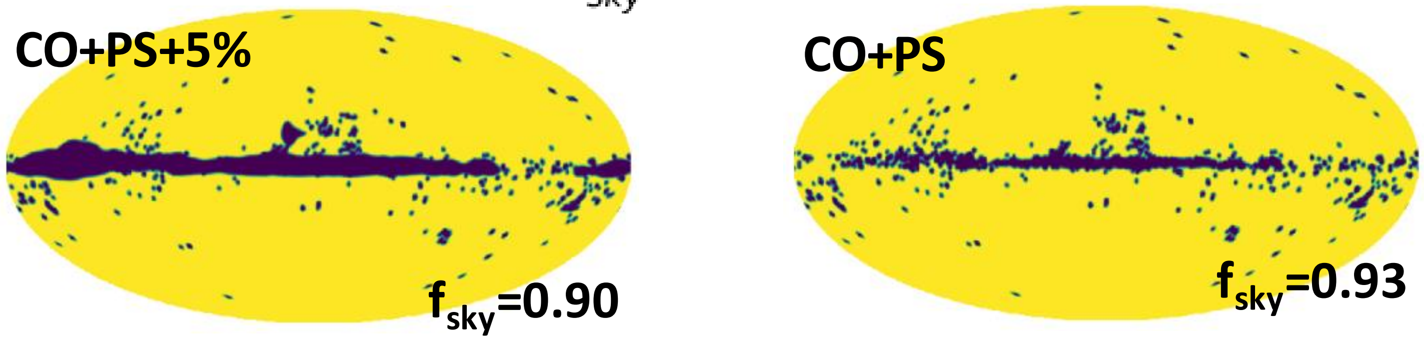

… but our inferred value of α depends on Galactic dust

Dust EB biases our estimation of miscalibration angles, dragging with them the measurement of β

Misalignment of dust filaments and Galactic magnetic fields produces TB and EB

Clark et al 2021, ApJ, 919, 53

- Dust **TB > 0** detected by ***Planck***

  Planck Collaboration XI. 2020, A&A, 641, A11

- Expected dust **EB > 0**

Indirect detection of dust EB

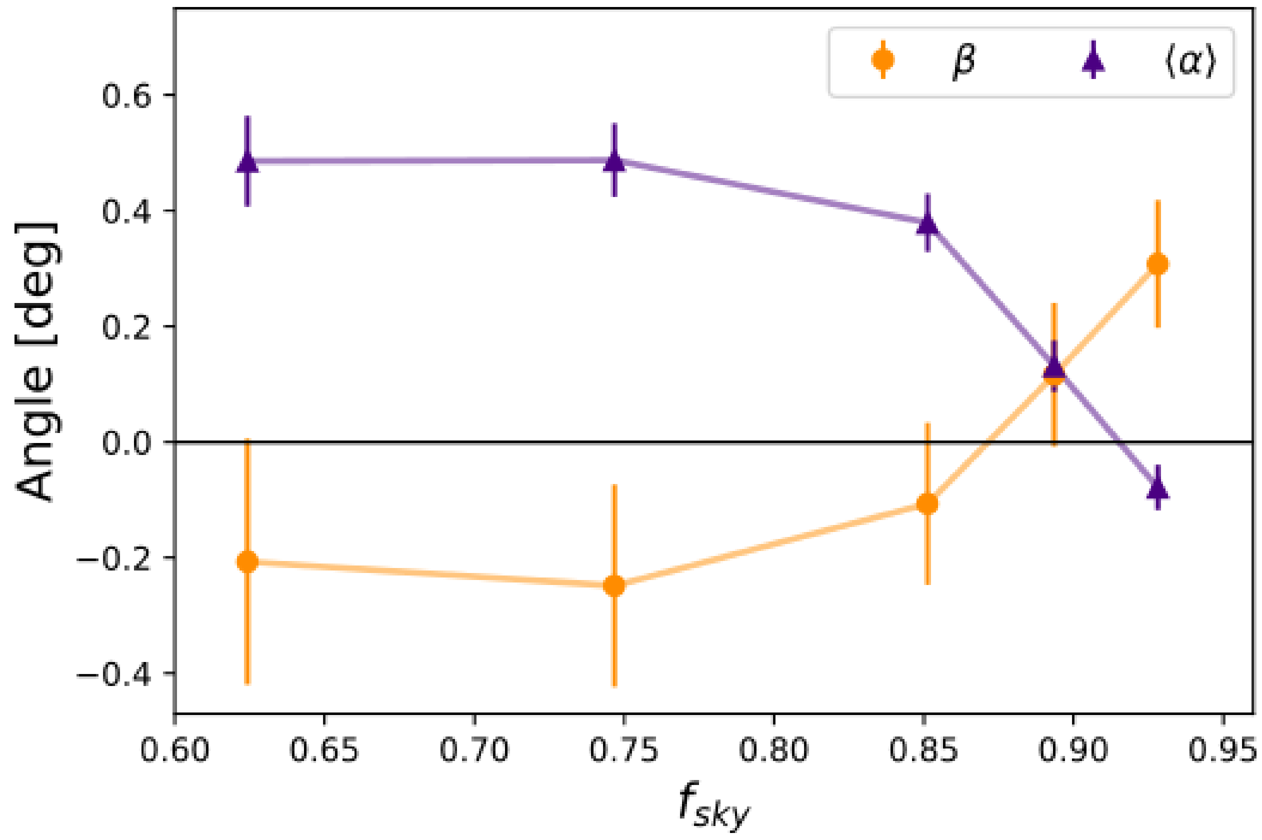

The EB signal created by birefringence exists regardless of the Galactic mask ...

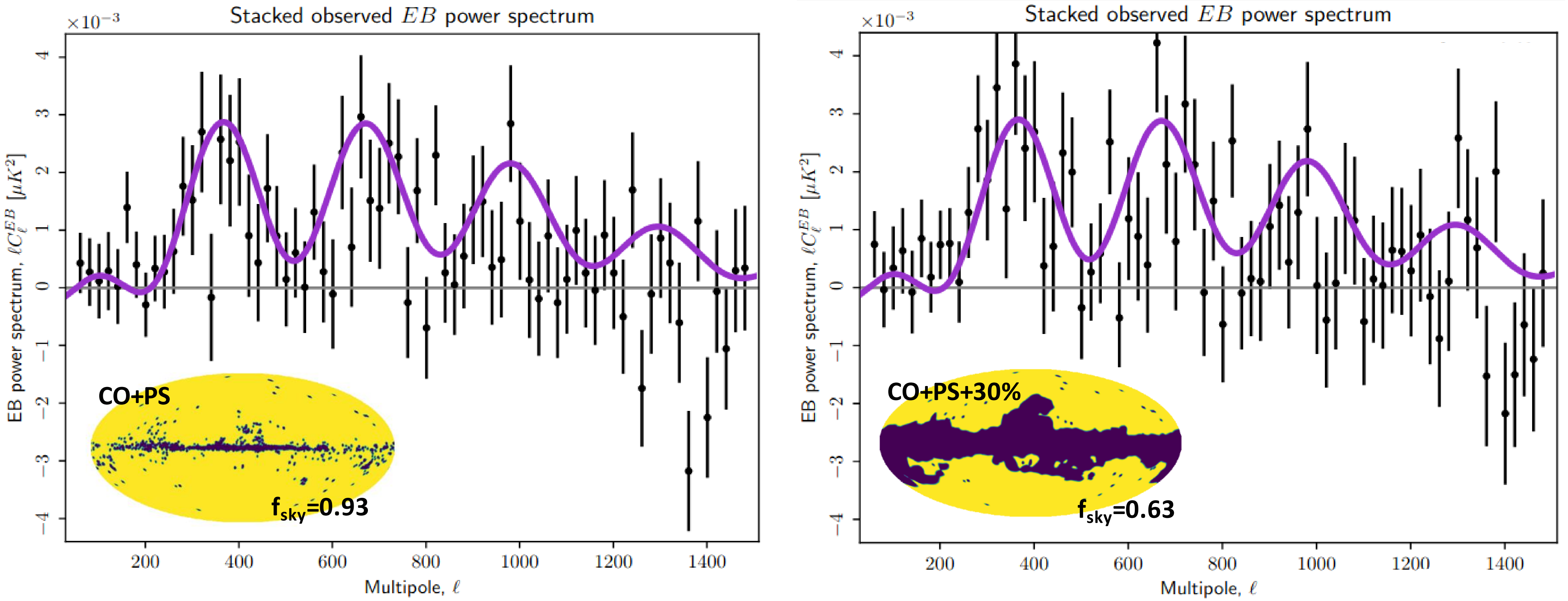

Eskilt & Komatsu 2022, PRD, 106, 063503

… but our inferred value of α depends on Galactic dust

Observed foreground signal can be rewritten as

$$C_\ell^{EB,\mathrm{fg,o}} = \tfrac{1}{2}\sin(4\alpha)\left(C_\ell^{EE,\mathrm{fg}} - C_\ell^{BB,\mathrm{fg}}\right) + \cos(4\alpha) C_\ell^{EB,\mathrm{fg}}$$
$$= \tfrac{1}{2}\sqrt{4\left(C_\ell^{EB,\mathrm{fg}}\right)^2 + \left(C_\ell^{EE,\mathrm{fg}} - C_\ell^{BB,\mathrm{fg}}\right)^2}\,\sin(4\alpha + 4\gamma_\ell)$$

Within the small angle approximation

$$\gamma_\ell \approx \frac{C_\ell^{EB,\mathrm{fg}}}{C_\ell^{EE,\mathrm{fg}} - C_\ell^{BB,\mathrm{fg}}}$$

If $C_\ell^{EB,\mathrm{fg}} \propto C_\ell^{EE,\mathrm{fg}} - C_\ell^{BB,\mathrm{fg}}$

then $\gamma_\ell = \gamma$ → **degenerate with α**

- **measure α + γ and β - γ**
- **does not affect α + β** → **By fixing α_i=0 we effectively measure β+⟨α⟩**

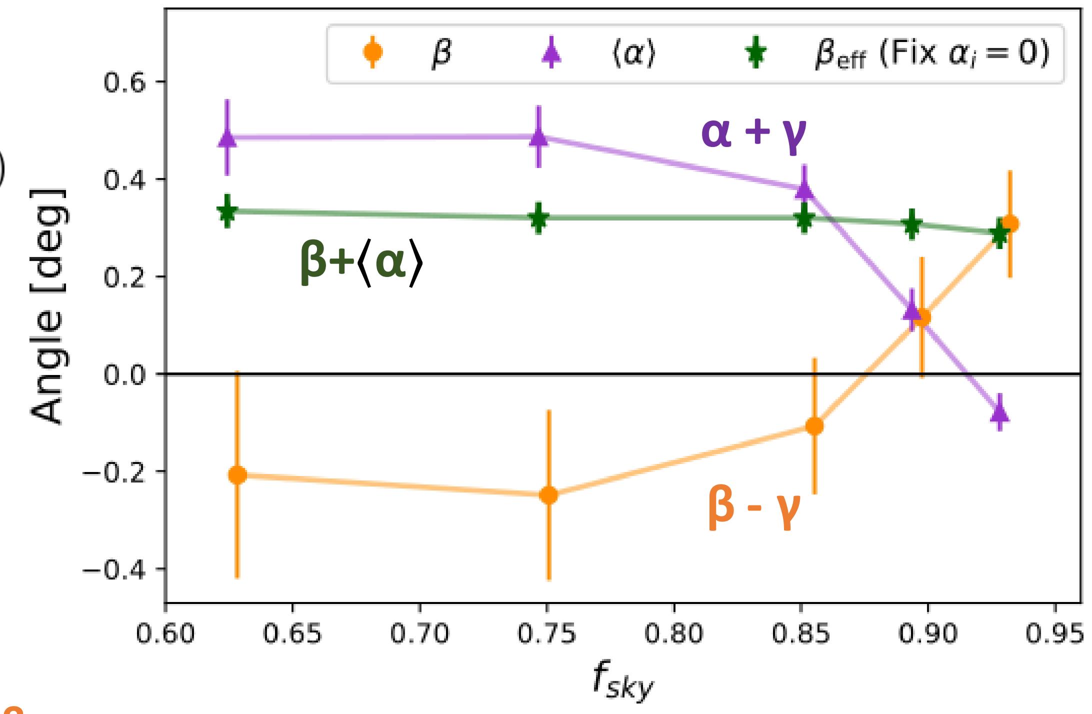

Planck Collaboration XI. 2020, A&A, 641, A11

Planck **reported dust TB > 0 → Plausible dust EB > 0 → Expect ↑α and ↓β**

Observed foreground signal can be rewritten as

$$C_\ell^{EB,\mathrm{fg,o}} = \frac{1}{2}\sqrt{4\left(C_\ell^{EB,\mathrm{fg}}\right)^2 + \left(C_\ell^{EE,\mathrm{fg}} - C_\ell^{BB,\mathrm{fg}}\right)^2}\,\sin(4\alpha + 4\gamma_\ell)$$

Within the small angle approximation $\gamma_\ell \approx \dfrac{C_\ell^{EB,\mathrm{fg}}}{C_\ell^{EE,\mathrm{fg}} - C_\ell^{BB,\mathrm{fg}}}$

If $C_\ell^{EB,\mathrm{fg}} \propto C_\ell^{EE,\mathrm{fg}} - C_\ell^{BB,\mathrm{fg}}$ then $\gamma_\ell = \gamma$ → degenerate with α { measure $\alpha + \gamma$ and $\beta - \gamma$; does not affect $\alpha + \beta$ }

Synch EB statistically compatible with null

Martire et al 2022, JCAP, 04, 003

No physical process known to produce synch EB

Misalignment between dust filaments and Galactic magnetic fields creates TB and EB correlations

Clark et al 2021, ApJ, 919, 53

Planck reported :

- Dust TB > 0
- A hint of dust EB > 0 (still statistically compatible with null)

Planck Collaboration XI. 2020, A&A, 641, A11

→ Expect $\gamma > 0$ leading to ↑α and ↓β

Planck Collaboration LVII. 2020, A&A, 643, A42

PDP et al 2022 [arXiv:2210.07655]

NPIPE end-to-end simulations

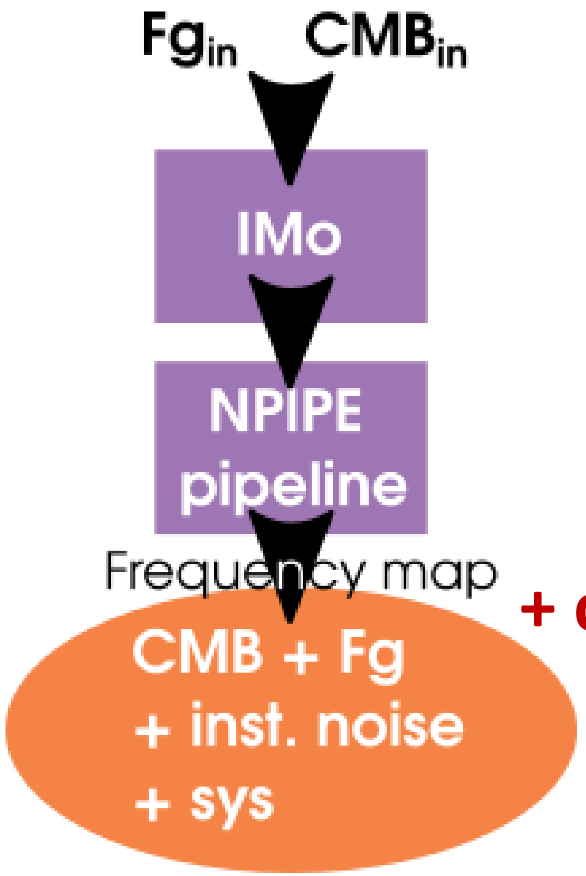

+ α, β

Ignoring dust EB

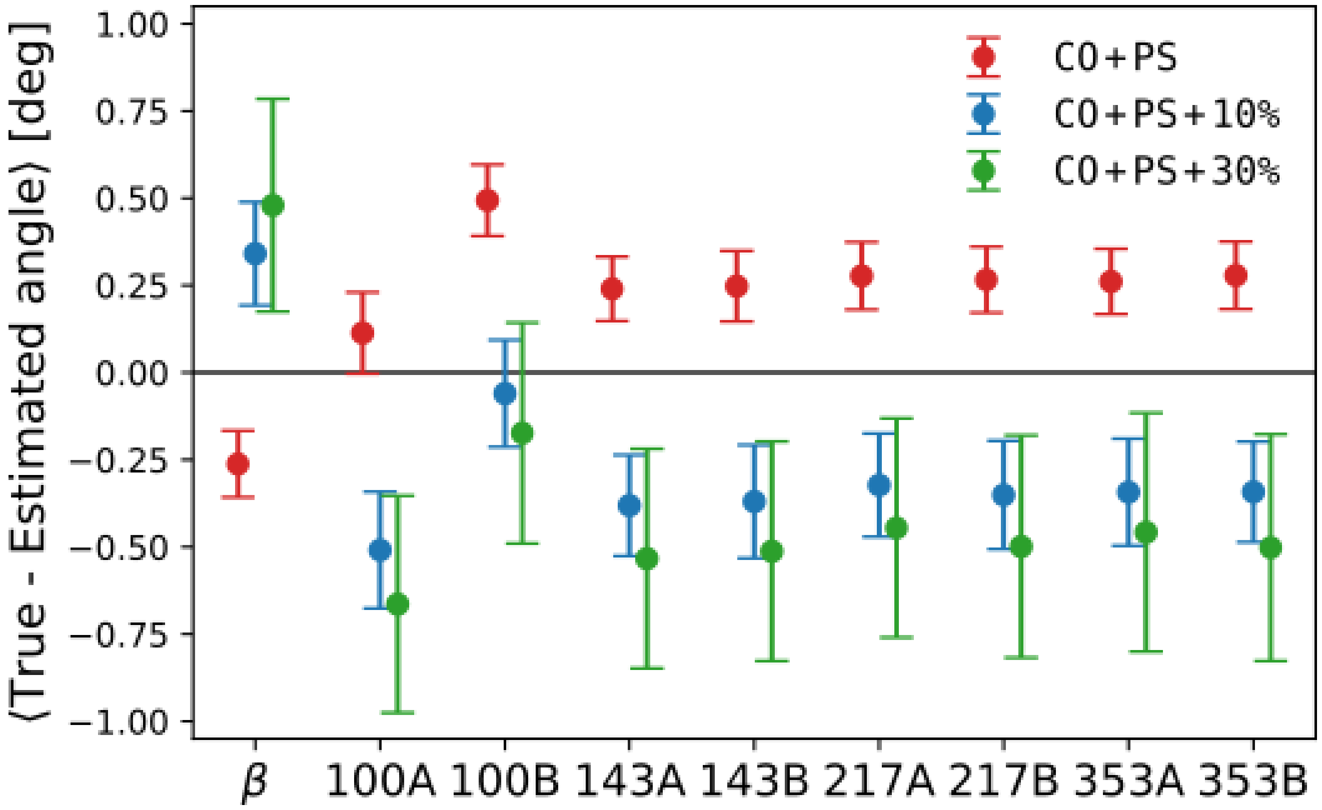

Average over 100 simulations
Error bar = simulations dispersion

Planck Collaboration LVII. 2020, A&A, 643, A42

PDP et al 2022 [arXiv:2210.07655]

NPIPE end-to-end simulations

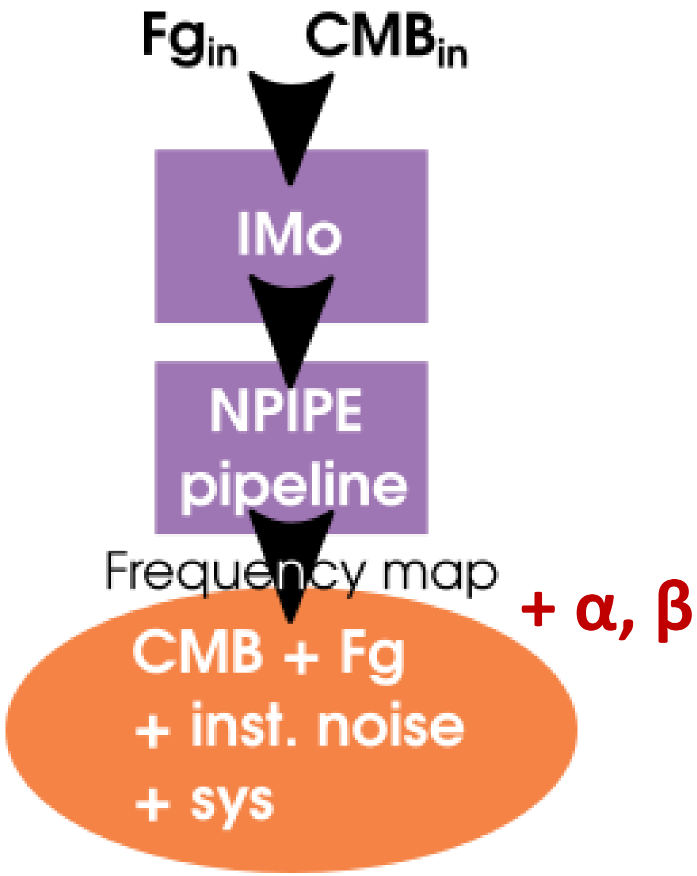

Correcting for dust EB

Exact description of the fiducial foreground model

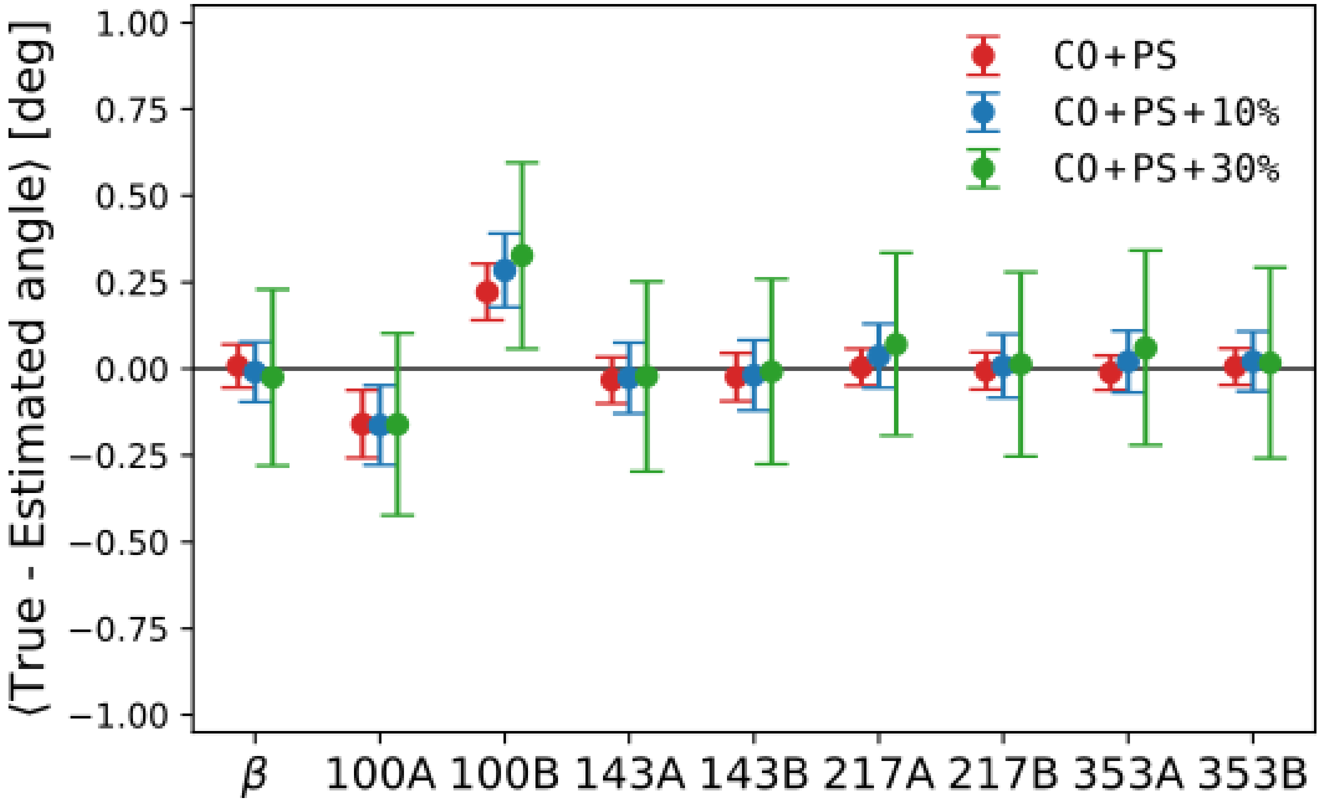

Average over 100 simulations

Error bar = simulations dispersion

Planck Collaboration LVII. 2020, A&A, 643, A42

PDP et al 2022 [arXiv:2210.07655]

NPIPE end-to-end simulations

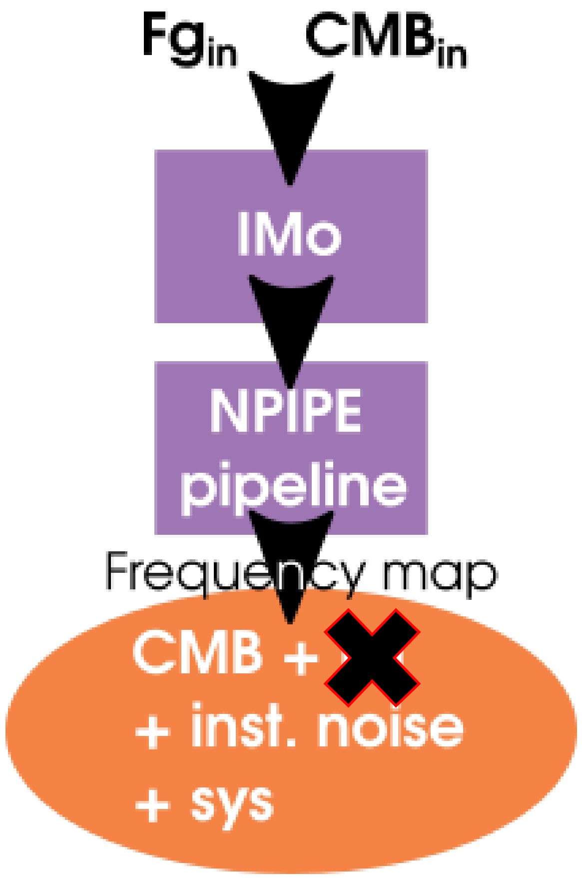

Removing foregrounds

Sims of CMB + Noise + Systematics

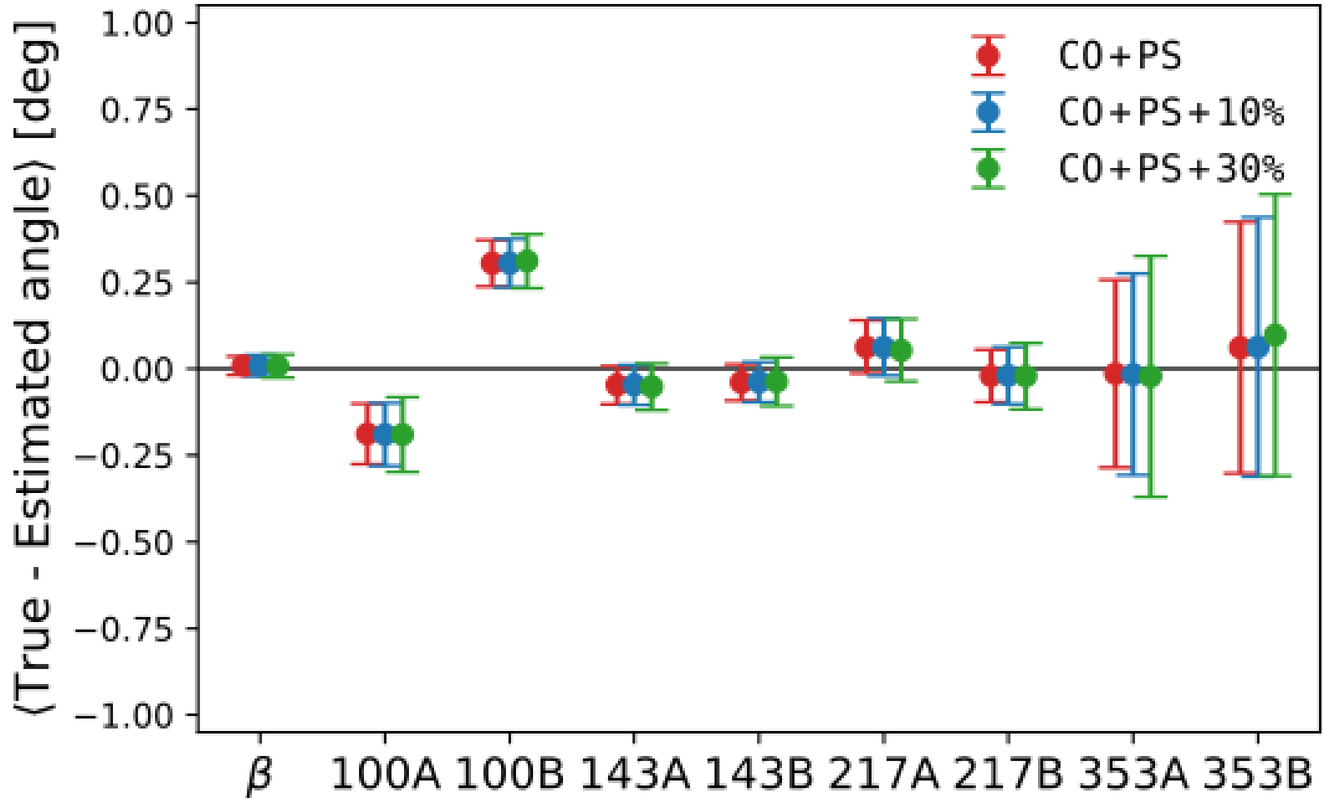

Average over 100 simulations
Error bar = simulations dispersion

Huffenberger et al 2020, ApJ, 899, 31
Clark et al 2021, ApJ, 919, 53

Misalignment between the filamentary dust structures of the ISM and the plane-of-sky orientation of the Galactic magnetic field

Filament
Magnetic Field

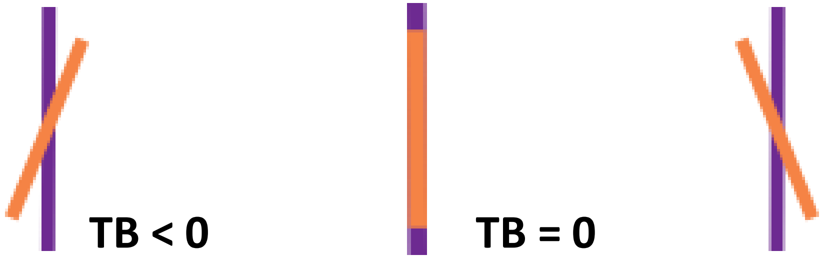

TB < 0	TB = 0	TB > 0
TE > 0	TE > 0	TE > 0
EB < 0	EB = 0	EB > 0

$$C_\ell^{TB,\mathrm{dust}} \propto \sin(2\psi)$$
$$C_\ell^{TE,\mathrm{dust}} \propto \cos(2\psi)$$
$$C_\ell^{EB,\mathrm{dust}} \propto \sin(4\psi)$$

Sign and magnitude of EB can be predicted by measuring TE and TB

$$C_\ell^{EB,\mathrm{dust}} = r_\ell^{TB,\mathrm{dust}} \sqrt{C_\ell^{EE,\mathrm{dust}} C_\ell^{BB,\mathrm{dust}}} \sin\left(2 \arctan\left(\frac{C_\ell^{TB,\mathrm{dust}}}{C_\ell^{TE,\mathrm{dust}}}\right)\right)$$

Our take

Small angle approximation

$C_\ell^{BB,\mathrm{dust}} \propto C_\ell^{EE,\mathrm{dust}}$ **thus** $\sqrt{C_\ell^{EE,\mathrm{dust}} C_\ell^{BB,\mathrm{dust}}} \rightarrow C_\ell^{EE,\mathrm{dust}}$

$|r_\ell^{TB,\mathrm{dust}}| \rightarrow A_\ell$ **free amplitude parameter** $0 \leq A_\ell \ll 1$

$$C_\ell^{EB,\mathrm{dust}} \approx A_\ell C_\ell^{EE,\mathrm{dust}} \frac{C_\ell^{TB,\mathrm{dust}}}{C_\ell^{TE,\mathrm{dust}}}$$

Huffenberger et al 2020, ApJ, 899, 31
Clark et al 2021, ApJ, 919, 53
Cukierman et al 2022 [arXiv:2208.07382]

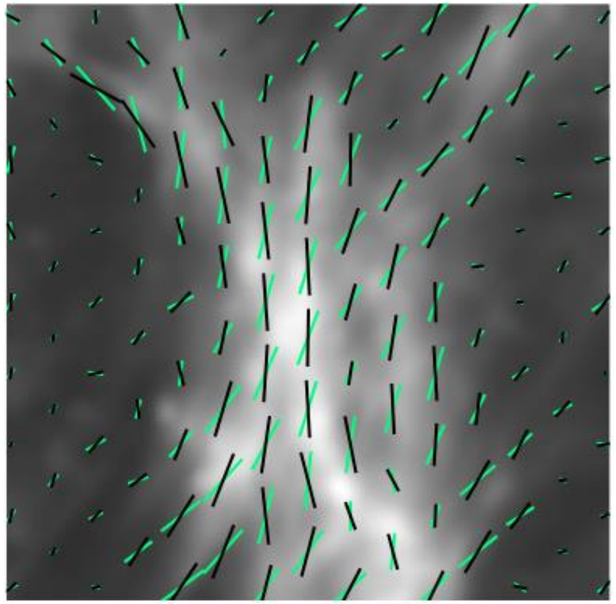

Misalignment between the dust filaments of the ISM and the plane-of-sky orientation of the Galactic magnetic field sources TE, TB, EB correlations

Filament
Magnetic Field

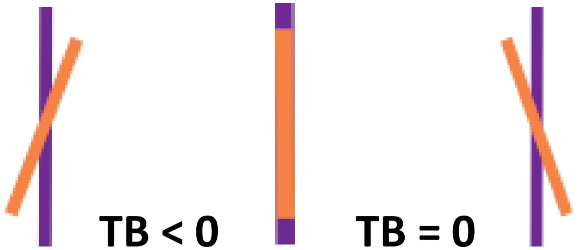

TB < 0	TB = 0	TB > 0
TE > 0	TE > 0	TE > 0
EB < 0	EB = 0	EB > 0

$$C_\ell^{TB,\text{dust}} \propto \sin(2\psi)$$
$$C_\ell^{TE,\text{dust}} \propto \cos(2\psi)$$
$$C_\ell^{EB,\text{dust}} \propto \sin(4\psi)$$

Sign and magnitude of EB predicted from EE, TE, and TB

$$C_\ell^{EB,\text{dust}} \approx A_\ell C_\ell^{EE,\text{dust}} \frac{C_\ell^{TB,\text{dust}}}{C_\ell^{TE,\text{dust}}}$$

Take dust C_ℓ to be that of NPIPE @ 353GHz

A_ℓ **free amplitude parameter** $0 \leq A_\ell \ll 1$

Caveats and limitations

- **Assumes that all dust is sourcing the misalignment while only filaments are expected to produce EB**
- **Noisy proxy as it is built from Planck polarization measurements**

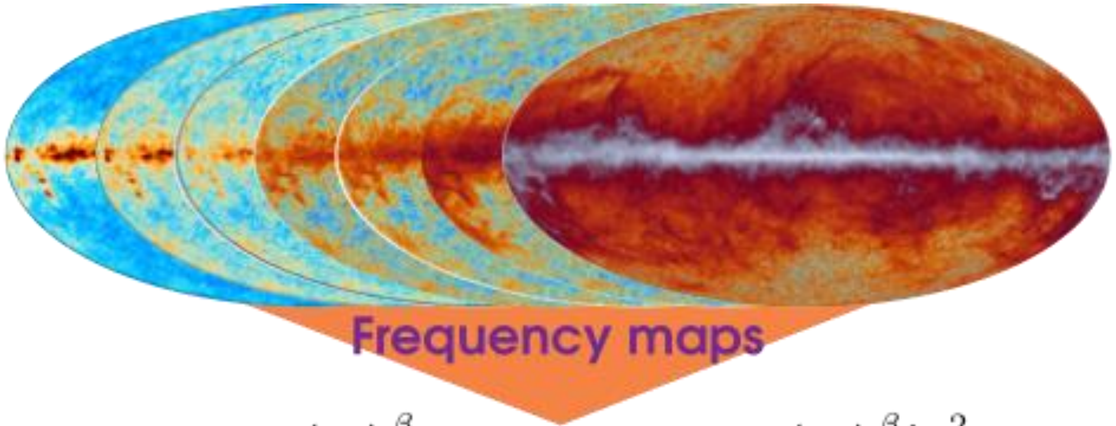

$$\begin{pmatrix} Q \\ U \end{pmatrix}_p = \begin{pmatrix} q^{\mathrm{cmb}} \\ u^{\mathrm{cmb}} \end{pmatrix}_p + \frac{1}{f(\nu)} \left(\frac{\nu}{\nu_s}\right)^{\beta_s} \begin{pmatrix} q^{\mathrm{synch}} \\ u^{\mathrm{synch}} \end{pmatrix}_p + \frac{1}{f(\nu)} \left(\frac{\nu}{\nu_d}\right)^{\beta_d - 2} \frac{B(\nu, T_d)}{B(\nu_d, T_d)} \begin{pmatrix} q^{\mathrm{dust}} \\ u^{\mathrm{dust}} \end{pmatrix}_p$$

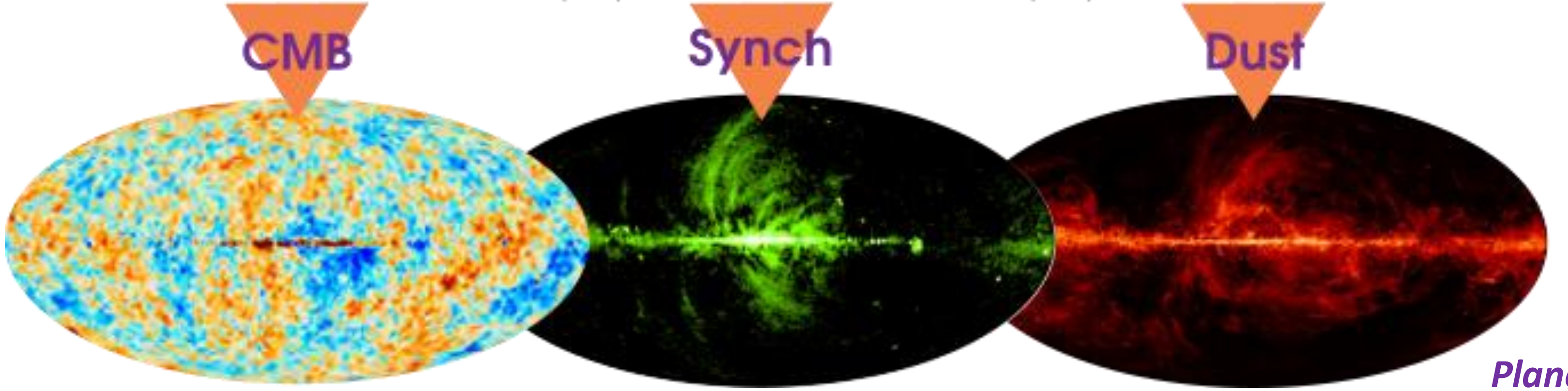

$f(\nu)$ conversion from thermodynamic to antenna units

$B(\nu, T)$ Planck's law

Power law synchrotron and one-component modified blackbody dust models

Commander

Planck Collaboration IV. 2020, A&A, 641, A4

Take the Commander sky model as our foreground model

$$C_\ell^{EB,\mathrm{o}} = \frac{\tan(4\alpha)}{2}\left(C_\ell^{EE,\mathrm{o}} - C_\ell^{BB,\mathrm{o}}\right) + \frac{\mathcal{D}}{\cos(4\alpha)} C_\ell^{EB,\mathrm{fg}} + \frac{\sin(4\beta)}{2\cos(4\alpha)}\left(C_\ell^{EE,\mathrm{cmb}} - C_\ell^{BB,\mathrm{cmb}}\right)$$

Commander

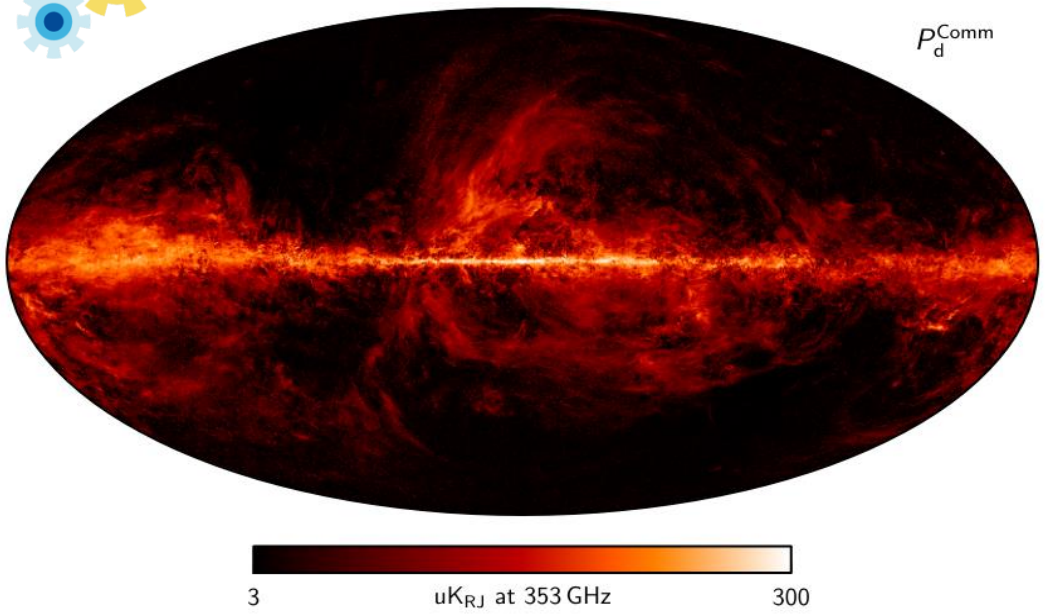

$$\frac{1}{f(\nu)}\left(\frac{\nu}{\nu_d}\right)^{\beta_d-2}\frac{B(\nu,T_d)}{B(\nu_d,T_d)}\begin{pmatrix} q^{\rm dust} \\ u^{\rm dust}\end{pmatrix}_p$$

Caveats and limitations

- **Limited signal-to-noise** of EB template leads to a 20% underestimation of uncertainties

  PDP et al 2022 [arXiv:2210.07655]

  → **High-precision measurements from next-generation experiments**

- Spurious EB correlations through **ignoring instrumental polarization angles** in the SED model

  → **Inclusion of polarization angles in SED**

  de la Hoz et al 2022, JCAP, 03, 032

- Spurious EB correlations from the **integration of different dust clouds along the line-of-sight**

  Vacher et al 2022 [arXiv:2210.14768]

  → **Dust model beyond the single modified blackbody**

NPIPE end-to-end simulations

Simulations of CMB + Foregrounds + Noise + Systematics

Baseline analysis (ignoring foreground EB)

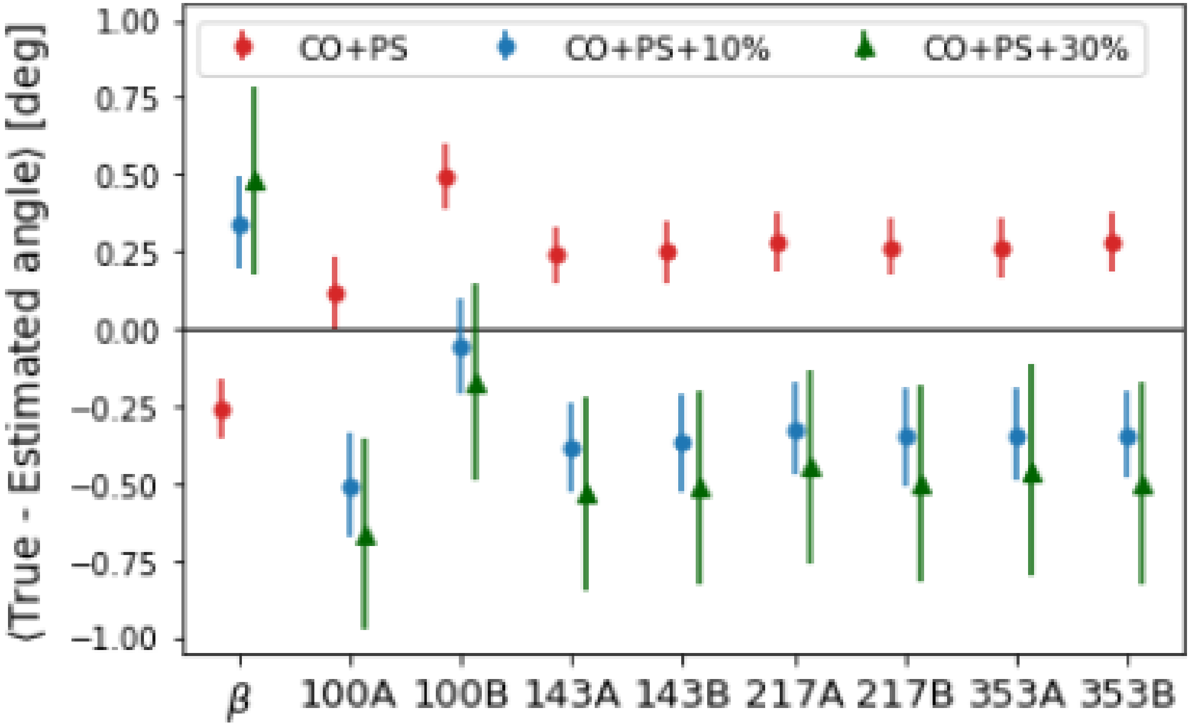

Modeling foreground EB (Commander)

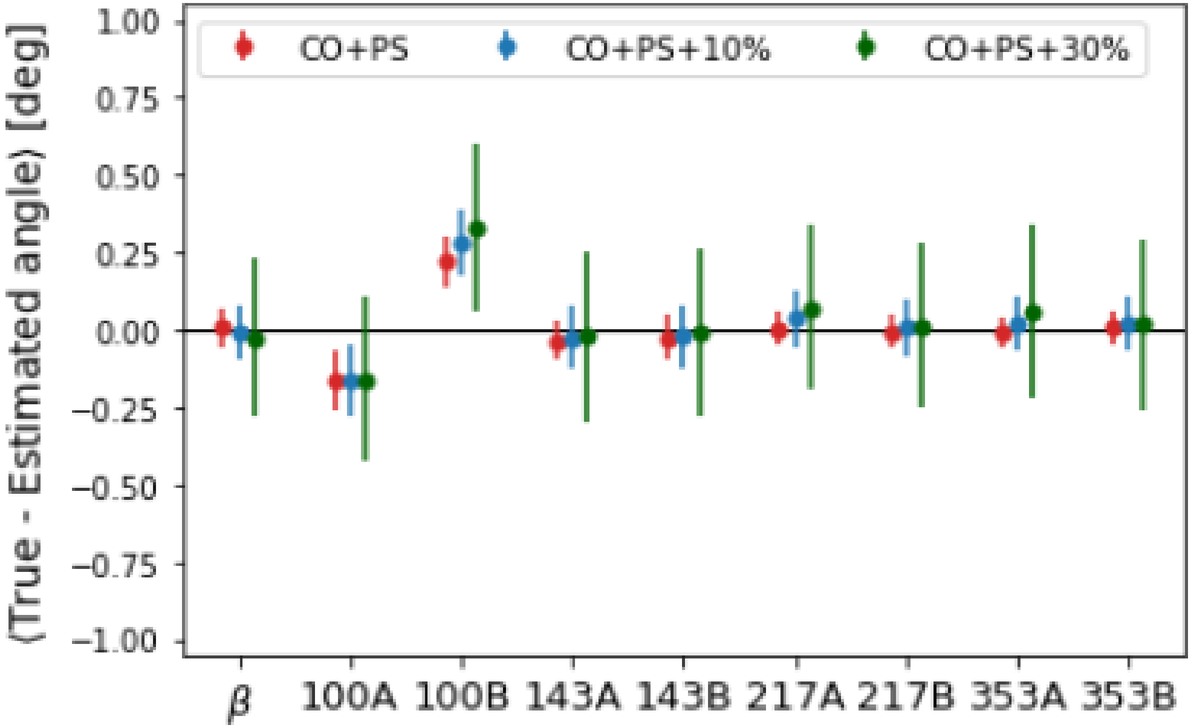

Average over 100 simulations
Error bar = simulations dispersion

PDP et al 2022 [arXiv:2210.07655]

Quantifying systematics with NPIPE end-to-end simulations

PDP et al 2022 [arXiv:2210.07655]

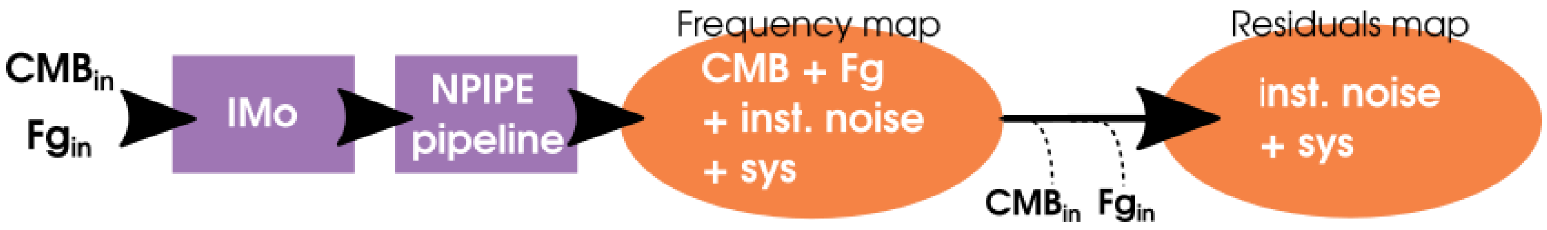

Simulations of CMB + Noise + Systematics

No foreground to break the α+β degeneracy

- different angle for each detector split → α_i
- same angle for all frequency bands → β

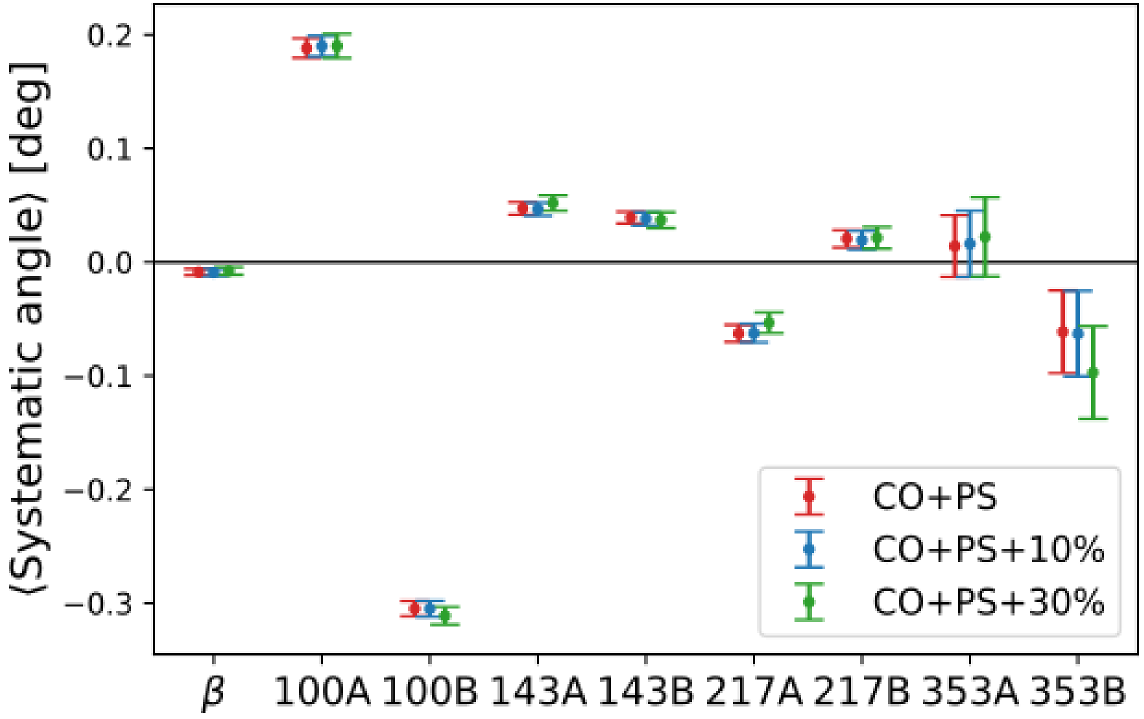

Average over 100 sims
Error bar = sim' dispersion / sqrt(100)

	From sims	σ_{stat} fit to data
$\langle\alpha_{100A}\rangle$ =	0.188° ± 0.009°	0.13°
$\langle\alpha_{100B}\rangle$ =	- 0.305° ± 0.007°	0.13°

→ cross-polarization effect

$\langle\alpha_{143A}\rangle$ =	0.047° ± 0.006°	0.11°
$\langle\alpha_{143B}\rangle$ =	0.039° ± 0.005°	0.11°
$\langle\alpha_{217A}\rangle$ =	- 0.063° ± 0.008°	0.11°

→ beam leakage

α_{sys} don't need to agree with data
→ simulations can't include the real α_i in the data

Negligible impact on β

$\langle\beta_{sys}\rangle$ =	- 0.009° ± 0.003°	0.11°

Intensity-to-polarization leakage → $C_\ell^{EB} \propto C_\ell^{TT}$

Cross-polarization effect → $C_\ell^{EB} \propto C_\ell^{EE}$

A combination of both → $C_\ell^{EB} \propto C_\ell^{TE}$

Beam leakage

$$C_\ell^{EB} = \omega_{\ell,\mathrm{pix}}^2 \sum_{XY} W_\ell^{EB,XY} C_\ell^{XY,\mathrm{cmb}}$$

$$XY \in \{TT, EE, BB, TE\}$$

QuickPol's polarization matrices
Hivon et al 2017, A&A, 598, A25

PDP et al 2022 [arXiv:2210.07655]

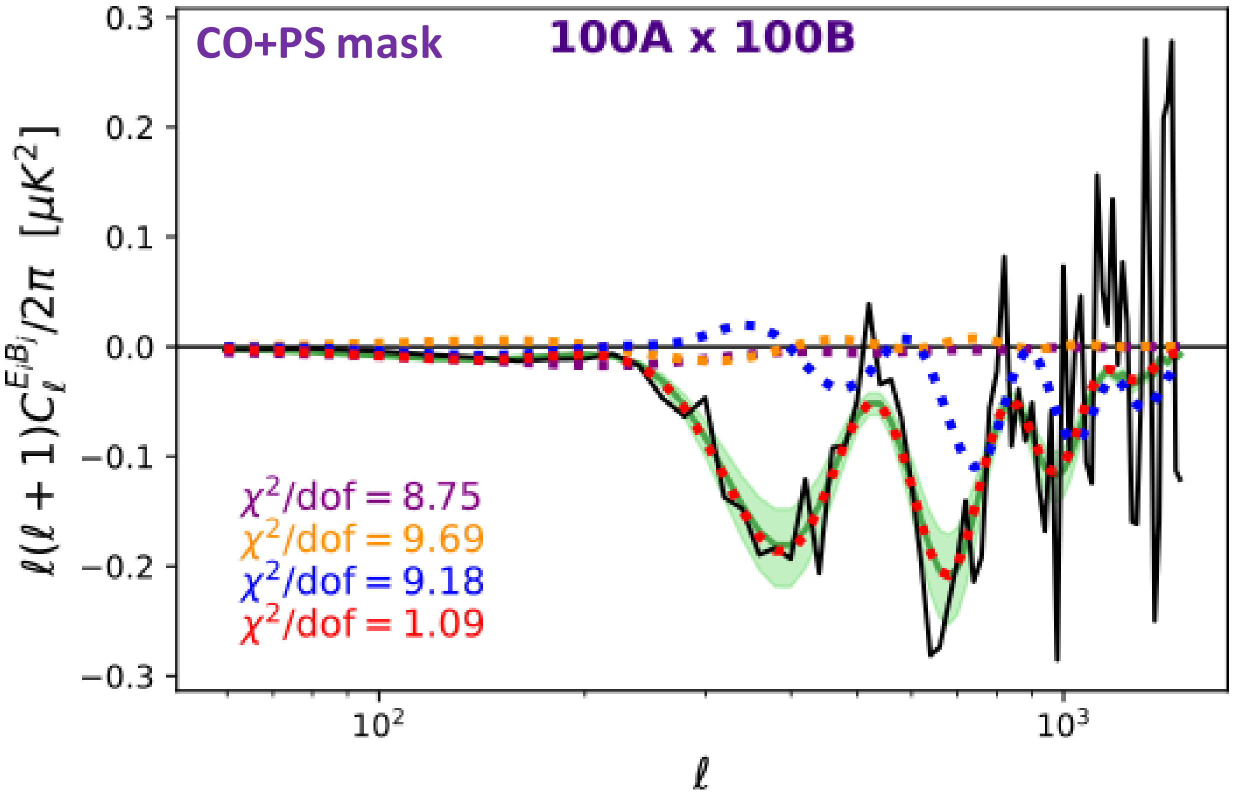

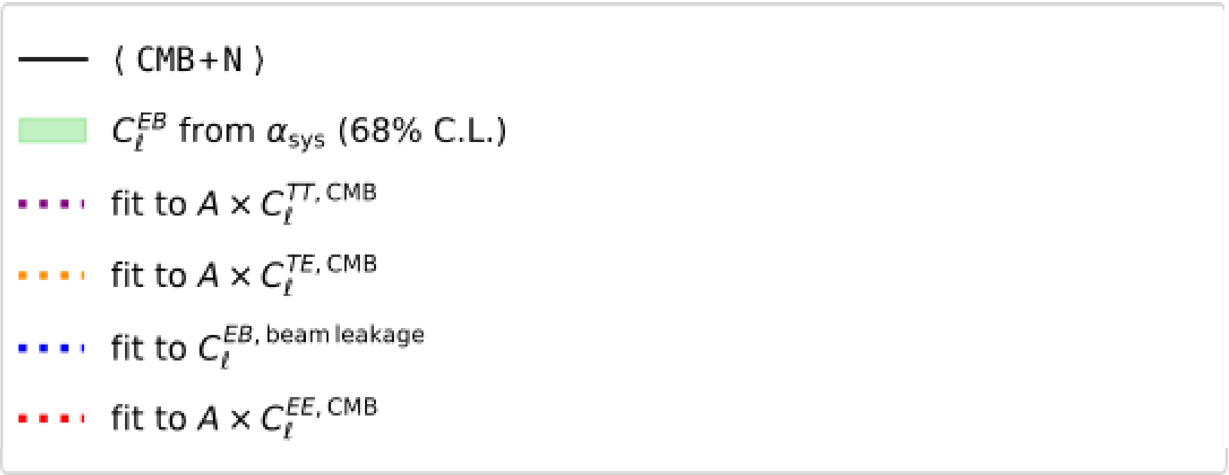

Particularly dangerous since our estimator relies on finding a signal resembling $EE^{\rm cmb}$ in EB

Intensity-to-polarization leakage → $C_\ell^{EB} \propto C_\ell^{TT}$

Cross-polarization effect → $C_\ell^{EB} \propto C_\ell^{EE}$

A combination of both → $C_\ell^{EB} \propto C_\ell^{TE}$

Beam leakage

$$C_\ell^{EB} = \omega_{\ell,\mathrm{pix}}^2 \sum_{XY} W_\ell^{EB,XY} C_\ell^{XY,\mathrm{cmb}}$$

$$XY \in \{TT, EE, BB, TE\}$$

QuickPol's polarization matrices

Hivon et al 2017, A&A, 598, A25

PDP et al 2022 [arXiv:2210.07655]

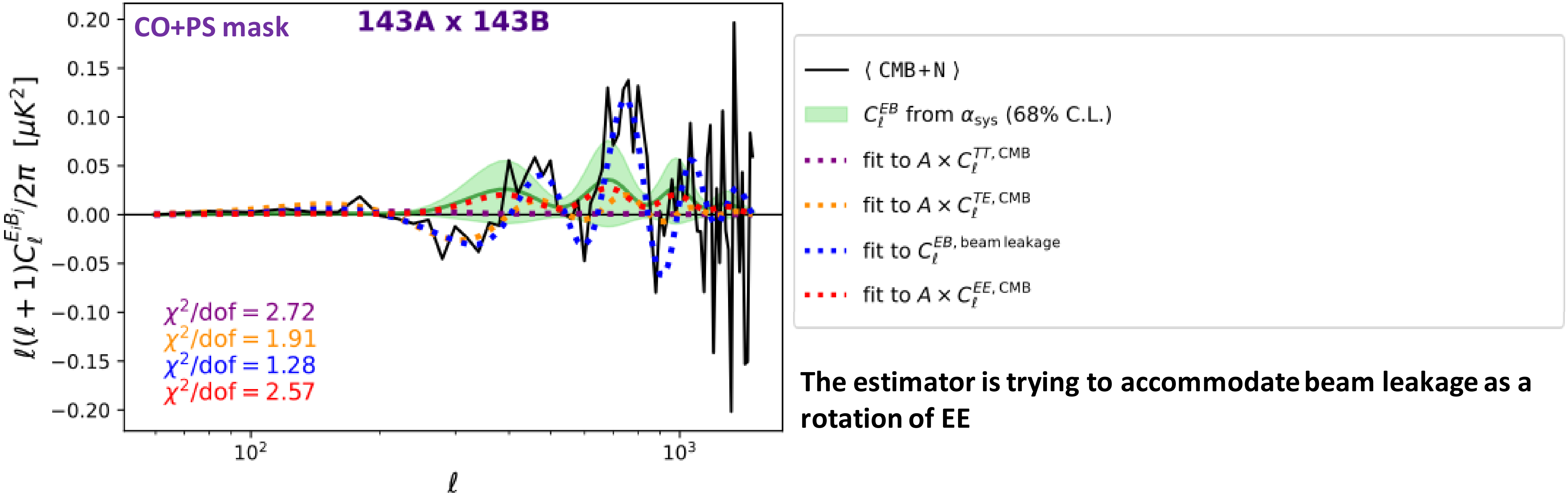

The estimator is trying to accommodate beam leakage as a rotation of EE

Frequency-dependent constraints on cosmic birefringence from the LFI and HFI Planck data release 4

Eskilt 2022, A&A, 662, A10

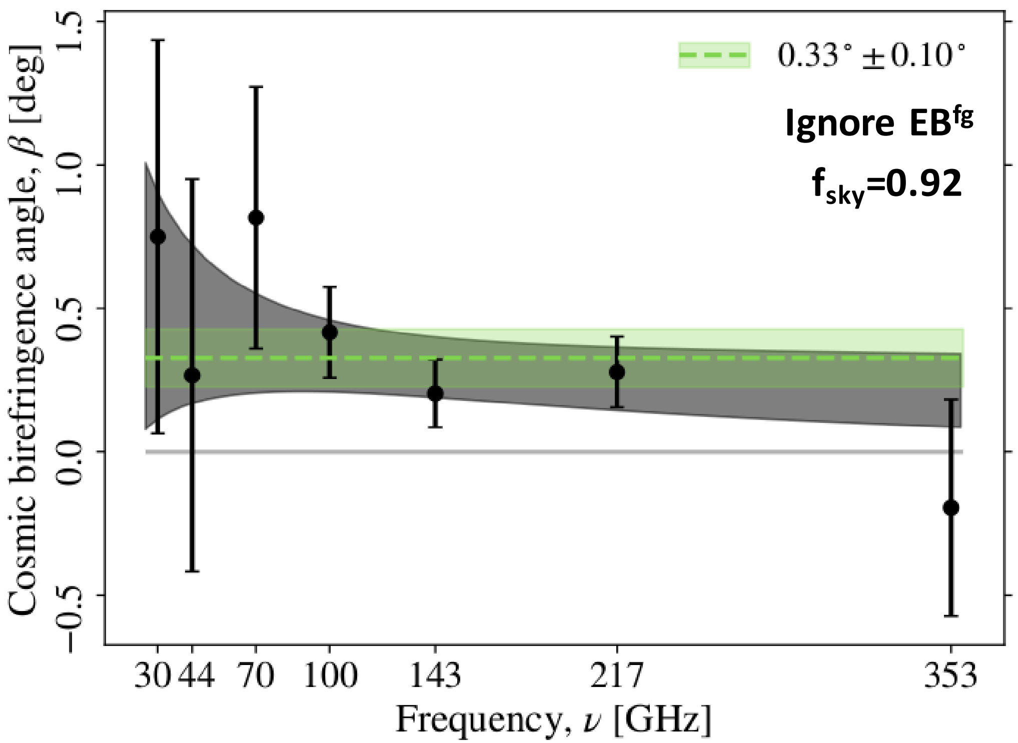

$$\beta_\nu = \beta_o(\nu/\nu_o)^n \begin{cases} \beta_o = 0.29^{+0.10}_{-0.11}\,\text{deg} \\ n = -0.35^{+0.48}_{-0.47} \end{cases}$$

First follow-up work adding *Planck* low-frequency bands

→ $\beta = 0.33° \pm 0.10°$ (3.3σ) for nearly full-sky data

Forcing an integer index

n	$\Delta\chi^2$ - Ignore EB^{fg}	$\Delta\chi^2$ - Model EB^{fg}
2	8.21	9.45
1	4.67	5.60
0	0.00	0.00
-2	2.25	3.01

Data seems to favor a frequency-independent birefringence

→Quantum gravity theories $\beta \propto \nu^2$

→Lorentz-violating electrodynamics $\beta \propto \nu$

→Chern-Simons coupling to a light pseudoscalar field $\beta \propto \nu^0$

→Faraday rotation from primordial magnetic fields $\beta \propto \nu^{-2}$

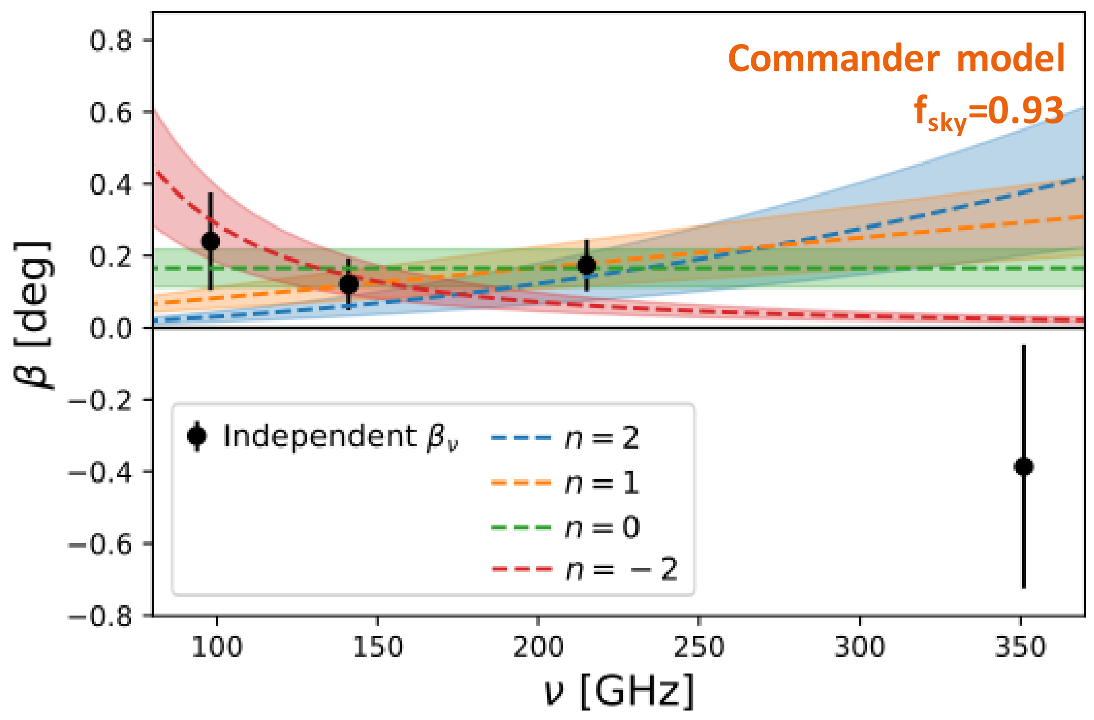

n	β_0 [deg]	$\Delta\chi^2$
2	0.07±0.03	5.08
1	0.13±0.04	1.77
0	0.17±0.05	0.00
-2	0.13±0.05	2.15

Independent β_ν for each frequency

$\beta_\nu=\beta_0\nu^2$ Quantum gravity models that modify the dispersion relation of photons

Gleiser & Kozameh 2001, PRD, 64, 8, 083007

$\beta_\nu=\beta_0\nu$ Superluminal Lorenzt-violating electrodynamics emerging from a non-vanishing Weyl tensor

Shore 2005, Nucl Phys B, 717, 86118

$\beta_\nu=\beta_0$ Chern-Simons coupling to a light pseudoscalar field like that of axion-like particles

$\beta_\nu=\beta_0\nu^{-2}$ Faraday rotation from Galactic or Primordial magnetic fields

Subramanian 2016, Rep Prog Phys, 79, 076901

Data seems to favor a frequency-independent birefringence

See Eskilt 2022, A&A, 662, A10 for a more detailed analysis

Constraining power of CMB observations on ALP parameter space

Fujita et al 2021, PRD, 103, 063508

Assuming:

- A **simple potential** $V(\phi) = \frac{1}{2} m_\phi^2 \phi^2$
- A **scale-invariant** power spectrum for the ALP field

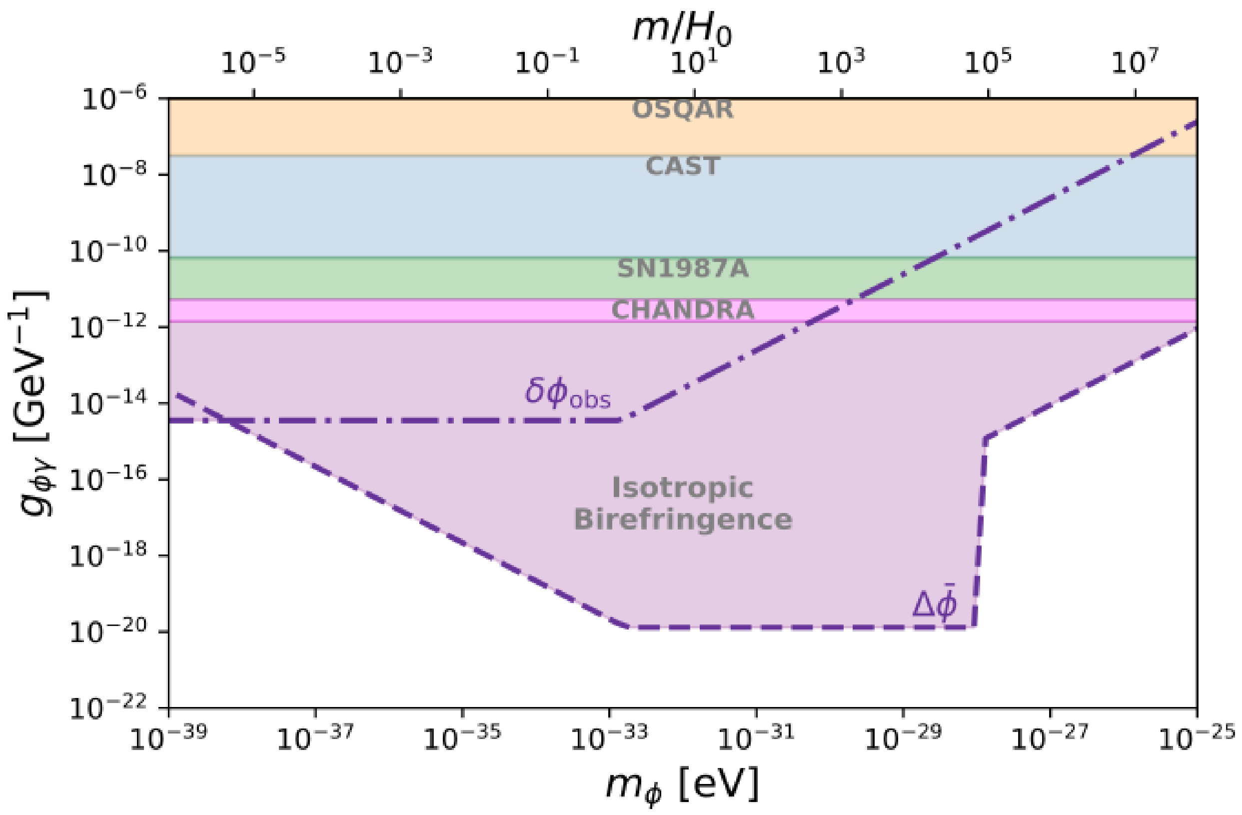

- A spatially flat FLRW universe, leading to **EoM**

$$\bar{\phi}'' + 2\mathcal{H}\bar{\phi}' + a^2 m_\phi^2 \bar{\phi} = 0$$
$$\delta\phi'' + 2\mathcal{H}\delta\phi' - \nabla^2\delta\phi + a^2 m_\phi^2 \delta\phi = 0$$

- The **largest allowed ALP abundance**

$$\Omega_\phi \begin{cases} \Omega_\Lambda = 0.69 & m_\phi \leq 9.26 \times 10^{-34}\mathrm{eV} \\ 0.006h^{-2} & 10^{-32}\mathrm{eV} \leq m_\phi \leq 10^{-25.5}\mathrm{eV} \end{cases}$$

Planck Collaboration VI. 2020, A&A, 641, A6

- **r<0.032** Tristram et al 2022, PRD, 105, 083524
- **β≈0.30°**

Chern-Simons coupling to a light ($m < 10^{-27}$eV) pseudoscalar field

$$\mathcal{L} = -\frac{1}{2}\partial^\mu\phi\partial_\mu\phi - V(\phi) - \frac{1}{4}F_{\mu\nu}F^{\mu\nu} + \frac{1}{4}g_{\phi\gamma}\phi F_{\mu\nu}\tilde{F}^{\mu\nu}$$

Marsh 2016, Phys Rep, 643, 1

Axion-like particles (ALP)

Initially proposed to solve the strong-CP problem

Evolved beyond the QCD axion to the more general axion-like particles from supersymmetry or string theories (10^{-33}eV < m < 10^{-18}eV)

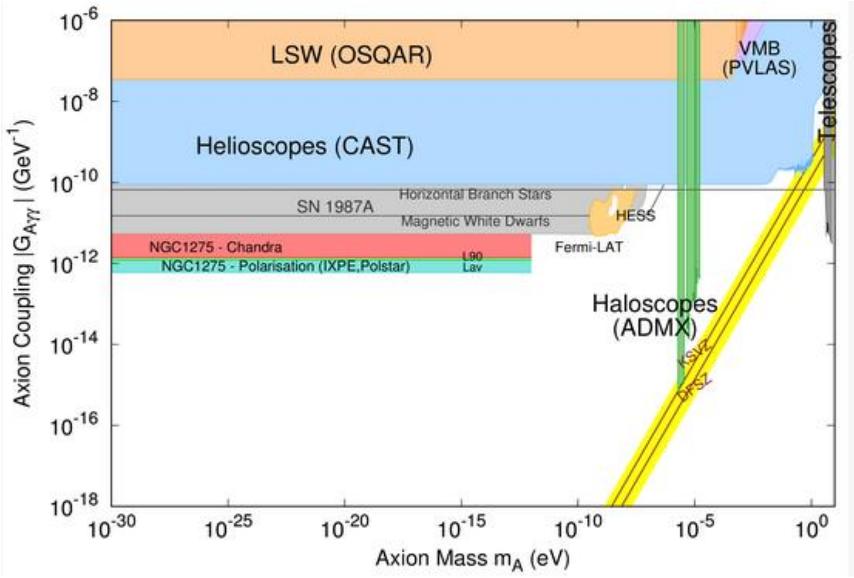

Day & Krippendorf 2018, Galaxies 2018, 6(2), 45

Kamionkowski & Riess 2022 [arXiv:2211.04492]

Early Dark Energy (EDE)

Early-time solution to the Hubble tension that modifies the sound horizon, increasing the H_0 inferred from CMB data

Fluid that behaves like a cosmological constant before matter-radiation equality (≈10% contribution to the total energy density briefly before recombination) and decays faster than radiation afterward so that late-time evolution is unchanged

Suppresses the growth of perturbations at early times, potentially increasing σ_8

→ worsening the tension between CMB and LSS measurements

Hill et al 2020, PRD, 102, 043507

Poulin et al 2019, PRL, 122, 221301
Hill et al 2020, PRD, 102, 043507

Global U(1) shift symmetry, broken by non-perturbative effects (instantons)

$$V(\phi) = m_\phi^2 f^2 \left[1 - \cos\left(\frac{\phi}{f}\right)\right]^n$$

Integer values of n

Around the minimum behaves as

$$w_\phi = \frac{n-1}{n+1}$$

$$\Omega_\phi \propto a^{-3(w_\phi+1)}$$

Axion-like particles (ALP)

$$n = 1$$

$$V(\phi) \rightarrow \frac{1}{2} m_\phi^2 \phi^2$$

$$\Omega_\phi \propto a^{-3}$$

ALP dilute like matter

Early Dark Energy (EDE)

$$n \geq 3$$

$$\Omega_\phi \propto a^{-4.5}$$

(or steeper)

☑ **EDE dilutes faster than radiation**

Nakatsuka et al 2022, PRD, 105, 123509

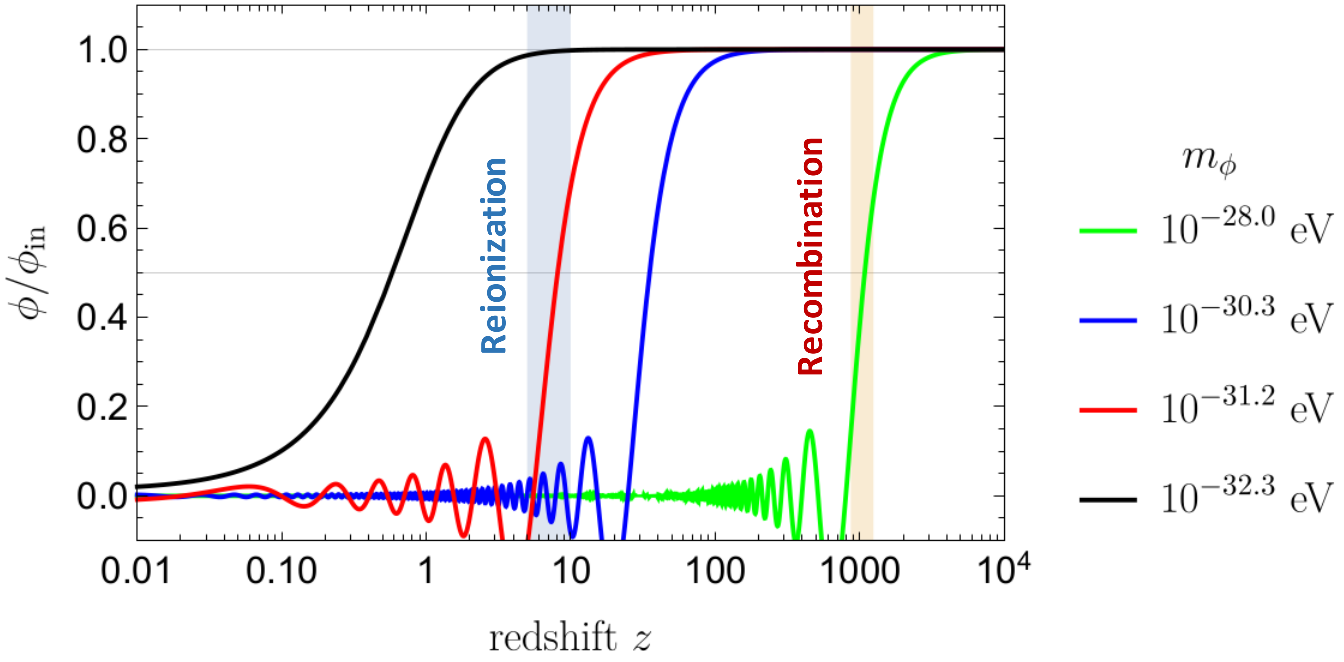

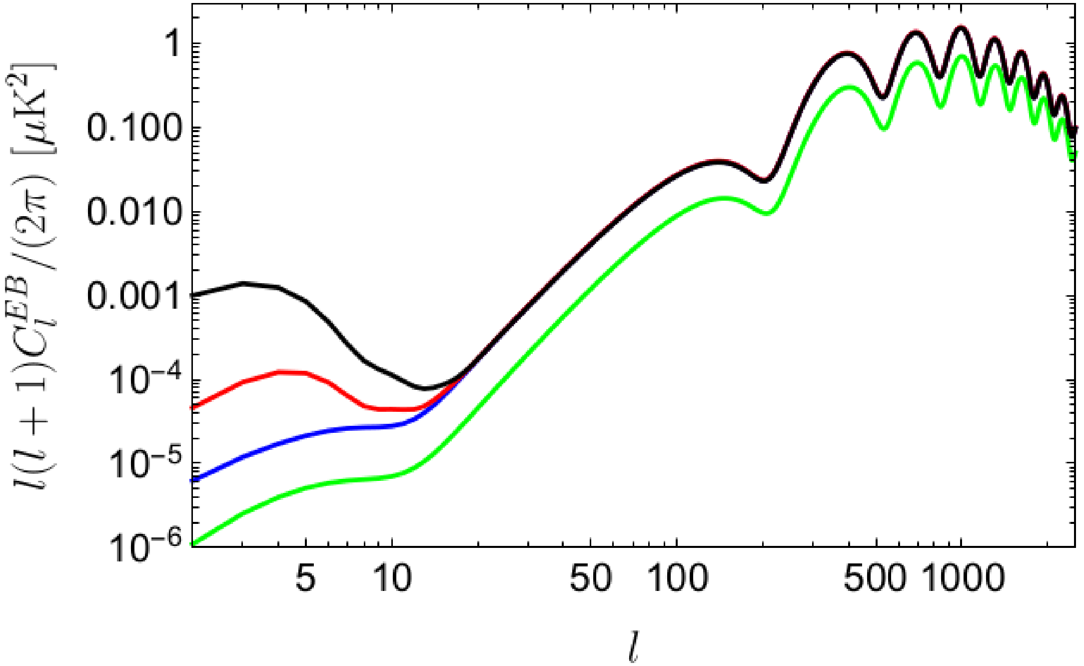

$$\beta = -\frac{1}{2} g_{\phi\gamma} \int \frac{\partial \phi}{\partial t} dt$$

Birefringence depends on the value of the field at photon emission and absorption

$$\beta(z) = \begin{cases} 0 & \text{for} \quad z = 0 \\ \beta_{\rm rei} & \text{for} \quad 0 < z \leq 10 \,, \\ \beta_{\rm rec} & \text{for} \quad 10 < z \end{cases}$$

CMB photons emitted at recombination and reionization will suffer different rotations

$$C_\ell^{EB,{\rm o}} \approx \frac{1}{2}\sin(4\beta_{\rm rec}) C_\ell^{E_{\rm rec}E_{\rm rec}} + \frac{1}{2}\sin(4\beta_{\rm rei}) C_\ell^{E_{\rm rei}E_{\rm rei}} + \sin(2\beta_{\rm rec} + 2\beta_{\rm rei}) C_\ell^{E_{\rm rec}E_{\rm rei}}$$

For fields undergoing a significant evolution during the epoch of recombination...

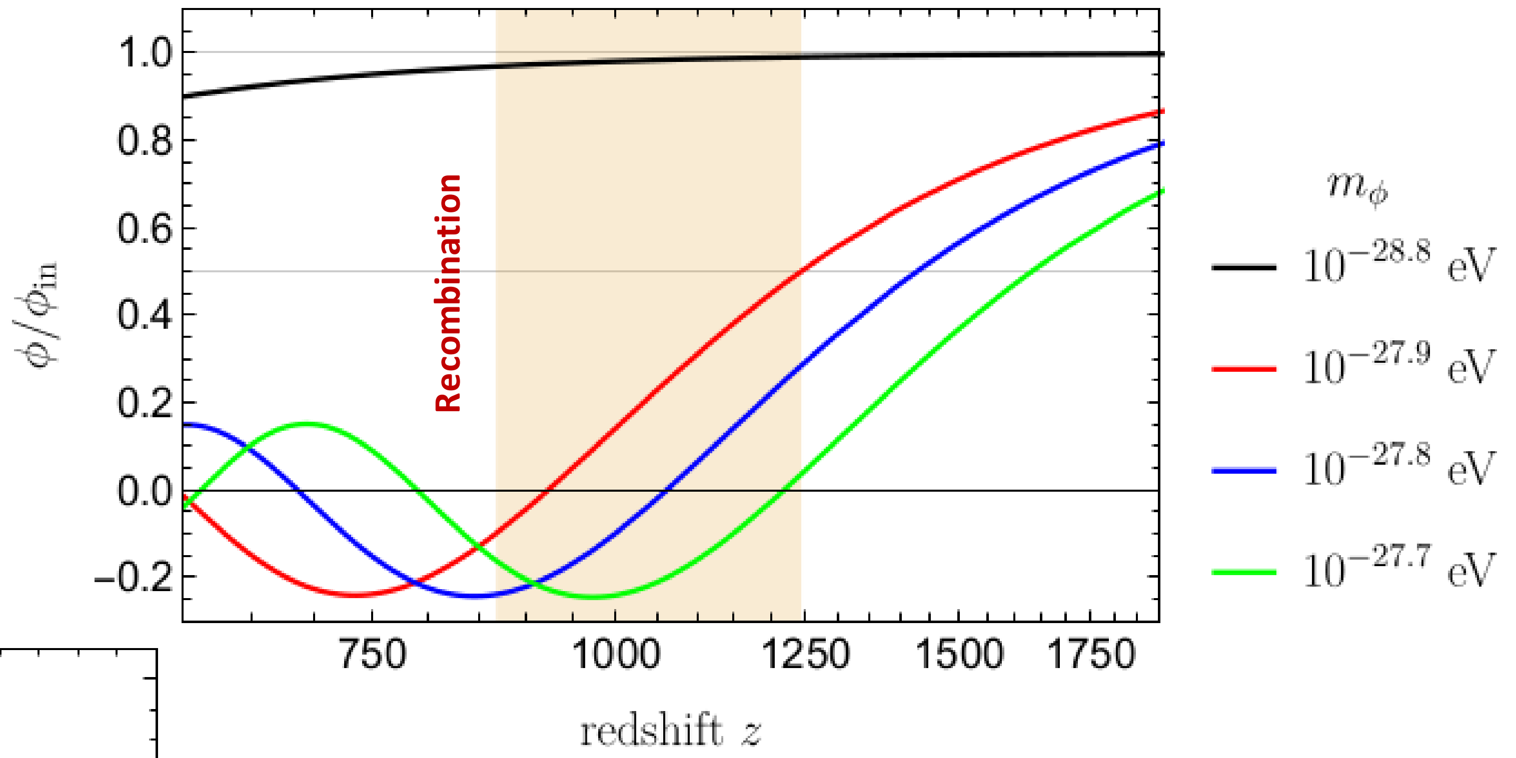

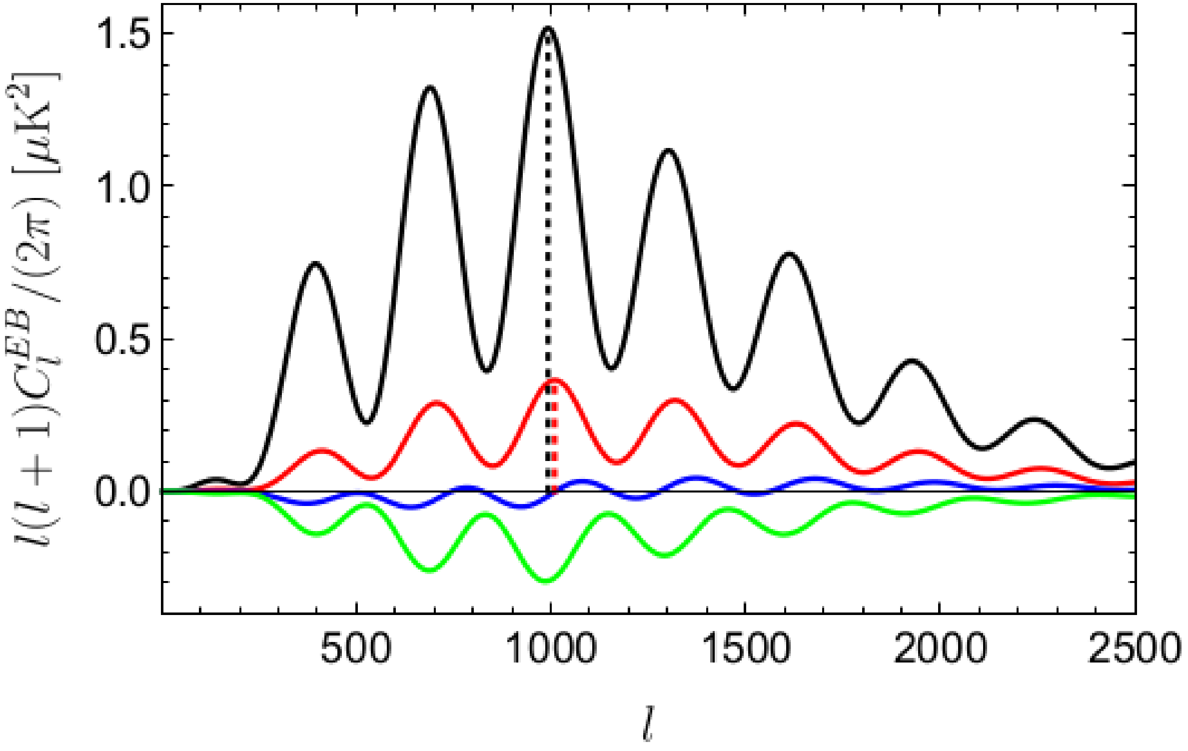

... the EB spectrum produced by birefringence no longer resembles a constant rotation of EE

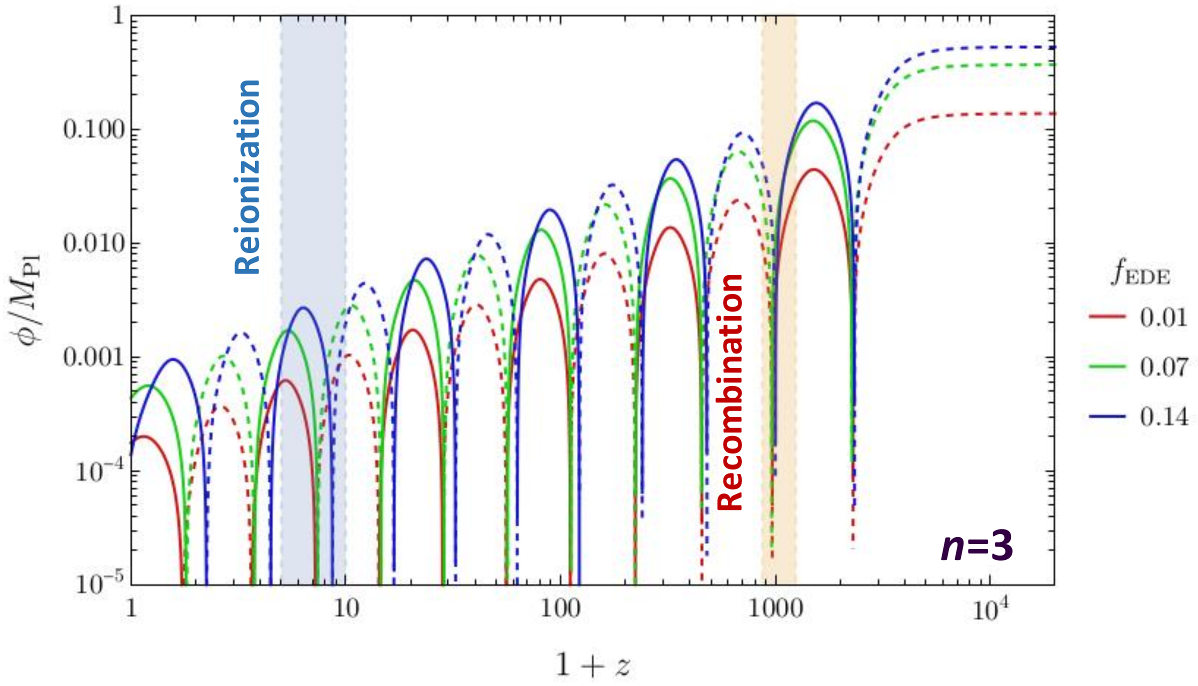

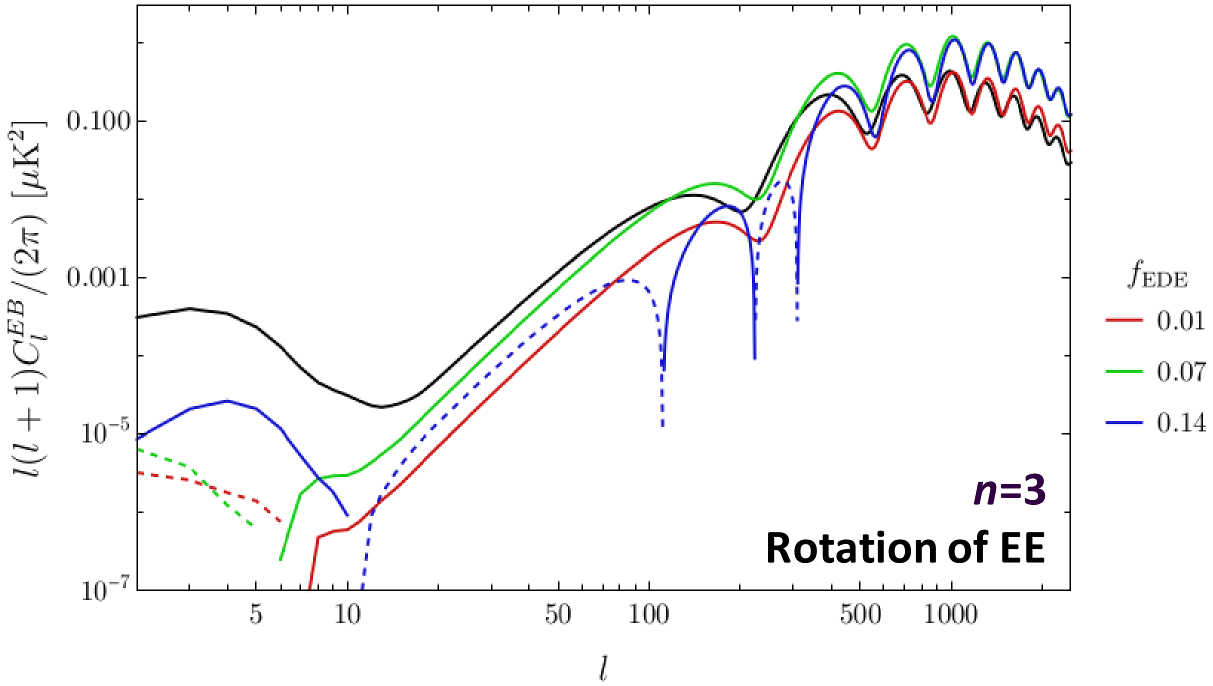

Murai et al 2022 [arXiv:2209.07804]

By definition, the EDE field must evolve before recombination

EB no longer resembles a constant EE rotation

EB is strongly dependent on the EDE model (*n* and f_{EDE})

CMB data alone can discern between ALPs and EDE as the source of birefringence

→ in the next decade, experiments like CMB-S4 will have enough sensitivity

WIP:

Obtain the first measurement of β from the epoch of reionization using only low-ℓ information